Meta-Analysis of Climate Change Data

Investigation of High Effect Climate Factors

Greenhouse Effect, Proxies and Reconstructions of Temperature and CO_2 (ppm), Instrumental Records of Temperature, Fossil Fuel Production, Solar Variation: Orbit, Magnetic and Sunspot Cycles, Irradiance, Radiation Bands, and Albedo. Temperature Statistical Model, Ocean Currents, Sea and Glacier Levels, Climate Extremes, Climate Cycle Analysis, Fundamental Models, Search for Anthropogenic Climate Fingerprints, and Potential Solutions for AGW.

http://www.leapcad.com/Climate_Analysis/Meta-Analysis_of_Climate_Change_Data.xmcd Rev April 18, 2016

An Application of the LeapCad Methodology and Philosophy in providing a Virtual Laboratory for
Learning, Exploring, and Developing Models using Tutorial Analytical Math Scripts.
These analytic climate model Mathcad (Version14) scripts and data are directly accessible from LeapCad.com.

Greenhouse Effect (GH), Anthropogenic Global Warming (AGW) Theory, and Evidence

The earth receives mostly visible **shortwave** (**< 1µm**) energy from the **sun**, the majority of which passes through the atmosphere. The atmosphere near the **surface** is largely **opaque to mid IR, thermal radiation (5-15µm)** (with important exceptions for "window" bands - See Section V. Solar Radiation Spectrum), and most heat loss from the surface is by sensible heat and latent heat transport. However, **CO_2 radiative effects** become **increasingly important higher in the atmosphere** as the higher levels become progressively more transparent to thermal radiation, largely because the **atmosphere is drier** and **water vapor -** an important greenhouse gas (**GHG**) - becomes **less**. GHG will absorb light only in a set of specific wavelengths, which show up as thin dark lines in a spectrum. In a gas at **sea-level** temperature and pressure, the countless molecules colliding with one another at different velocities each absorb at slightly different wavelengths, so the **lines are broadened and overlap** to a considerable extent. At **low pressure** the spikes become much more **sharply defined,** like a picket fence. There are gaps between the H2O lines where radiation can get through unless blocked by CO2 lines. **Thus CO2 absorption in the stratosphere does not saturate**. If the concentration of CO_2 is doubled, the GH effect **model** adds 4 W/sq. meter, which results in a global average temperature increase of 2.8C.
It is more realistic to think of the greenhouse effect as applying to a **"surface" in the mid-troposphere**, which is effectively coupled to the surface by a temperature lapse rate. Within the mid-troposphere region where **radiative effects are important**, the presentation of the Idealized Greenhouse Model becomes more reasonable: a layer of atmosphere with greenhouses gases will re-radiate heat in all directions, both upwards and downwards, thereby warming the surface (324 W/m^2) and simultaneously cooling (195 W/m^2) the atmosphere by transmitting heat to deep space at 2.7K. Increasing the concentration of these gases increases the amount of radiation, and thereby **warms the surface** and **cools the atmosphere** more. GHG shift the balance between incoming shortwave solar radiation and IR thermal radiation. This GH effect increase the land & ocean by about 20 C. See the illustration below.
AGW Mechanism: The Industrial Era has doubled CO_2. CO_2 is only 0.04% of the atmosphere, (its highest atmospheric concentration in at least 650,000 years), but it modifies the balance of shortwave incoming and IR. It is a strong absorber of infrared wavelengths, so it traps energy that would otherwise escape to space and nudges upward the temperature at which the radiation balance occurs. Another critical factor is that CO_2 lingers for decades to centuries, while water vapor rains out.

For the following discussion refer to the "Energy Balance Intensities" figure on page 2.

If we average the **incoming shortwave solar radiation** that is absorbed by the earth's climate over the surface of the earth we get around **235 W/m2**.
If we average the **outgoing longwave** radiation from the **top of atmosphere** we get the same value: **235 W/m2**.
If the atmosphere didn't't absorb any terrestrial radiation then the surface of the earth must also be emitting 235 W/m2. The only way that the surface of the earth could emit this amount is if the temperature of the earth was around **255K or -18°C. See Section IX-2.** And **yet we measure** an average **surface temperature** of the earth around **15°C** – which corresponds to an emission of radiation of 396 W/m2 from the **surface of the earth**.
If the atmosphere wasn't't absorbing **and re-radiating longwave** then the surface of the earth would be -18°C. **The actual warmer temperature of the earth results from the inappropriately-named "greenhouse" effect.**
In reality, of course, the situation is **more complicated**. Warmer air holds more water vapor, which is itself an important greenhouse gas. If we add carbon dioxide to the atmosphere, **water vapor becomes more abundant and amplifies the temperature increase** that would result from the carbon dioxide alone. Indeed, somewhat more than half of any AGW warming comes from this and other feedback processes.

Main Feedback Factors: Note - We currently have a limited understanding of these feedback factors.
1. Evaporation increases water vapor content of the atmosphere (provides both cloud shading, but water vapor is a GHG). It causes both cooling from clouds reflecting sunlight and heating from the greenhouse effect.
2. Albedo is the ratio of reflected to absorbed sunlight. This is affected by the ratio of ice to dark land (ice is reflective, while dark land absorbs sunlight). AGW causes increased heating and thus melting of polar ice.
3. Volcanic dust reflects sunlight and cools the planet. 4. Ocean currents/upwelling can change ocean heat flux.

Graphic Illustrations for Greenhouse Effect

The earth is an **isolated planet**, that is, it is surrounded by the vacuum of space. The energy-in is by short wave solar radiation and the only energy out must also be by radiation (longwave). For Energy Balance, the shortwave solar heat coming in must equal the long wave IR re-radiated heat going out.
The energy out comes from the **IR transparent region in the upper Troposphere**, which is at a lower temperature (on average, the temperature drops by 6.5 degrees C for every thousand meters of altitude you climb). If **GHG** is added, then **more energy is absorbed in the lower atmosphere** which **cools the upper** troposphere. According to the Stefan-Boltzmann Law, the radiated power is proportional to T^4. Thus the GHG IR molecules **radiated less power to space** than they absorb from the surface. Thus the temperature must rise to maintain energy balance. This is the greenhouse effect.

In the graph below, more that the energy leaving the earth, 452 W/m^2, is much greater than the solar radiation absorbed from the sun, 235 W/m^2. The **absorption and re-radiation** by "greenhouse" gases in the atmosphere is responsible. This is another indication of the greenhouse effect. The earth system **recirculates long wave mid IR**

Energy Balance Intensities (Power Density)

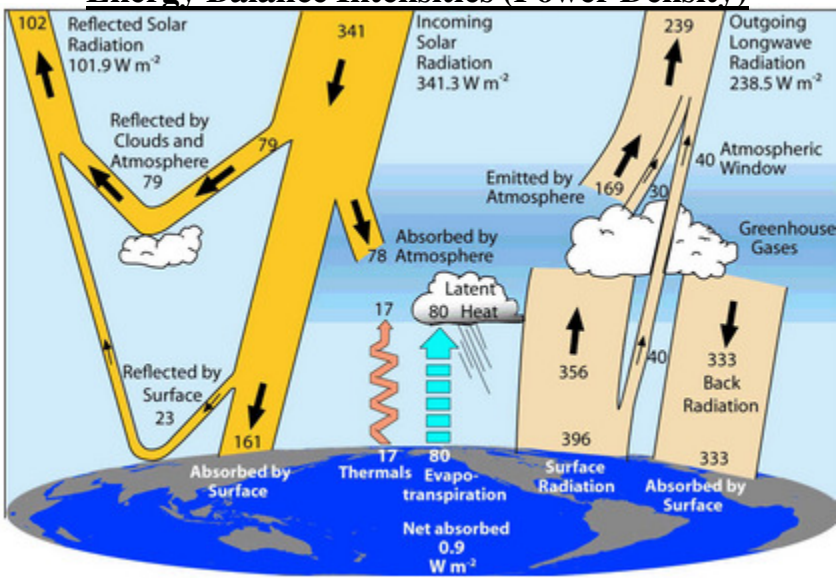

TABLE OF CONTENTS

A. Investigation of Climate Change Data

Testing the Anthropogenic Greenhouse Gas Global Warming Model

Looking for Unique Fingerprints of Global Warming

B. CONCLUSIONS - EVALUATION OF EVIDENCE

"Science and skepticism are synonymous, and it's okay to change your mind if the evidence changes."- Michael Shermer
"The first principle is that you must not fool yourself and you are the easiest person to fool." - Richard Feynman

1. The evidence shows "global" warming over the last 300 years. But, is the degree of **AGW** significant?
2. Section II. Warming over the last 100 years has been unusually rapid. Global +0.8 C for last 65 years.
3. Section V#3: Test 00: High Res Spectral Measurements gives 3.5 W?m^2 increase to CO2 AGW.
4. Section XIII: Test 0: Regressions reproduce both natural fluctuations & CO2 trend line of global temp
5. Section XIV: Test 1 through 7 show unique AGW fingerprints.
6. Section XIV: T8- Measurements of downwelling long wave radiation vs time --> 0.2 W/m^2 per decade
   Correlates with decadal 22 ppm CO2 increase - 10% of the trend in long wave downwelling radiation
7. Section XV to XVIII show increased sea levels, decreased glacier mass, and decrease north sea ice.
8. 2009 to 2013 US winters show destabilized polar vortex. Result: extremes of winter temperature.

Concern: Increased CO_2 in the oceans causes increased carbonic acid, which attacks coral.

Summary:

Climate is a complex phenomena. Much is not known. Models are incomplete &poor predictors.
There is definitely a spike in the recorded global temperature over the last 100 years. Data has verified unique fingerprints of AGW. The global temperature trend has been +0.8 C from 1950 to 2015.
Because of the chaotic nature of climate, climate models results must be presented as ensembles.
Therefore only probalistic conclusions are meaningful. Climate prediction is difficult because climate is chaotic.
The evidence shows that AGW contributes significantly to the total Global Warming in our industrial era.
Increased acidity of the oceans are also a major anthropogenic concern.
There is still much we do not know about climate. We have a poor understanding of feedback factors. Factors are at best guesses. **IPCC Assessment Report**, AR 5, Chapter 9.8.3 "Unlike shorter lead forecasts, longer-term climate change **projections push models into conditions outside the range** observed in the historical period used for evaluation."
We also have limited data, e.g. volcanic, sun, and cosmic ray activity, 3D data on clouds, threshold for convection, and aerosols.
Because of the verified footprints of anthropomorphic greenhouse gas production, that is, tests #1 - 8, it i unlikely that natural global warming be occurring due to solar variation or other mechanisms (cosmic ray ocean currents, or unknown feedback factors) is the cause of recent global warming.
Considering all the above factors, the evidence shows that antropogenic CO_2 production is4 causing a significant increase in downwelling long wave radiation power density with resultant global warming and increased startospheric cooling.

C. POTENTIAL SOLUTIONS TO GLOBAL WARMING

I. Alternative Energy Sources-

See • Models: Other Energy Technology- Nuclear Fusion, e.g. MIT ARC

II. Climate Engineering - Mitigating Climate Change:

The observed spike in temperature carries risks such as increases in ocean heights. The outlook for mitigating the AGW component by political change is very dim. Climate Engineering may target differen areas of the climate system; possess varying mechanics, costs, and feasibility; have diverse environmental and societal impacts on varying scales; and create their own sets of risks, challenges, and unknowns. The are commonly divided into two non-exhaustive suites:

• Carbon Dioxide Removal (CDR) methods attempt to absorb and store carbon from the atmosphere; either by technological means, or by enhancing the ability of natural systems (e.g. oceans) to do so.

• Solar Radiation Management or Sunlight Reflection Methods aims to reduce the amount of heat trappe by GHG by reflecting sunlight back into space, either by reflectivity of the earth or atmospheric particles.

Investigation of Climate Change Data

SECTION 0. History of Climate Change

The Nature of Ice Ages

Ice ages are times when the entire Earth experiences notably colder climatic conditions. During an ice age, the polar regions are cold, there are large differences in temperature from the equator to the pole, and large, continental-size glaciers can cover enormous regions of the Earth.

Ever since the Pre-Cambrian (600 million years ago), ice ages have occurred at widely spaced intervals of geologic time—approximately 200 million years—lasting for millions, or even tens of millions of years.

At least five major ice ages have occurred throughout Earth's history: the earliest was over 2 billion years ago, and the most recent one began approximately 3 million years ago and continues today (yes, we live in an ice age!). The most recent ice age was almost 10,000 years ago.

We are currently coming out of an ice ages and the Vostok Ice Core data in Section I. Plot 2-1 shows this more clearly.

Simplified chart showing when the five major ice ages occurred in the past 2.4 billion yrs of Earth's history.

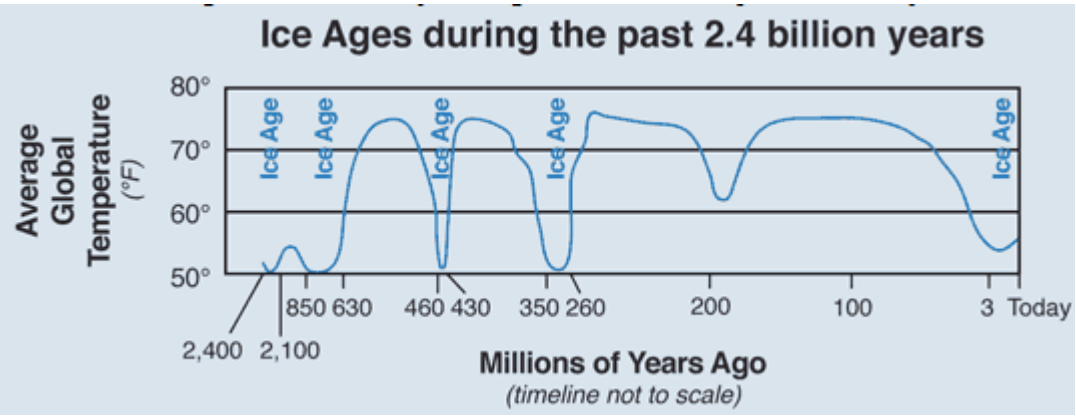

Era - a long period of time (intervals of hundreds of millions of years) which is marked by the definite beginning and end.
Period - a cycle of time (intervals of tens of millions of years long).
Epoch - a more recent period (intervals of tens of thousands to millions of years).

Today
Cenozoic
Quaternary
Holocene

The earth's temperature has oscillated between cold ice ages and hot "tropical" periods.

Today we are in the Cenozoic Era /Quaternary Period /Holocene Epoch -------

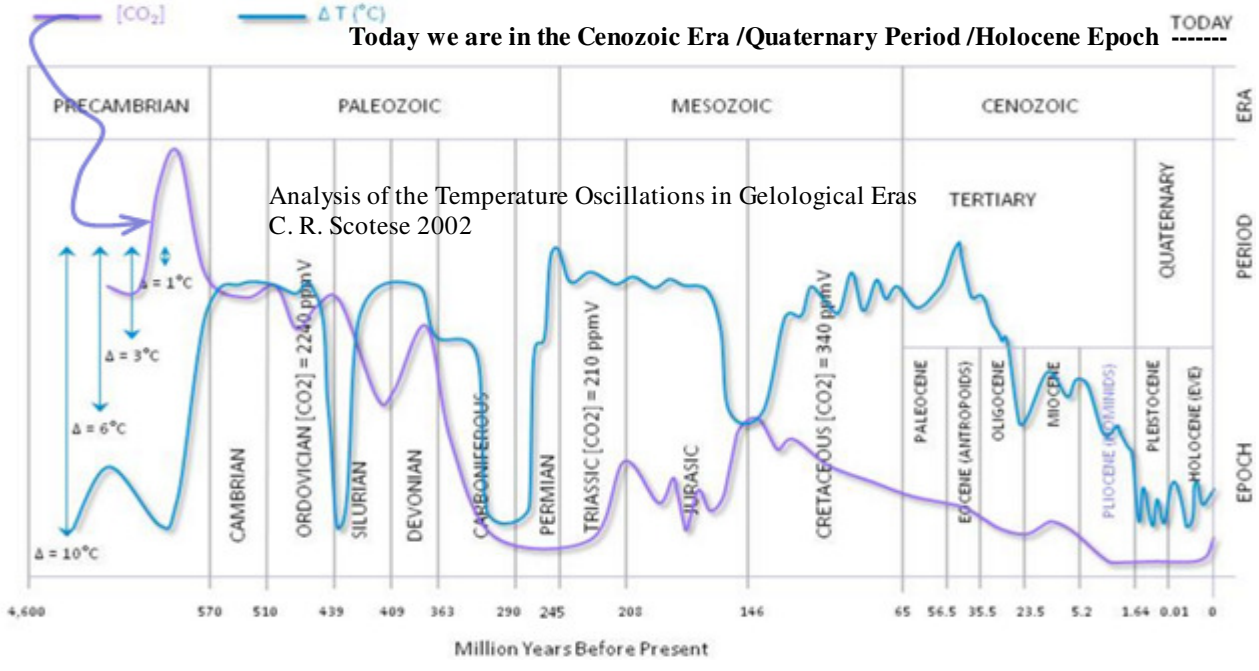

SECTION I. Paleological Isotopic Temp Record - the Vostok Ice Core - 1999

http://www.heartland.org/publications/NIPCC%20report/PDFs/Chapter%203.1.pdf
http://en.wikipedia.org/wiki/Ice_core
Petit, "Climate and atmospheric history of the past 420,000 years from the Vostok ice core, Antarctica", Nature 399: 429-436 CO2: Gas age CO2 (ppmv) File: co2vostokPetit.txt
Carbon Dioxide Information Analysis Center
http://cdiac.esd.ornl.gov/ftp/trends/temp/vostok/vostok.1999.temp.dat
Depth (m), Age of ice (yr BP), Deuterium content of the ice (D), Temperature Variation (deg C)

$Temp_{Vostok}$:= READPRN("vostok.1999.temp.txt CO2Vostok := READPRN("CO2vostokPetit.txt")

Glacials/Ice Ages and Their Temp Cycles over the Past 450,000 Years - Vostok Ice Core

Note: The 100,000 Year Cycle, which corresponds the the Earth's Orbital Variation
CO_2 actually lags temperature by around 1000 years.
IS CO_2 SAVING US FROM ANOTHER GLACIAL?

2-1. Vostok Ice Temperature/Glacials (Blue) & CO2 (Black) over 420,000 Years

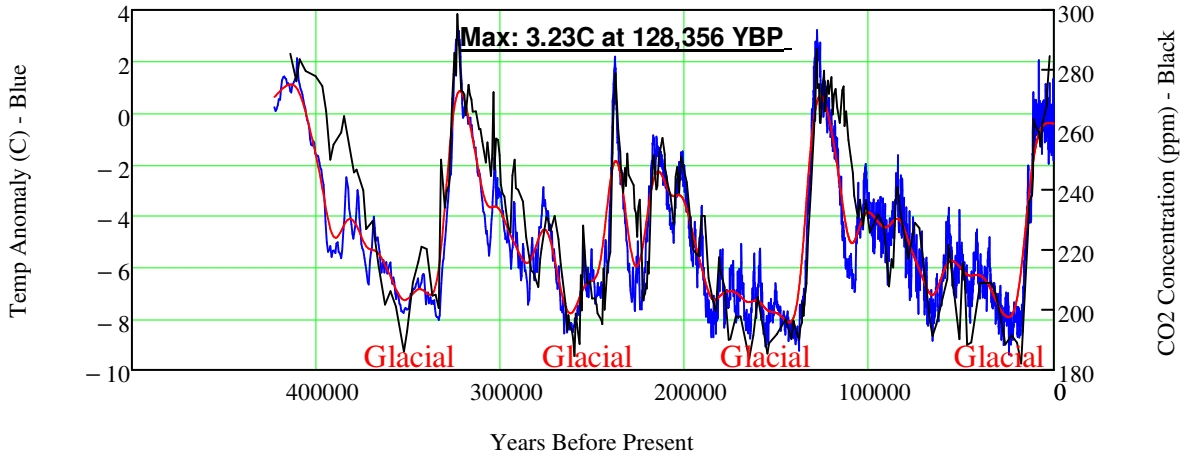

2-2. Vostok Antartica CO2 Concentration

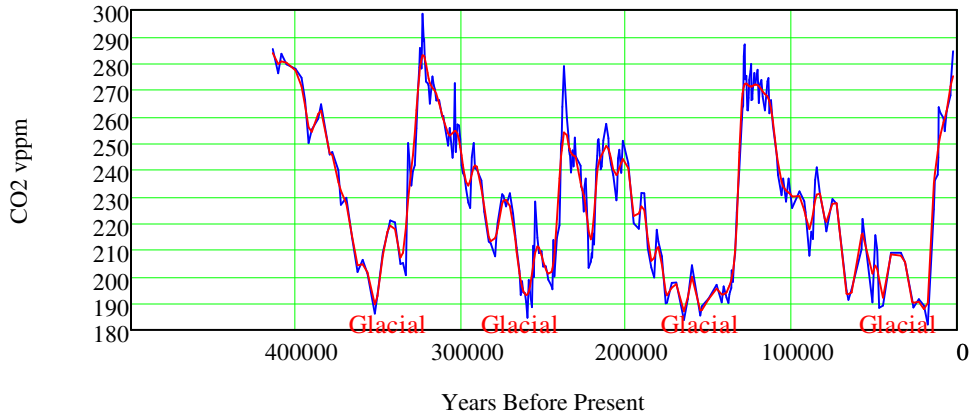

2.2-3. Vostok Antartica Temperature

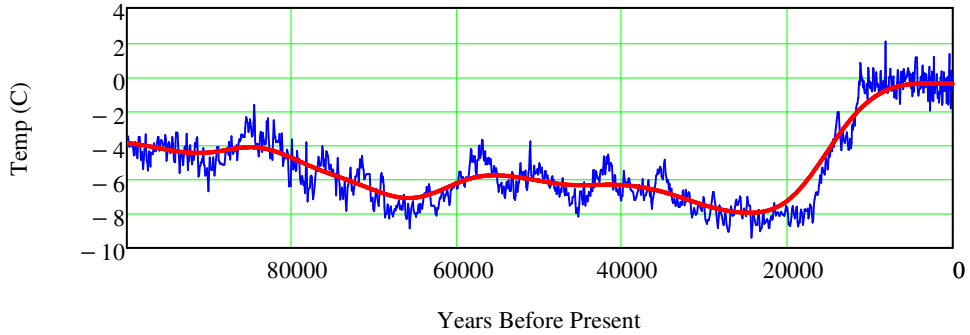

3. The Present Holocene Interglacial with 1500 Year Warming/Cooling Cycles
Spatio-temporal Analysis of Glacier Fluctuations in the European Alps after 1850

http://www.geo.uzh.ch/~mzemp/Docs/Zemp_PhD_2006.pdf

Holocene Climate Maximum

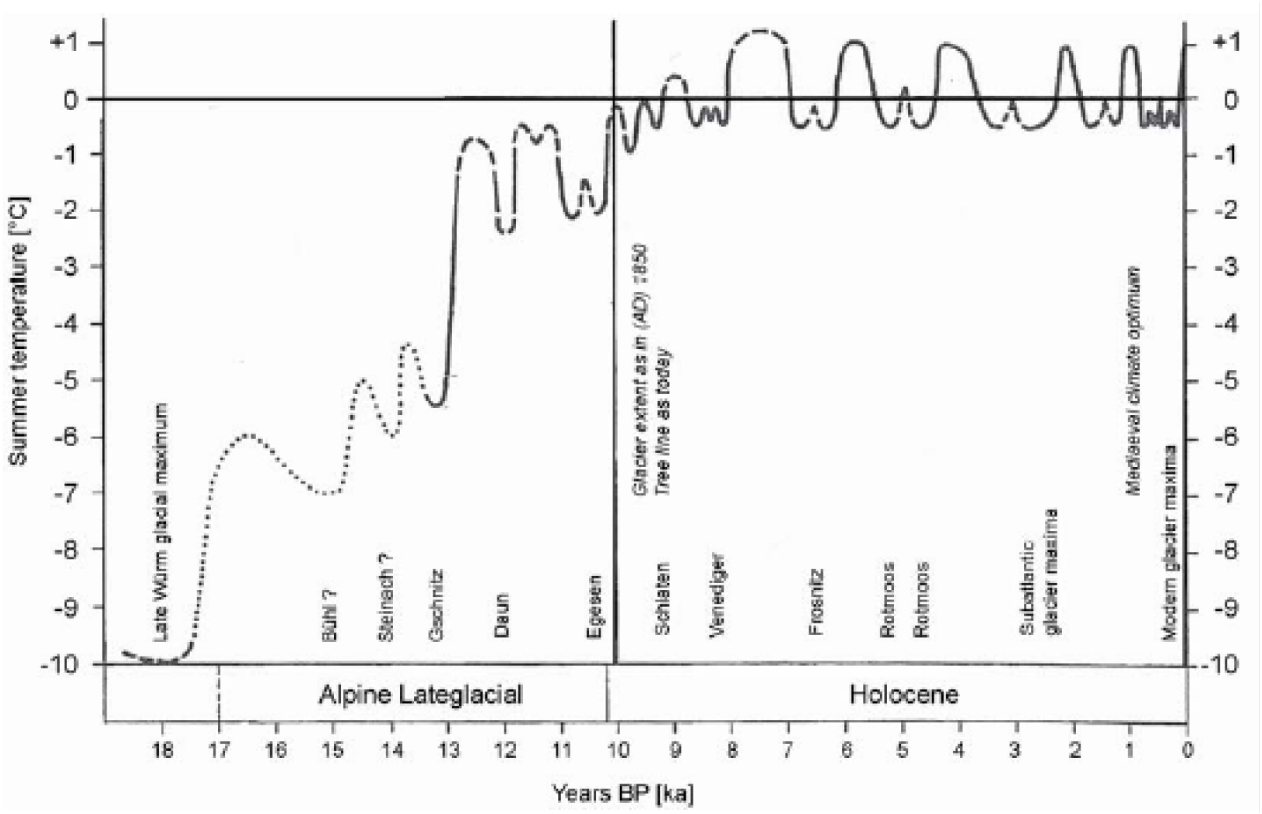

Figure 3: Alpine summer temperatures of the Lateglacial and the Holocene, as estimated from tree line and snow line variations. Slightly modified after Patzelt (1980).

4. The Little Ice Age and Medieval Warm Period in the Sargasso Sea (Local Area-May not be Typical)

Lloyd D. Keigwin

ftp://ftp.ncdc.noaa.gov/pub/data/paleo/contributions_by_author/keigwin1996/fig4bdata
http://lv-twk.oekosys.tu-berlin.de/project/lv-twk/002-Sargasso-Sea-surface-temperature.htm

This graph shows the Sargasso Sea surface temperature, which was derived from oxygen isotope ratios. This is an indicator of evaporation and, therefore, a proxy for sea-surface temperature. The Sargasso Sea is a two-million-mi2 body of water in the North Atlantic Ocean that lies roughly between the West Indies and the Azores from approximately 20-35oN. It is relatively static through its vertical column so that potential interference from mixing with other water masses and sediment sources is minimal. The isotopic ratios are derived from biotic debris that has precipitated onto the sea floor. Wide and abrupt variations in temperature are indicated. The relative temperature variations of the Little Ice Age (LIA) and the Medieval Warm Period (MWP) are prominently recorded in the data. Note that the temperature has been increasing since about 300 years before present (1700 A.D.) The horizontal line is the average temperature for this 3000-year period.

No indication of Error Bars. These are huge zig-zag changes, may be local shifts in currents, not global.

$Temp_{Paleo} := READPRN("Paleo\ Temp\ Keigwin\ 1996.TXT")$

$Temp_{Recent} := READPRN("Paleo\ Temp\ Keigwin\ 1955\text{-}1995.TXT")$

$Years := Temp_{Paleo}^{\langle 0 \rangle}$ $Temp := Temp_{Paleo}^{\langle 1 \rangle}$

$TSmooth := ksmooth(Years, Temp, 200)$ $WRITEPRN("TSmooth.txt") := TSmooth$

$TSmooth := READPRN("TSmooth.txt")$

4. The Little Ice Age and Medieval Warm Period. Sargasso Sea Surface Temperature

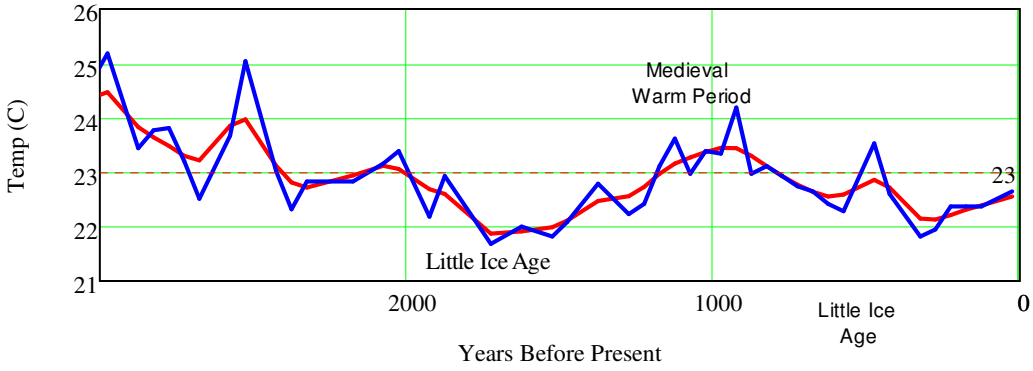

5. 2000-Year Global Temperature Reconstruction Based on Non-Tree Ring Proxies - Loehle - 2007

There are reasons to believe that tree ring data may not capture long-term climate changes (100+ years) because tree size, root/shoot ratio, genetic adaptation to climate, and forest density can all shift in response to prolonged climate changes, among other reasons Most seriously, typical reconstructions assume that tree ring width responds linearly to temperature, but trees can respond in an inverse parabolic manner to temperature, with ring width rising with temperature to some optimal level, and then decreasing with further temperature increases. Only 3 of the data sets is from Europe.

This reconstruction does not show the "hockey stick". **Thus the MWP and Little Ice Age were global.**

$Loelhe := READPRN("LoehleE\&E2007.csv")$ "Loehle, E&E Nov. 2007", calendar date,dev. deg C

5. Means of Temperature from 18 Non Tree Ring Series (30 Yr Running Means)

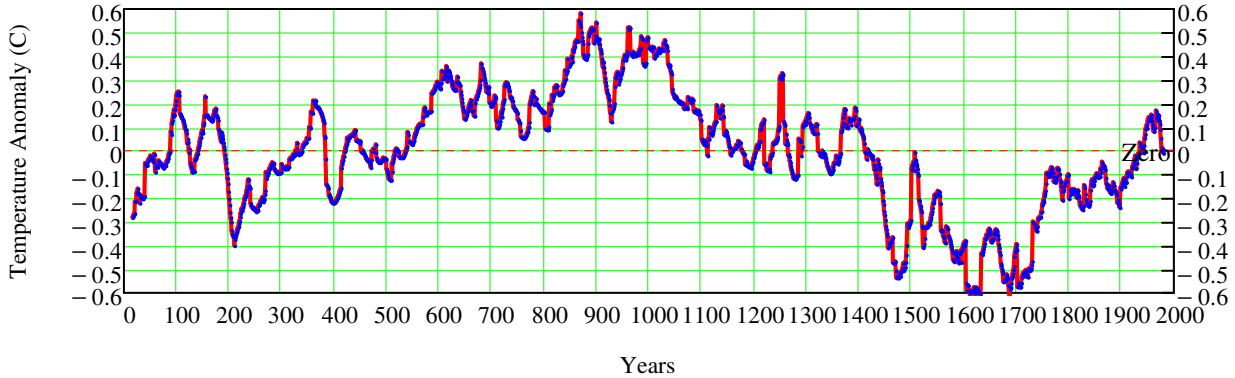

6. Millennial (Yrs 1000 to 2000) temperature reconstruction intercomparison and evaluation

M. N. Juckes, M. R. Allen, K. R. Briffa
supplement: http://www.clim-past.net/3/591/2007/cp-3-591-2007-supplement.zip
mitrie_cited_reconstructions_v01.csv

Reconstructions; Name Date-Column (Color)

crowley_lowery 2000-4 Northern (Red) mann_jones 1999 -10 Global (Violet)
hegerl_etal 2006-6 " (Blue) oerlemans2005-12 " (Blue-Green)
huang_etal 1998-7 x 0 " (Green)

Observed "Instrument"

Supplement 2007 (Blue)
See SECTION II -3: **Berkeley Land Surface (Not Land/Sea)** Temp Data - BerkTemp from 1800 to 2014 (Black)

BerkTemp := READPRN("BerkTemp2.txt") BkYr := $BerkTemp^{\langle 0 \rangle} + (BerkTemp^{\langle 1 \rangle} - 1) \cdot 0.08333$

BerkTempS := ksmooth(BkYr1800, BerkTemp1800, 10)

Mitrie_T2006 := READPRN("mitrie_instrumental_2006.txt")

Mitrie_T2006S := ksmooth$(Mitrie_T2006^{\langle 0 \rangle}, Mitrie_T2006^{\langle 1 \rangle})$, Yr_{mr} := READPRN("YrMitrie.txt")

MitrieTempf := READPRN("mitrie reconstructions1.txt") MitrieTemp := MitrieTempf

cols(MitrieTempf) = 13 **Mann Hockey Puck Curve (Rose Color)**

Note that the rise within the last 100 years has been **much more rapid** than in the past.

6. Millennial Temperature Reconstructions (Last 1000 yrs from 5 sources) and Insturment Temp (2)

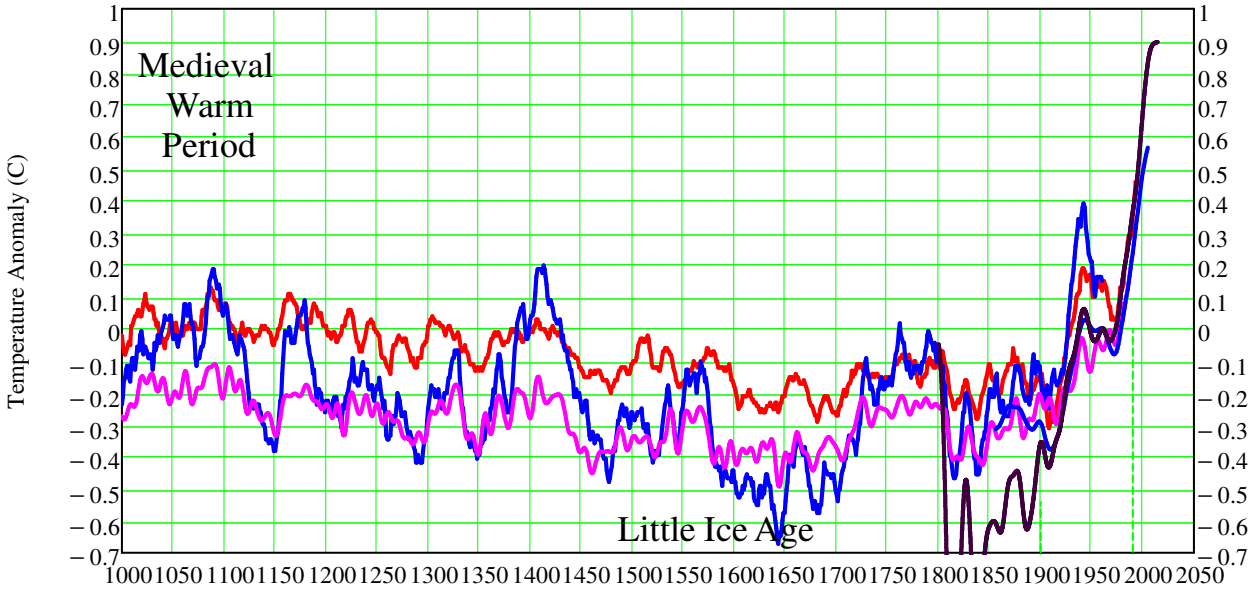

7. Temperature reconstructions and anomalies taken from the references listed below

ftp://ftp.ncdc.noaa.gov/pub/data/paleo/treering/reconstructions/n_hem_temp/briffa2001jgr3.txt
Re calibrations given in Briffa et al. (2001) J Geophys Res 106, 2929-2941

Years: 1000 to 1997

1: Jones et al. (1998) Holocene
2: Mann et al. (1999) Geophys Res Lett
3: Briffa et al. (2001) J Geophys Res
4: Briffa (2000) Quat Sci Rev
5: Overpeck et al. (1997) Science
6: Crowley & Lowery (2000) Ambio
7: Observed temperatures from Jones et al. (1999) Rev Geophys

TempMill7 := READPRN("Temp 7 Reconstructions-briffa.txt")

YearMill := $TempMill7^{\langle 0 \rangle}$ TempS := MKSmooth(TempMill7)

MKSmooth is a Matrix ksmooth over 12 points

7. Millenial Temperature Anomaly Reconstructions (5)

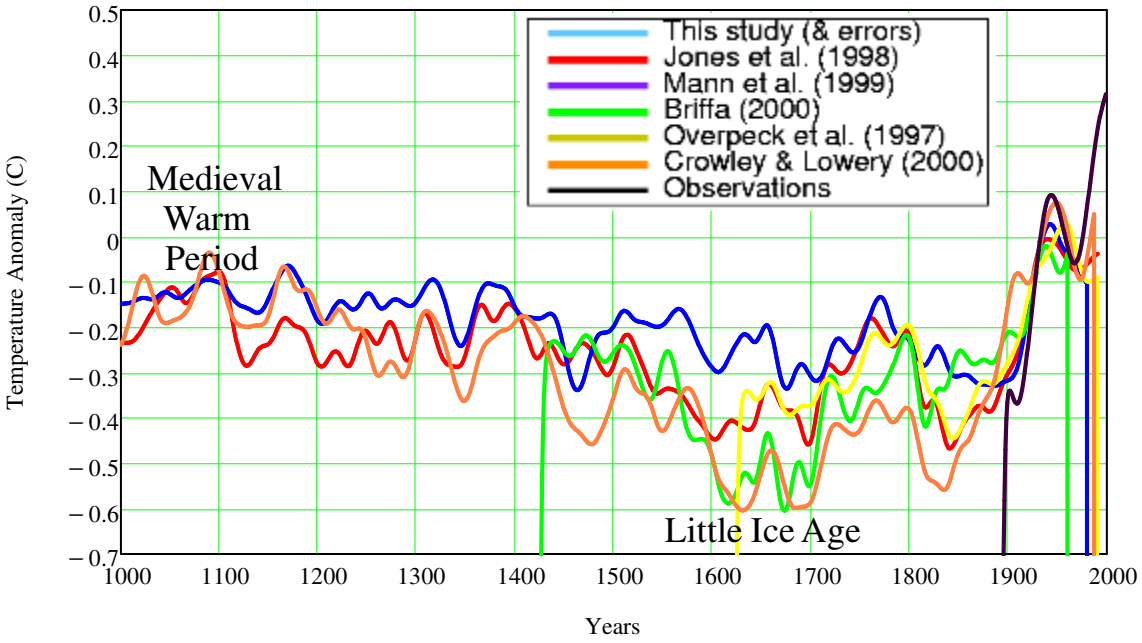

8. Highly variable Northern Hemisphere temperatures reconstructed from low- and high-resolution proxy data, Anders Moberg1, Dmitry M. Sonechkin2, Karin Holmgren3, Nina M. Datsenko2, Nature 2005

NHTC := READPRN("Highly variable NH temps reconstructed-Moberg.TXT")

$NHTC_{yr} := NHTC^{\langle 0 \rangle}$ $NHTC_{Temp} := NHTC$ cols(NHTC) = 9

8. Multi-Proxy Reconstructioned North Hemisphere Temperature Anomaly

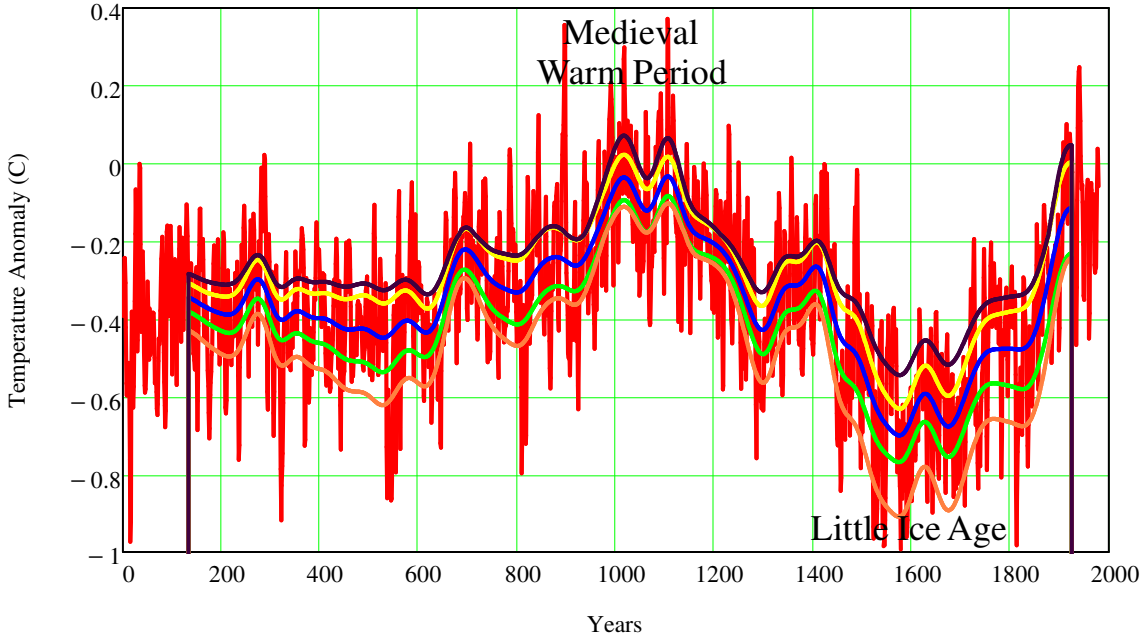

9. Roman, Medieval, and Modern Warm Periods - Modern same as Roman and Medieval

This reconstruction is the first to show a distinct Roman Warm Period c. AD 1-300, reaching up to the 1961-1990 mean temperature level, followed by the Dark Age Cold Period c. AD 300-800. The last 2,000 years of proxy reconstructed temperature variations for the Northern Hemisphere shows that the
Modern Warm Period (today) is not significantly different from the Medieval Warm Period of ~1,000 years ago, or the Roman Warm Period of ~2,000 years ago (Ljungqvist, 2010):

Read Data from: Ljungqvist, F.C. 2009, N. Hemisphere Extra-Tropics 2,000yr Decadal Temperature Reconstruction
Source: ftp://ftp.ncdc.noaa.gov/pub/data/paleo/contributions_by_author/ljungqvist2010/ljungqvist2010.txt

	Line Color
Column 0: Begin Decade AD	
Column 1: End Decade AD	
Column 2: Reconstructed temperature anomaly in degrees C with respect to 1961–1990	Blue
Column 3: Upper Red Trace - 2 standard deviation error bar	Red
Column 4: Lower Red Tracde- 2 standard deviation error bar	Red
Column 5: Instrumental temperature data from the variance adjusted CRUTEM3+HadSST2 90–30°N Smoothed Data for Temp Anomaly	Heavy Green

Data Columns: Decade ReconT Up.err. Lo.err. Inst.Temp.

$T_{LMillenial} := READPRN("Temp\ NH\ \ 1\ to\ 2000AD\ Ljungquist2010.txt")$

Smooth the Temp Anomaly Data, Green Line

$TLSmooth := ksmooth\left(T_{LMillenial}^{\langle 0 \rangle}, T_{LMillenial}^{\langle 2 \rangle}, 50\right)$

Lungquist Reconstruction data from year 0 to 2000.
Added GISS USA 1880 to 2014 Data from Section II.2 below

$USTemp := READPRN("GISS\ NH\ TempC-2014.txt")$

$USTS := ksmooth\left(USTemp^{\langle 0 \rangle}, USTemp^{\langle 13 \rangle} \cdot 0.01, 10\right)$

Units 0.01 Celsius,
J-D Mean in Col 13
Smooth for decadal
Black Dotted Trace

Temp Reconstruction for North Hemisphere with 2 Sigma Error Limits. Added USA (black dots)

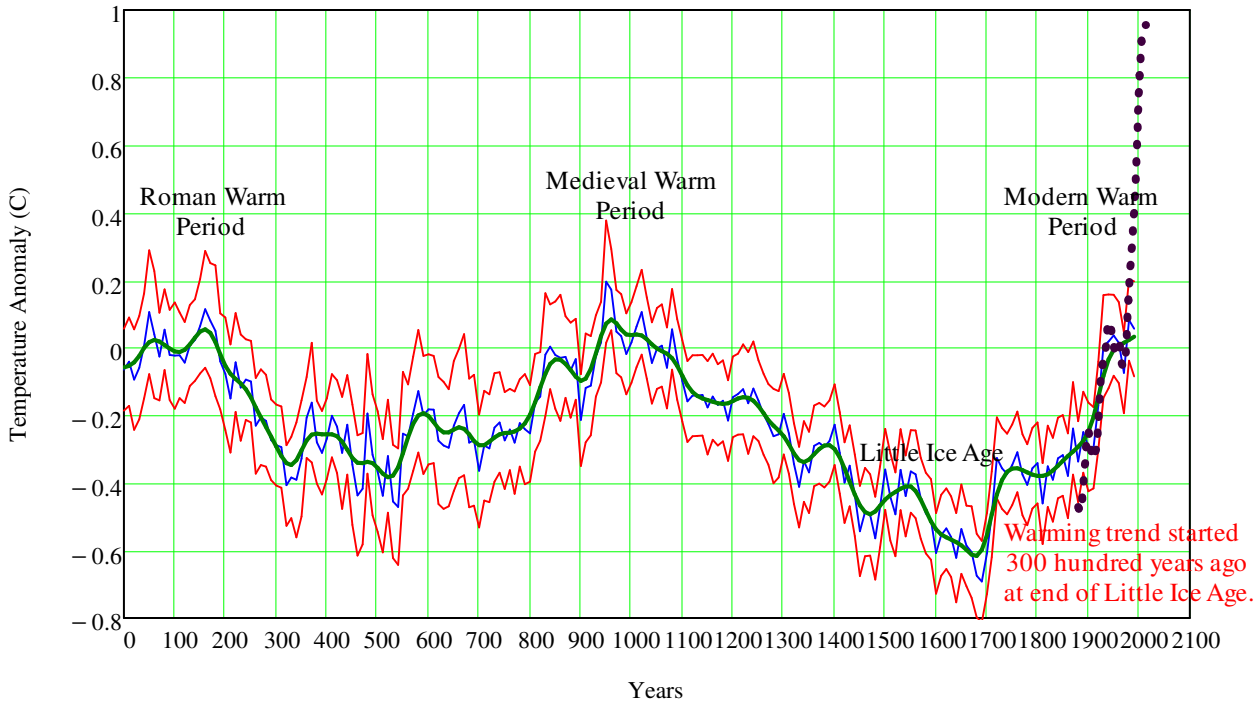

SECTION II. Instrument Direct Temp: NOAA, NASA, Berkeley Earth Records

1. Global from 1880: 2006 & 2014 Datasets Direct Inst Temp Time Series Records

Latitude Range -90 to 90, Longitude Range -180 to 180
(from the Global Historical Climatology Network dataset)
http://www.co2science.org/cgi-bin/temperatures/ghcn.pl

BerkT := READPRN("BerkTemp2.txt")

GHCN := READPRN("GHCN Temp Anomally 1880 - 2006.txt") BYr := $BerkT^{\langle 0 \rangle}$ + $BerkT^{\langle 1 \rangle}$ 0.08333

GHCN2 := READPRN("GHCN Temp Anomally 1880 - 2014.txt")

National Climatic Data Center's website: http://www.ncdc.noaa.gov/oa/climate/ghcn-monthly/index.php
Berkeley Earth Decadal Land-Surface Temperatures: http://berkeleyearth.org/summary-of-findings

USATSmth := ksmooth$\left(GHCN^{\langle 0 \rangle}, GHCN^{\langle 1 \rangle}, 5\right)$ WRITEPRN("USATSmth.txt") := USATSmth

1. Global Temp Anomaly: GHCN Dataset (Red) & Berkeley Land/Surface 1&5Yr Avg

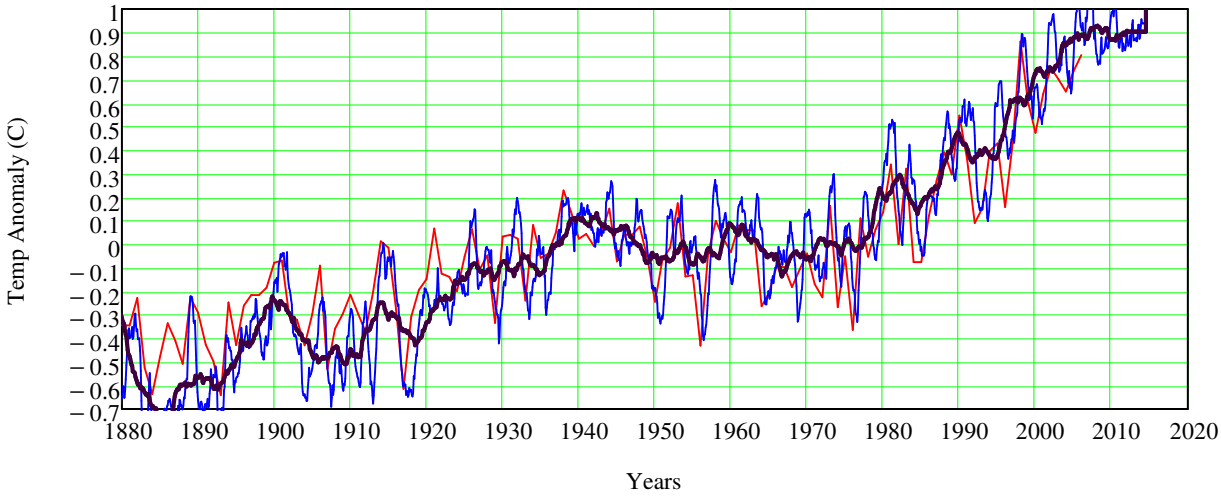

2. NASA GISS Surface Temperature Analysis - US and Zonal 1880 - 2014

Goddard Institute Space Studies: Annual Mean US & Global Temperature Change

http://data.giss.nasa.gov/gistemp/graphs/Fig.D.txt - Blue & Red /Fig.A2.txt - Green
Annual and five-year running mean surface air temperature in the contiguous 48 United States (1.6% of the Earth's surface) relative to the 1951-1980 mean. 2014 http://data.giss.nasa.gov/gistemp/ Data in C.
This is an update of Figure 6 in Hansen et al. (1999). Fields: year Annual_Mean 5-year_Mean

USTemp0 := READPRN("Contiguous 48 US Tempt Anomaly.TXT") Red 2009 Averaging Method
USTemp := READPRN("GISS NH TempC-2014.txt") Units 0.01 Celsius, J-D Mean in Col 13
GTemp0 := READPRN("GISS NASA Global Temp Mean Fig2A.TXT") reen 2013 Revised Method
GTemp := READPRN("GISS GLB TempC-2014.TXT") Units 0.01 Celsius, J-D Mean in Col 13

USTSmth := ksmooth$\left(USTemp^{\langle 0 \rangle}, USTemp^{\langle 13 \rangle} \cdot 0.01, 5\right)$

GLB2014 := READPRN("/Source Temp Files/GLB.Ts+dSST-2014X.txt")

Note: On the 2008 scale the warmest year in US was 1934

2. US(Blue) and Global (Red) Annual Mean Temp Anomaly in Celcius- GISS- 1880

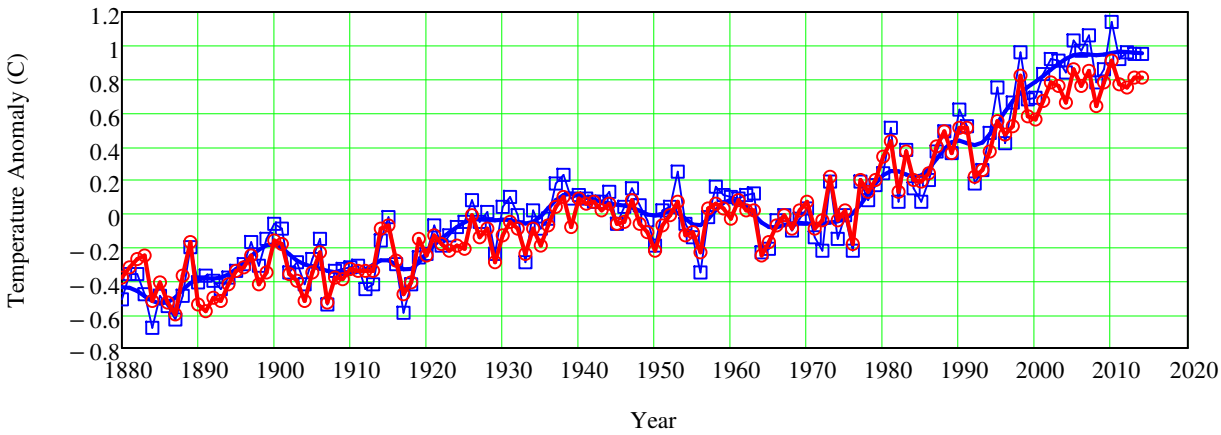

3. Berkeley Earth Land Average Temp and Simple CO2 and Volcano Temperature Fit

Focused (Richard A. Muller) on land temperature data analysis. Berkeley Earth was founded in early 2010 with the goal of addressing the major concerns of "skeptics" regarding global warming and the instrumental temperature record. The project's stated aim was a "transparent approach, based on data analysis.

http://berkeleyearth.org/summary-of-findings

Yr , Month, TempAnom&Unc: 1Yr, 5 Yr, 10Yr, 20 Yr

BerkTemp := READPRN("BerkTemp2.txt")

BkYr := BerkTemp⟨0⟩ + (BerkTemp⟨1⟩ − 1)·0.08333 *

BCVFit := READPRN("forcing-comparison-data2.txt") ==> Year, CO2, Volcano, ln(), Volcano, T, Tfit

α := 8.342105 β := 4.466369 γ := −0.01515 Fit := α − 8.8 + β·ln(BCVFit⟨1⟩·277.3^−1) + γ·BCVFit⟨2⟩

MLCO2 := READPRN("NOA_Mauna_Loa_Monthly_CO2_14.txt")

Berkeley Land 5 Year Average Temp (Blue), CO2 (Black) , and Simple CO2/Vocano Fit (Red)

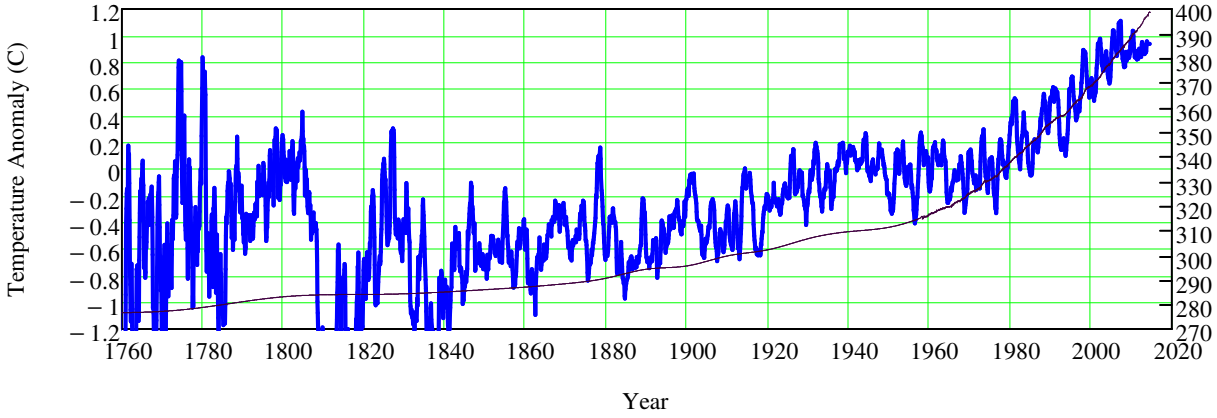

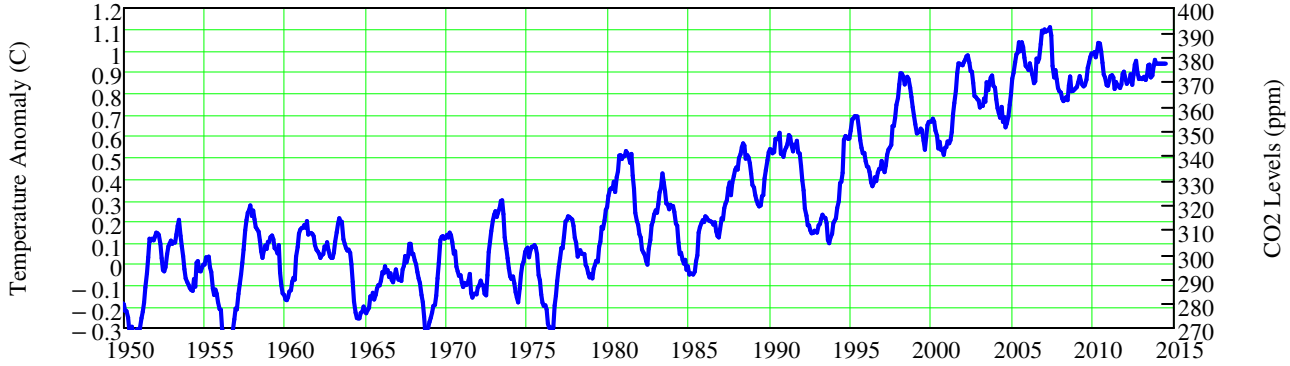

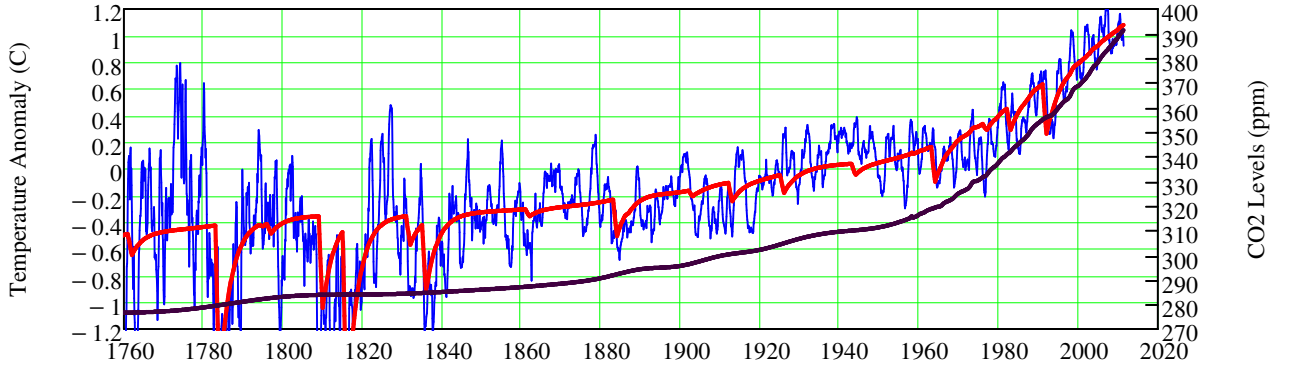

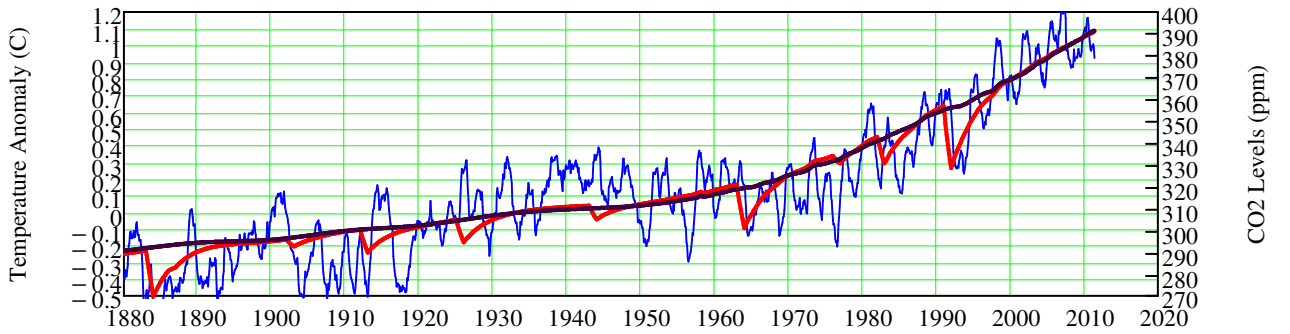

4. Hadley Center- Climate Research Unit: HadCrut Global Land Air Data 1860 to 2015: See Section III-A (CO2) - 5 for Plots of CO2 vs HadCrut Global Temp.

http://www.cru.uea.ac.uk/cru/data/temperature/CRUTEM4-gl.dat Monthly and Yearly Data

Read HadCrut Formatted File (Different Number of Cols/Row): HadCrutE4 = Insert File Input (HadCrutE4.dat)

Read every other row

5. GISS Zonal: Annual mean Land-Ocean Temperature - Selected zonal means 1880 - 2013

http://data.giss.nasa.gov/gistemp/tabledata_v3/ZonAnn.Ts.txt

Fields: Year Glob NHem SHem -90N -24N -24S -90N -64N -44N -24N -E

USZTemp := READPRN("ZonAnnT1880-2013.txt' NHTSmth := ksmooth$\left(USZTemp^{\langle 0\rangle}, USZTemp^{\langle 2\rangle} \cdot 0.01, 5\right)$

USZTSmth := ksmooth$\left(USZTemp^{\langle 0\rangle}, USZTemp^{\langle 3\rangle} \cdot 0.0\right.$ GTSmth := ksmooth$\left(USZTemp^{\langle 0\rangle}, USZTemp^{\langle 1\rangle} \cdot 0.01, 5\right)$

3. Hemispheric Temperature Change NH (Blue) SH (Red) Global (Black)

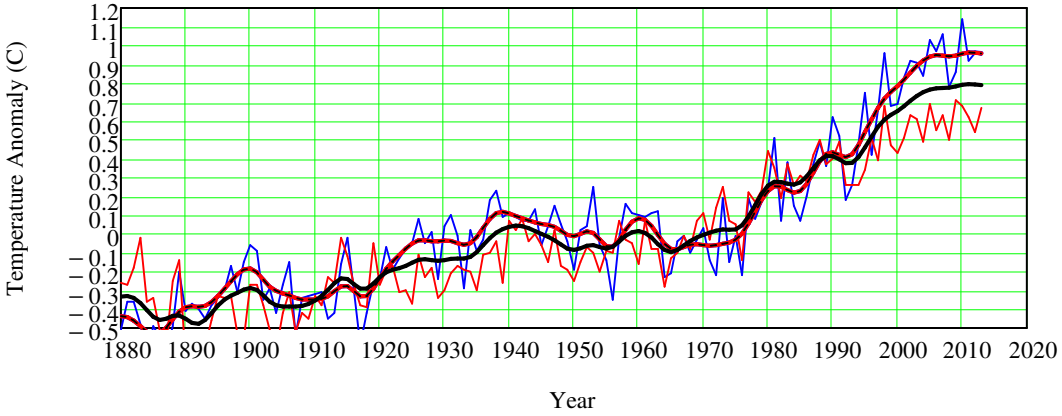

6. NOAA: No Slowdown in Global Warming

Science: Possible artifacts of data biases in the recent global surface warming hiatus - June 4, 2015

ftp://ftp.ncdc.noaa.gov/pub/data/scpub201506/NewAnalysis/NewAnalysis.aravg.mon.land_ocean.90S.90N.asc

ftp://ftp.ncdc.noaa.gov/pub/data/scpub201506/NewAnalysis/NewAnalysis.aravg.mon.land.90S.90N.asc

Global_New := READPRN("NewAnalysis.aravg.ann.land_ocean.90S.90N.asc")

Global_NewMon := READPRN("NewAnal.mon.global.txt")

rd := rows(Global_New) $Date_{1950} := submatrix\left(Global\_New^{\langle 0\rangle}, 70, rd-1, 0, 0\right)$

$L_{1950} := line\left(Date_{1950}, submatrix\left(Global\_New^{\langle 1\rangle}, 70, rd-1, 0, 0\right)\right)$

$Trend_{1950}(Year) := L_{1950_0} + L_{1950_1} \cdot Year$ $\Delta T1950 := L_{1950_1} \cdot 65 = 0.85271$

$L_{1880} := line\left(Global\_New^{\langle 0\rangle}, Global\_New^{\langle 1\rangle}\right)$ Last 65 Year: $\Delta T\_Century := L_{1950_1} \cdot 100 = 1.31186$

$Trend_{1880}(Year) := L_{1880_0} + L_{1880_1} \cdot Year$ $Temp\_Change\_Century := L_{1880_1} \cdot 100 = 0.67615$

Global Temperature Change per Century = +0.68 C. Increased to +

5. No Slowdown in Global Warming. Trend line + 0.8 C from 1950 to 2015 - NOAA

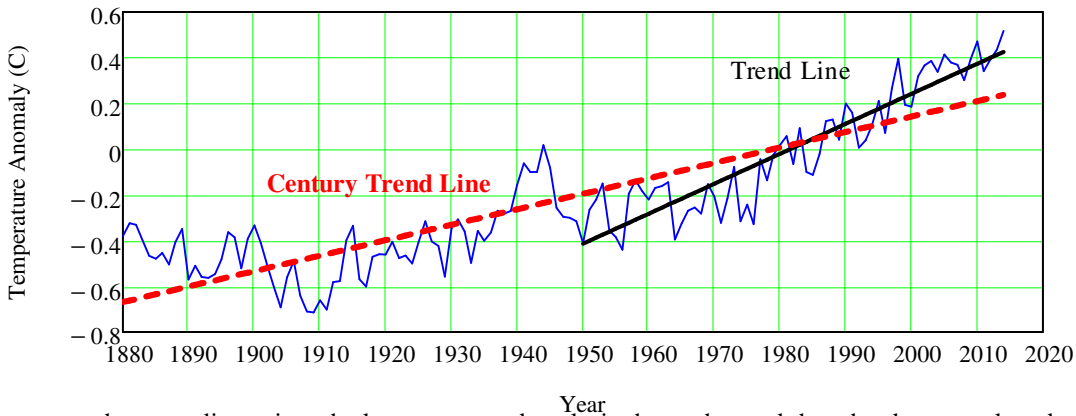

Contrary to much recent discussion, the latest corrected analysis shows that and there has been no slow down.

7. http://www.drroyspencer.com/latest-global-temperatures/

Year Mo Globe Land Ocean NH Land Ocean SH Land Ocean Trpcs Land Ocean NoExt Land Ocean SoExt Land Ocean NoPol Land Ocean SoPol Land Ocean USA48

$$Tsat13 := READPRN("uahncdc1978\ to\ 9\text{-}2014dat.txt") \qquad Yrsat13 := Tsat13^{\langle 0 \rangle} + \left(Tsat13^{\langle 1 \rangle} - 1\right) \cdot \frac{1}{12}$$

Ice Ages and Interglacials - Page 219
SOI Data: http://www.cpc.ncep.noaa.gov/data/indices/soi

Southern Oscillation Index (SOI): A standardized index based on the observed sea level pressure differences between Tahiti and Darwin.

Satellite Global Temp Anomaly and Southern Oscillation Index (SOI)

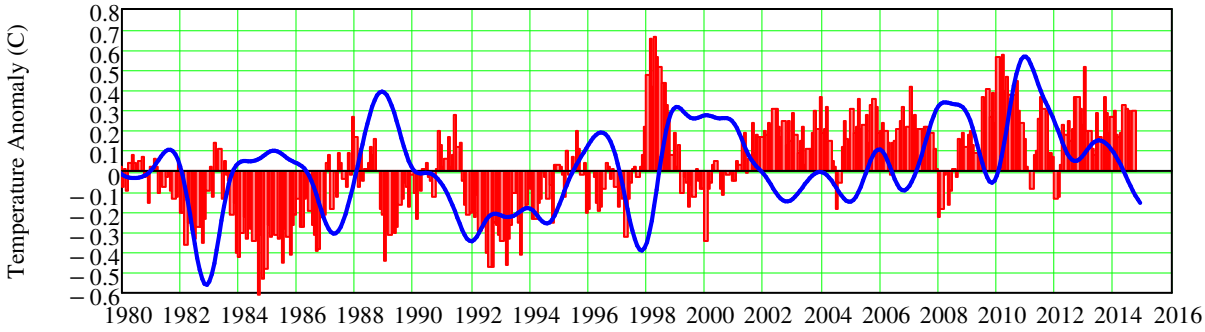

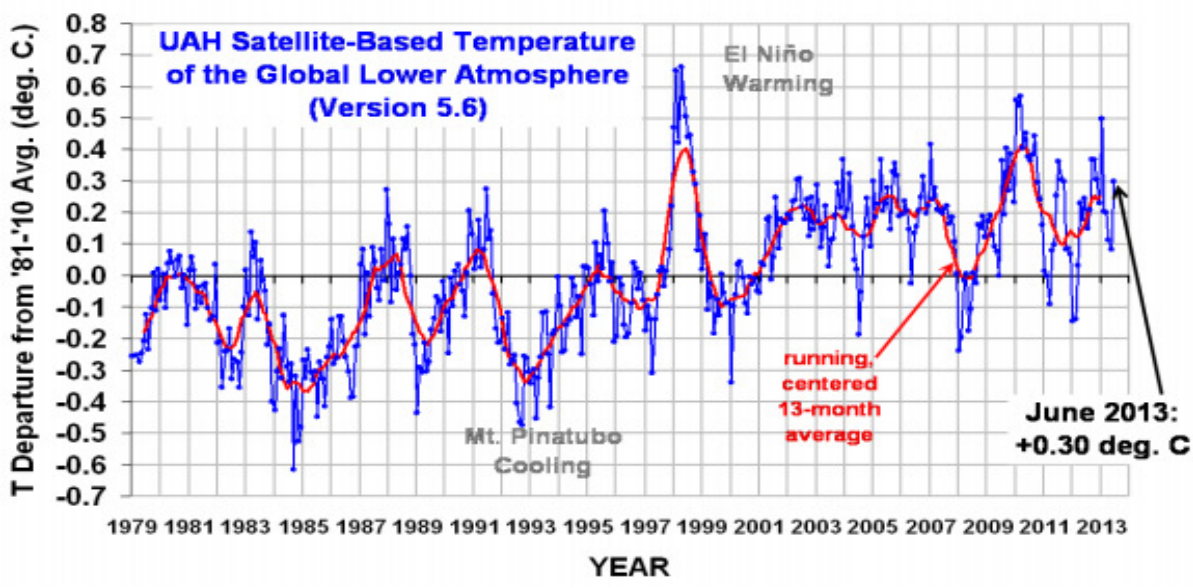

8. Greater Temperature Asymmetry of Northern versus Southern Hemisphere Since 2000

Interhemispheric Temperature Asymmetry over the Twentieth Century and in Future Projections - Andrew R. Friedman
Journal of Climate, Feb 2013

Northern Hemisphere has more land and less ocean than the Southern Hemisphere, and oceans warm relatively slowly. Prior to 1980, the long-term trend that would have been there from increased greenhouse gases during the 20th century was essentially cancelled out by man-made stratospheric sulphate aerosol emissions, which mostly cooled the Northern Hemisphere, the study found. Anthropogenic aerosols are believed to have masked GHGs over the middle of the twentieth century.

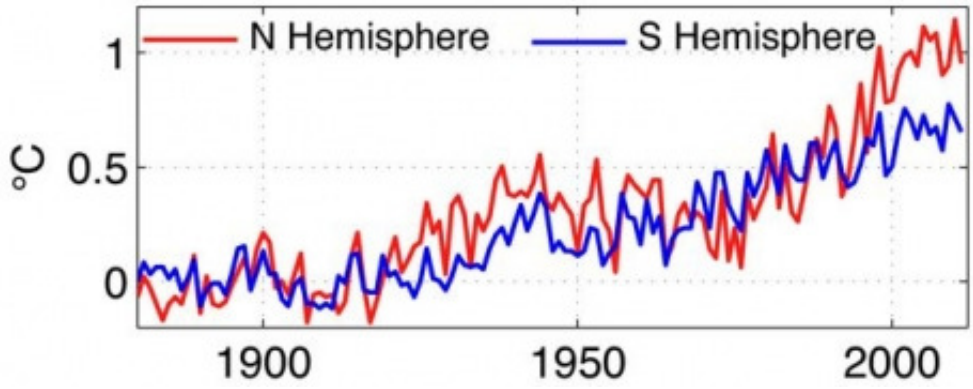

9. Heat Content of Oceans -Indisputable evidence of global warming, but ~ΔTavg= 0.025K

Levitus et al., Geophysical Research Letters 36 (2009): L07608.

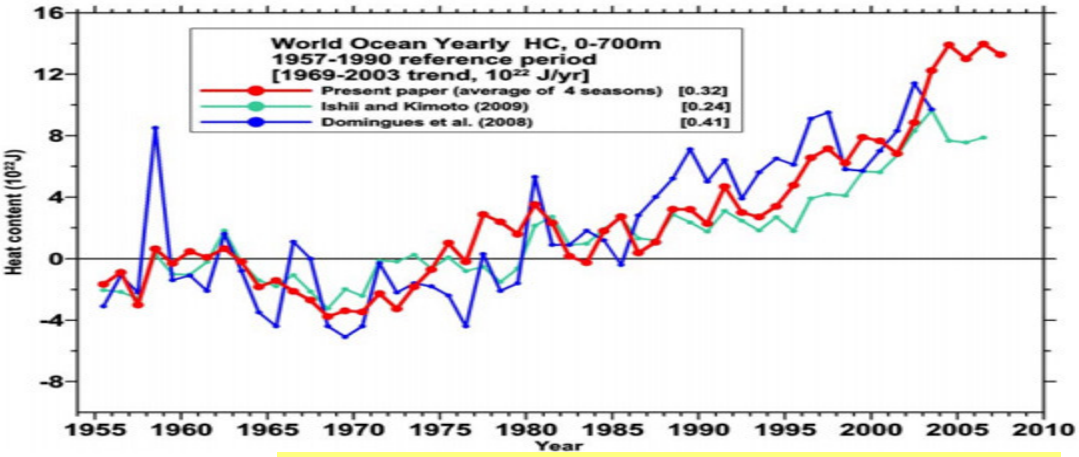

Mass_Ocean := $1.4 \cdot 10^{21}$kg $\quad \Delta T_{avg} := 14 \cdot 10^{22}\text{J} \cdot \left[\left[\text{Mass\_Ocean}\, 4000\text{J} \cdot (\text{kg} \cdot \text{K})^{-1}\right]^{-1}\right] = 0.025\,\text{K}$

10. IPCC Report "Climate Change 2007: "Synthesis Report - Summary for Policymakers.

Comparison of observed continental- and global-scale changes in surface temperature with results simulated by climate models using **either natural or both natural and anthropogenic forcings**. Decadal averages.

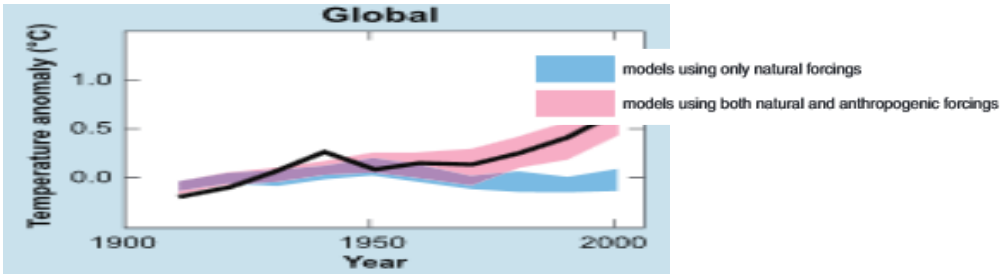

11. Analysis: Climate Change Stats - Mean Temp Rise is Non Monotonic - 70 Year Cycles

Reference: "ABRUPT GLOBAL TEMPERATURE CHANGE AND THE INSTRUMENTAL RECORD," Menne

Use GISS Global Temp Data: "GISS NASA Global Temp Mean Fig2A.TXT" from Above

Break into Four 35 Year Periods: 1880 to 1910, 1911 to 1945, 1946 to 1980 and 1981 to 2010

Use Analysis from: **http://www.leapcad.com/Climate_Analysis/Cycles_and_Trends_Average_Temp.xmcd**

GTemp2010 := READPRN("GISS NASA Global Temp Mean Fig2A.TXT") T_{abrupt} := READPRN("GAbrupt.txt")

Note: Temperature Plateaus and then Climbs in 70 (60) Year Cycles

"The solar system oscillates with a 60-year cycle due to the Jupiter/Saturn three-synodic cycle and to a Jupiter/Saturn beat tidal cycle" 9.1 year moon orbital cylce. See Scafetta "Empirical evidence for a celestial origin of .."

9. Analysis: Abrupt NOAA Global Annual Mean Temperature in 70 Year Cycles

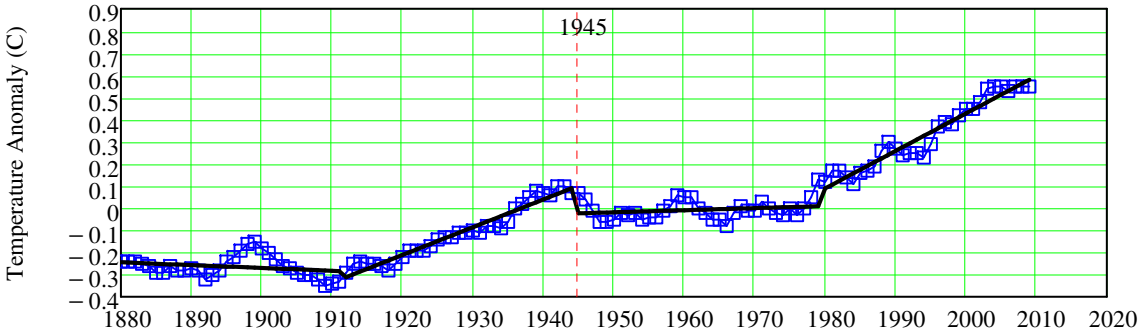

Correlation Coefficient: $\text{corr}\left(\text{GTemp2010}^{\langle 2 \rangle} \cdot 0.01, T_{abrupt}\right) = 0.98589 \quad \text{Stdev}\left(T_{abrupt}\right) = 0.23426$

t Test: $t := \dfrac{0.98622}{0.23434} = 4.2085$ These 70 year cycles are statistically significant

12. How The Pause Was Made To Disappear:

https://notalotofpeopleknowthat.wordpress.com/2016/03/09/how-the-pause-was-made-to-disappear/

"Corrections" were made to NOAA and RSS data that lowered early and raised more recent temperatures data.
As a result of these corrections to the data, the recent temperature pause was made to disappear.
Not all experts agree concerning the illegitimacy of the criteria that was used to make these adjustments.

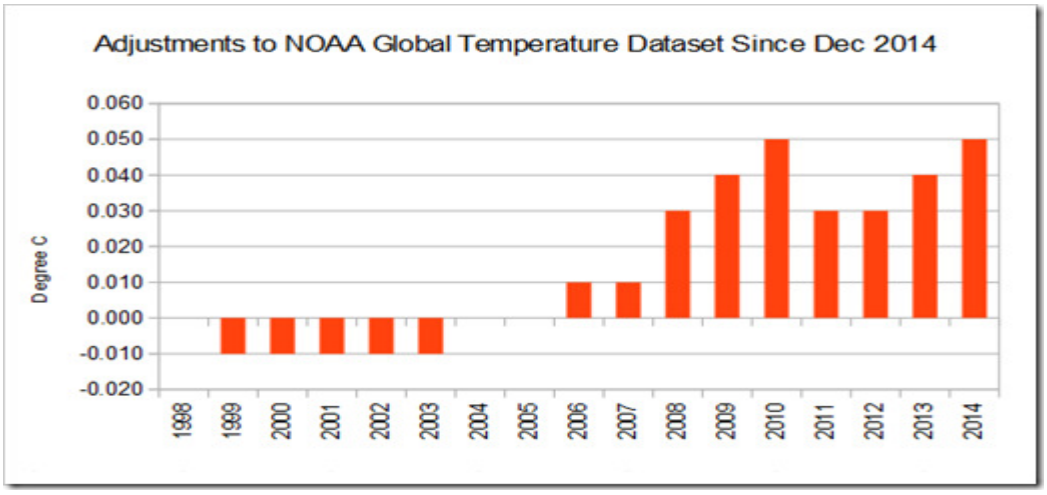

RSS Mid Troposphere temperatures, TMT, Satellite Data

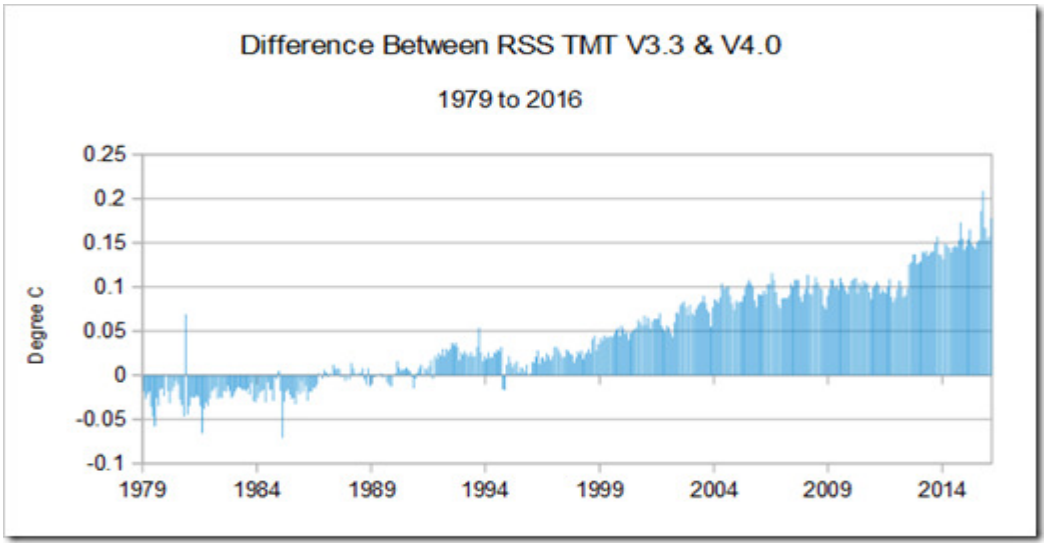

The effect of the change since 1998 in particular is startling. An essentially flat trend has been replaced by 0.74C/C.

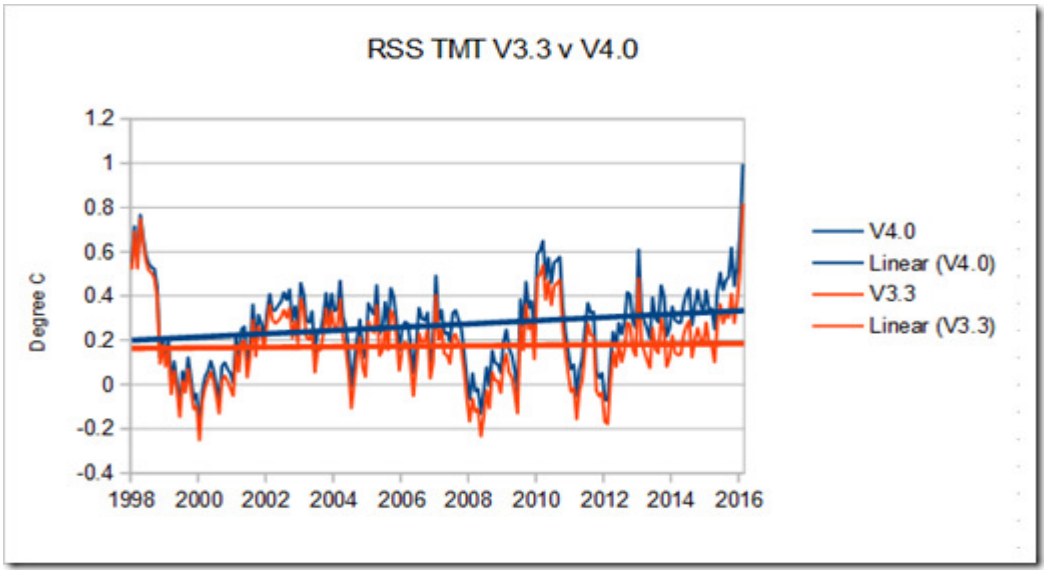

SECTION III-A. CO_2 Concentration Changes

1. Global Temperature and Atmospheric CO_2 over Geologic Time

Paleozoic, Mesozoic, Cenozoic: 600 to 0 Million Years BPA
Temperature: http://www.scotese.com/climate.htm
"GEOCARB III: A REVISED MODEL OF ATMOSPHERIC CO2 OVER PHANEROZOIC TIME", R.A. Berner, 2001
See also: **http://www.geocraft.com/WVFossils/CO_2_Temp_O2.html**

Late Carboniferous to Early Permian time (315 mya -- 270 mya) is the only time period in the last 600 million (Quaternary Period).

PaleoTemp := READPRN("Temp-Comparing CO2 -Temp over Geologic Time.txt")
RCO2 := READPRN("Effect of GCM Model Params - GEOCARB II.txt")
RCO2 = mass of atmos. CO2(t)/mass of CO2(0) ppm = 300 ppm x RCO2 $PaleoCO2 := RCO2^{\langle 1 \rangle} \cdot 300 \cdot \frac{4}{3}$

1. Comparing CO2 (Red) and Temperature (Blue) Over Geologic Time

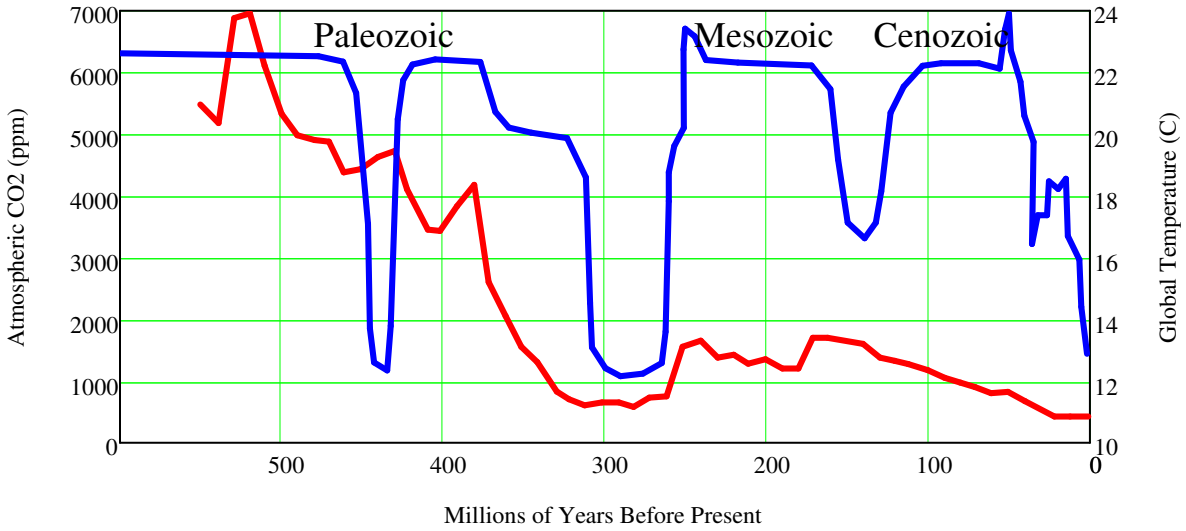

CO_2 Concentration Monthly Plot

2. The Keeling Curve: Mauna Loa Observation Hawaii Monthly CO2 Concentration Data

The carbon dioxide data, measured as the mole fraction in dry air, on Mauna Loa constitute the longest record of direct measurements of CO2 in the atmosphere. This data is the gold standard in climate research. They were started by C. David Keeling of the Scripps Institution of Oceanography in March of 1958 at a facility of the National Oceanic and Atmospheric Administration (Keeling, 1979). NOAA started its own CO2 measurements in May of 1974. The moving average is for seven adjacent seasonal cycles centered on the month to be corrected, except for the first and last three and one-half years of the record, where the seasonal cycle has been averaged over the first and last seven years, respectively. The estimated uncertainty in the Mauna Loa annual mean growth rate is 0.11 ppm/yr. This estimate is based on the standard deviation of the differences between monthly mean values.

Keeling had perfected the measurement techniques and observed strong diurnal behavior with steady values of about 310 ppm in the afternoon at three locations (Big Sur near Monterey, the rain forests of Olympic Peninsula and high mountain forests in Arizona). By measuring the ratio of two isotopes of carbon, Keeling attributed the diurnal change to respiration from local plants and soils, with afternoon values representative of the "free atmosphere". By 1960, Keeling and his group established the measurement record that was long enough to see not just the diurnal and seasonal variations, but also a year-on-year increase that roughly matched the amount of fossil fuels burned per year.

The Keeling Curve also shows a cyclic variation of about 5 ppmv in each year corresponding to the seasonal change in uptake of CO2 by the world's land vegetation. Most of this vegetation is in the Northern hemisphere, since this is where most of the land is located. The level **decreases from northern spring** (May) onwards as new plant growth takes carbon dioxide out of the atmosphere through photosynthesis and rises again in the northern fall as plants and leaves die off and decay to release the gas back into the atmosphere.
Read data from http://www.esrl.noaa.gov/gmd/ccgg/trends/co2_data_mlo.

Year Month decimal average interpolated trend #days
date ppm ppm (season corr)

MLCO2 := READPRN("NOA_Mauna_Loa_Monthly_CO2_14.txt")

Date := $MLCO2^{\langle 2 \rangle}$ $CO2_{ML} := MLCO2^{\langle 4 \rangle}$ TrendCO2 := $MLCO2^{\langle 5 \rangle}$ RD := rows(Date)

Get CO2 Trend Line from 1990 to 2010

$Date_{1990}$:= submatrix(Date, 383, RD − 1, 0 L_{co2} := line$\left(Date_{1990}, \text{submatrix}(TrendCO2, 383, RD - 1, 0, 0)\right.$

$$Trend_{co2}(Year) := L_{co2_0} + L_{co2_1} \cdot Year$$

$$Keeling(yr) := 1.054 \cdot 10^{-2}(yr - 1960)^2 + 9 \cdot 10^{-1} \cdot (yr - 1960) + 315.5$$

Mauna Loa CO2 Seasonal ppm vs. Time

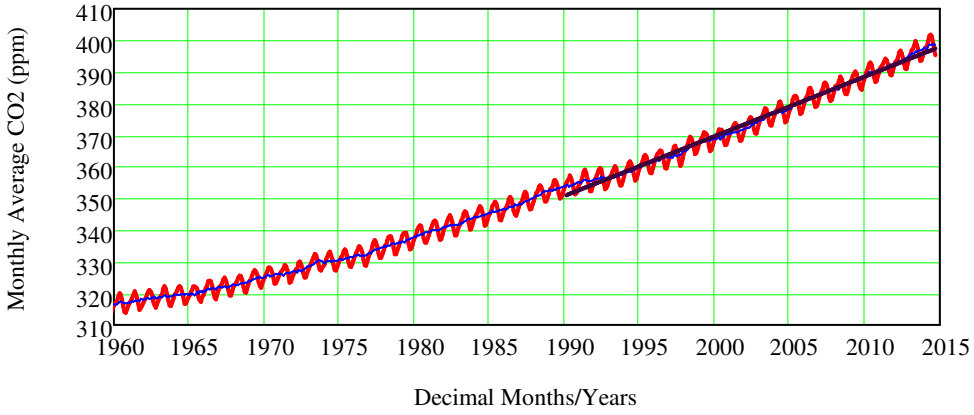

2b. Mauna Loa CO2: Seasonal ppm +- 3 ppm Seasonal Swing about Trend Line

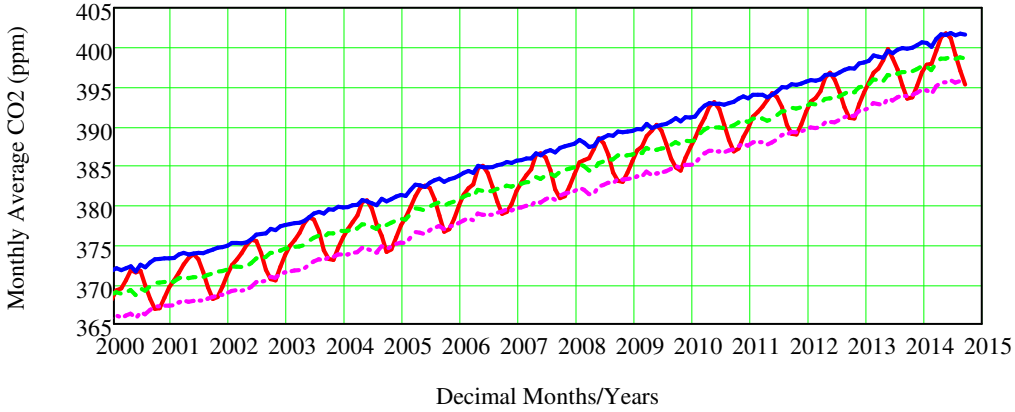

3. Neftel Siple Ice Station - 1847 to 1953

http://cdiac.ornl.gov/ftp/trends/co2/siple2.013

Avg depth (m) Gas age (yr AD) concentration (ppmv)

Increase per year (%)

$$\frac{(390 - 372) \cdot 100}{10 \cdot 372} = 0.48387$$

SipleCO2 := READPRN("Friedli Siple CO2 1986.TXT' IceCO2 := READPRN("CO2 Ice Core Data.txt")

http://www.wasserplanet.becsoft.de/180CO2/CO2tot1812-2007.txt

Column C: CO2 total 1812-1961 corrected. annual averages from raw data.

BeckCO2 := READPRN("Beck CO2 Corrected.TXT")

BeckSmth := ksmooth$\left(BeckCO2^{\langle 0 \rangle}, BeckCO2^{\langle 1 \rangle}, 10\right)$

See: "CO2: The Greatest Scientific Scandal of our Time", Zbigniew Jaworowski
This applies to all the CO2 Ice Core data shown in this worksheet

Jaworowski's worked on ice cores. He has suggested that the long-term CO2 record is an artifact caused by the structural changes of the ice with depth and by postcoring processes.

However, Jaworowski's views are rejected by the scientific community. Increases in CO2 and CH4 concentrations in the Vostok core are similar for the last two glacial-interglacial transitions, even though only the most recent transition is located in the brittle zone.

3. CO2 Yearly ppm: Composite Ice Core & Keeling (Hockey Stick) vs. Beck (Black)

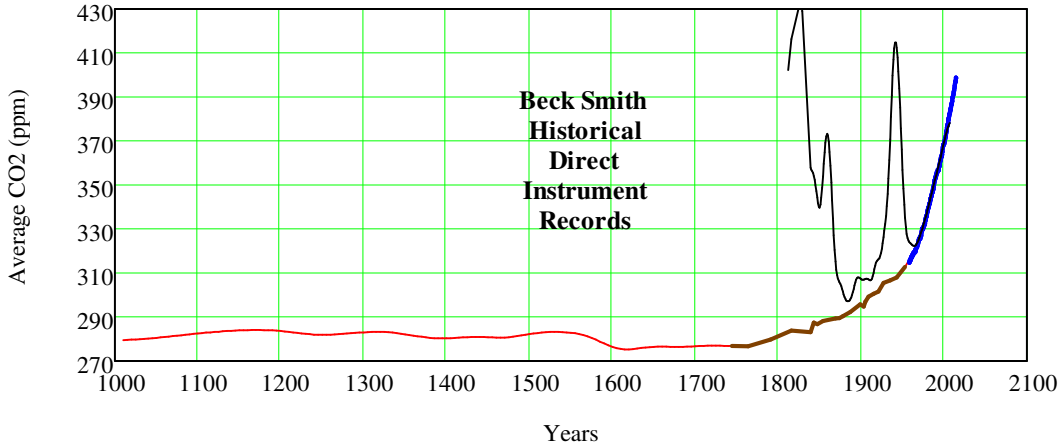

E.G. Beck "180 years accurate CO_2 analysis in air by chemical methods", In press Energy&Environment
After a more thorough review of the old literature, E.G.Beck concluded that there were indications that **current CO_2 concentrations were considerably exceeded in the 1820s** and again in the 1940s

Beck CO2 Yearly ppm

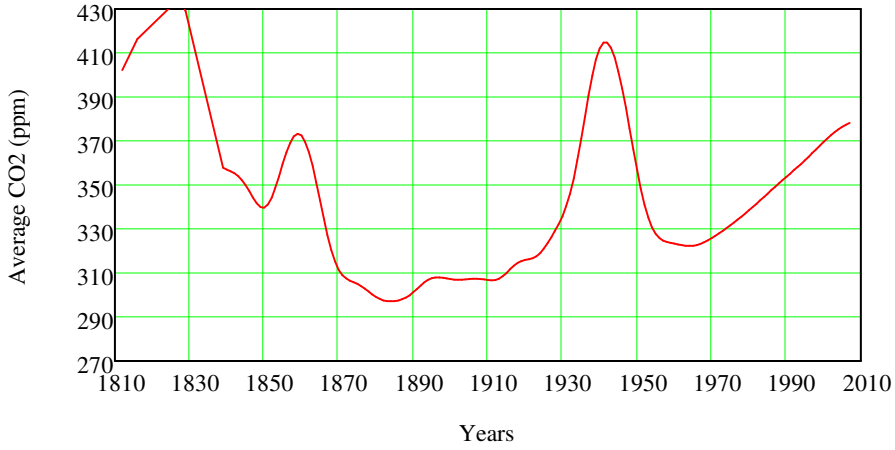

www.soest.hawaii.edu/GG/FACULTY/POPP/Lecture15.ppt
Measurements of CO_2 concentration - Core from rapidly accumulating ice
Merge well with instrumental data1763 - major improvements to the steam engine by the

Scottish engineer James Watt
1769 – first self-powered road vehicle, built by French inventor Nicholas Cugnot
1780 - formulation of the Law of Combustion by the French scientist Antoine Lavoisier
1790 - invention of the electrical battery by the Italian scientist Luigi Galvani
1807 - development of commercial steamboats by the American inventor Robert Fulton
1816 – first U.S. energy utility company and natural gas is used to light streets of Baltimore
1851 - height of the New England whaling industry
1886 – German mechanical engineer Karl Benz first patent for gasoline-powered ICE car
1903 – first sustained powered air flight, at Kill Devil Hills, North Carolina

4. Vostok Ice Core CO_2 Data: Barnola et al, Nature, 329, 408-414 (1987)

Depth (m), Ice Age(yrs), Gaz age (Yrs), CO2 (ppmv), minimum, maximum

BarnolaCO2 := READPRN("Barnola Vostok CO2 1987.TXT") IceAgeCO2Level := 205

Vostok cores show that CO_2 concentrations are at the highest level in 160,000 years.

4. Barnola Vostok and Trend CO2 Concentration Data - 160,000 Yrs.

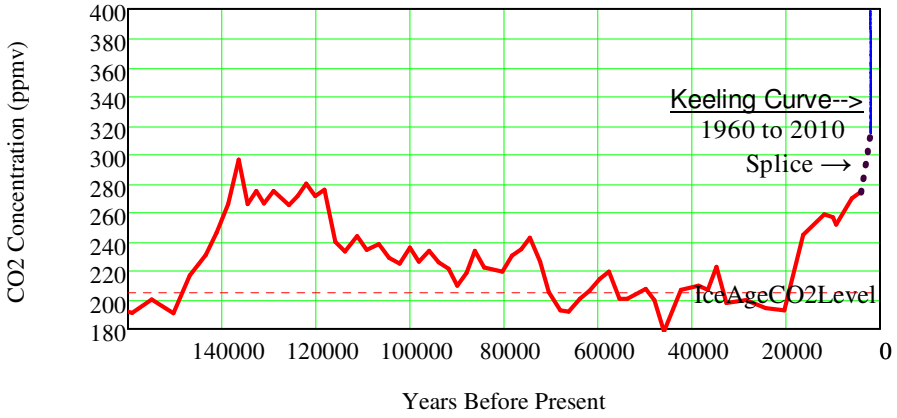

5. An imperative for climate change planning: tracking Earth's global energy

Kevin E Trenberth

http://www.cgd.ucar.edu/cas/Trenberth/trenberth.papers/EnergyDiagnostics09final2.pdf

Plot data from above article for Fig 1

http://www.cru.uea.ac.uk/cru/data/temperature/CRUTEM4-gl.dat Column 13 has yearly Temp data to 5-2015.

http://www.cru.uea.ac.uk/cru/data/temperature/HadCRUT4-gl.dat Monthly Temp Data 1850 to **Feb 2013**

http://www.cru.uea.ac.uk/cru/data/temperature/CRUTEM4-gl.dat Monthly Temp Data 1850 to Oct 2014

Note: For this plot, years 1980 - 2014 show a solid plus warming.

Global Temp (Bars) & CO2 Levels (Black Line) vs. Time

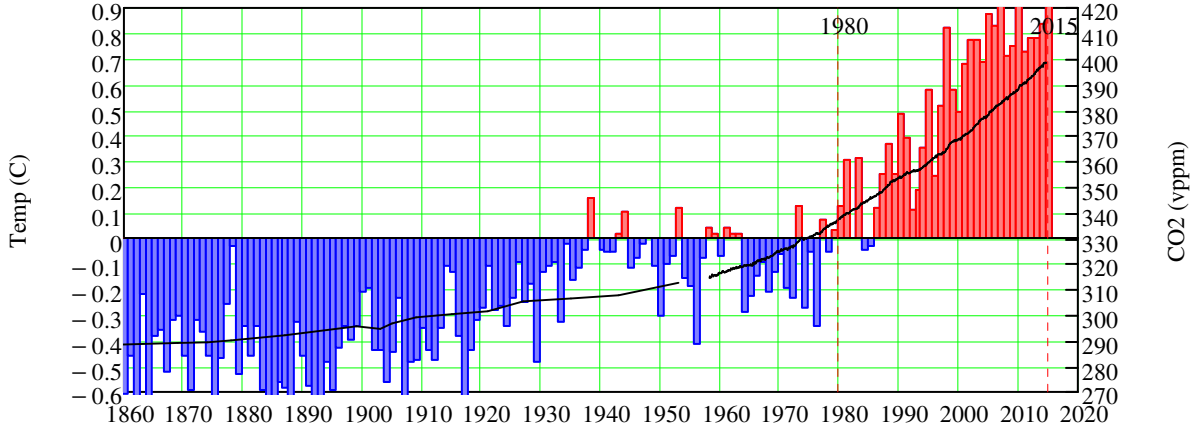

Does Temp track CO2? Fails Decadal Examination.

Note: Decadal forecasts are a known of weakness of generic numeric general circulation models.

Global Satellite Temperature Does NOT TRACK CO_2 During the Last 18 Years

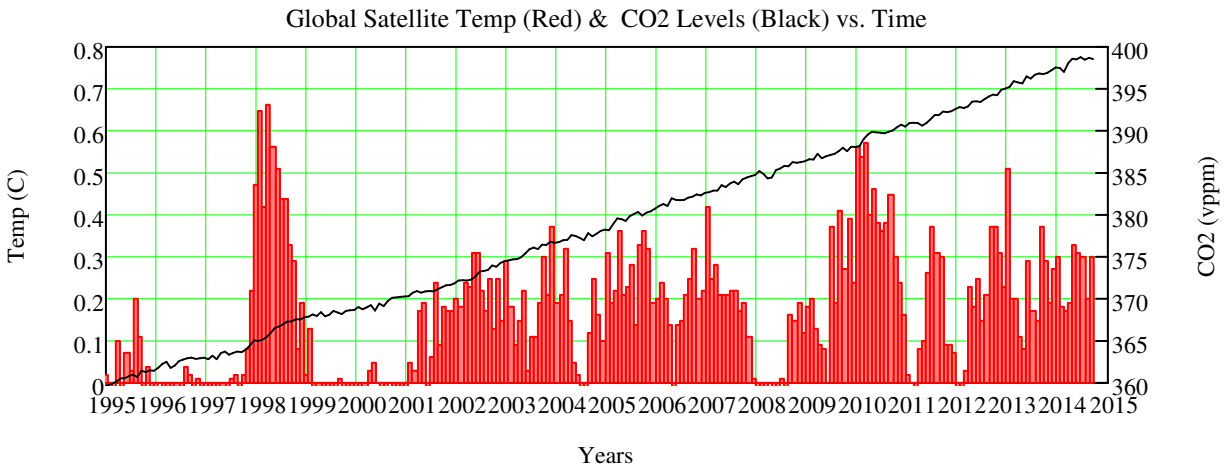

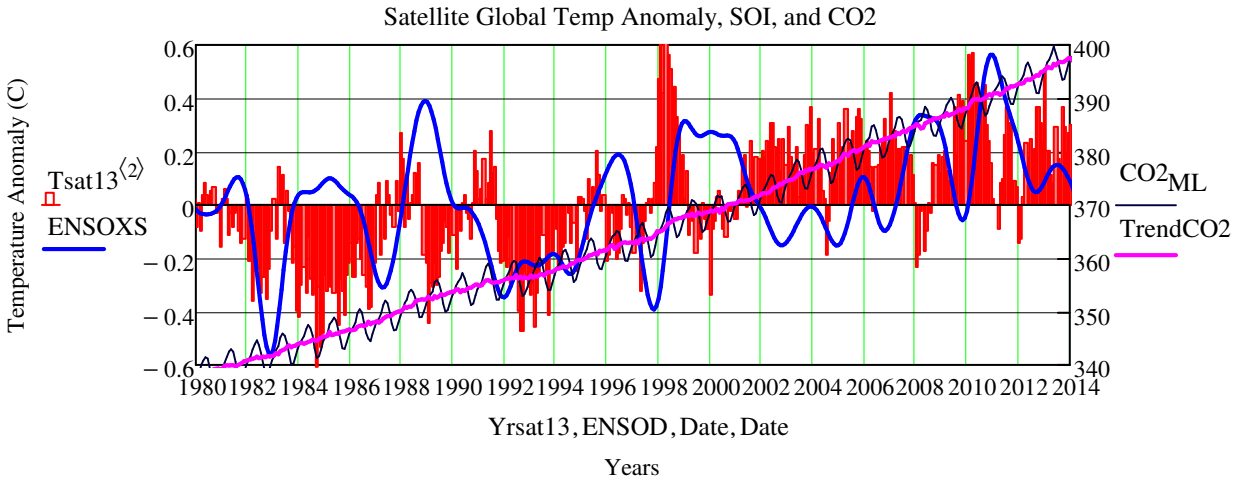

Use Ice Core and NOA _Mauna_Loa_Trend_CO2.txt versus hadcrut3glx.txt in file Correlation_Yr_CO2_Temp.TXT.

CorrCO2Temp := READPRN("Correlation_Yr_CO2_Temp.TXT")

RSquare := $\text{corr}\left(\text{CorrCO2Temp}^{\langle 1\rangle}, \text{CorrCO2Temp}^{\langle 2\rangle}\right)^2$ RSquare = 0.80882

s := $\text{slope}\left(\text{CorrCO2Temp}^{\langle 1\rangle}, \text{CorrCO2Temp}^{\langle 2\rangle}\right)$ = 0.00847

int := $\text{intercept}\left(\text{CorrCO2Temp}^{\langle 1\rangle}, \text{CorrCO2Temp}^{\langle 2\rangle}\right)$ = −2.82393 δT := int + s·$\text{CorrCO2Temp}^{\langle 1\rangle}$

Correlation (1854 to 2009) between CO_2 and Temperature Anomaly

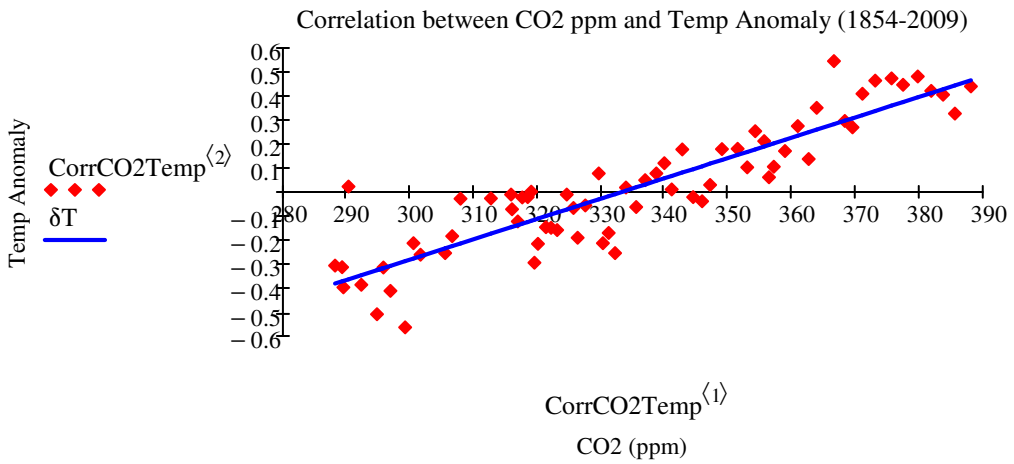

Covariation Between CO2 and δD

If the δD change reflects a proportional T drop, then more than ½ of the interglacial-to-glacial change occurred before significant removal of atmospheric CO2

Values shown normalized to their mean values during the mid-Holocene (5–7 kya BP) and the last glacial (18–60 kya BP) Clearly visible are the disproportionately low deuterium values during the mid-glacial (60–80 Kya BP), the glacial inception (95–125 KyaBP), and the penultimate glacial maximum (140–150 Kya BP)
Covariation of carbon dioxide and temperature from the Vostok ice core after deuterium-excess correction" Kurt M. Cuffey & Françoise Vimeux

SECTION III-B. CO_2 Production Projections, Scenarios, and Fossil Fuel Projections

ATMOSPHERIC CARBON DIOXIDE

The concentration of CO_2 in Earth's atmosphere has increased during the past century, as shown in Figure below. The magnitude of this atmospheric increase is currently about 4 giga tons (Gt C) of carbon per year. Total human **industrial CO_2 production**, primarily from use of coal, oil, and natural gas and the production of cement, is currently about **8 Gt C per year** (7,56,57). Humans also exhale about 0.6 Gt C per year, which has been sequestered by plants from atmospheric CO_2. Office air concentrations often exceed 1,000 ppm CO_2. To put these figures in perspective, it is estimated that the **atmosphere contains 780 Gt C**; the surface ocean contains 1,000 Gt C; vegetation, soils, and detritus contain 2,000 Gt C; and the intermediate and deep oceans contain 38,000 Gt C, as CO_2 or CO_2 hydration products. Each year, the surface ocean and atmosphere exchange an estimated 90 Gt C; vegetation and the atmosphere, 100 Gt C; marine biota and the surface ocean, 50 Gt C; and the surface ocean and the intermediate and deep oceans, 40 Gt C (56,57). So great are the magnitudes of these reservoirs, the rates of exchange between them, and the uncertainties of these estimated numbers that the sources of the recent rise in atmospheric CO_2 have not been determined with certainty (58,59). Atmospheric concentrations of CO_2 are reported to have varied widely over geo logical time, with peaks, according to some estimates, some 20-fold higher than at present and lows at approximately 200 ppm (60-62).

% Industrial Production per Atmosphere

$$\frac{8 \cdot 100}{780} = 1.02564$$

The Climate Catastrophe - A Spectroscopic Artifact

Is the airborne fraction of anthropogenic CO2 emissions increasing?

http://www.skepticalscience.com/Is-the-airborne-fraction-of-anthropogenic-CO2-emissions-increasing.html

Knorr finds that since 1850, the airborne fraction has remained relatively constant. When CO2 emissions were low, the amount of CO2 absorbed by natural carbon sinks was correspondingly low. As human CO2 sharply increased emissions in the 20th Century, the **amount absorbed by nature correspondingly increased**. The airborne fraction remained level at around 43%. The trend since 1850 is found to be 0.7 ± 1.4% per decade.

There are several differences in methodology between Knorr 2009and Le Quere 2009. Knorr's result does not include the filtering for ENSO and volcanic activity employed by Le Quéré. However, when filtering Knorr does include this in his analysis, he finds a trend of 1.2 ± 0.9% per decade. This is smaller than Le Quere's result but is statistically significant.

CDIAC - Carbon Dioxide Information Analysis Center - Global Anthropogenic CO2 Emissions

http://cdiac.ornl.gov/trends/emis/meth_reg.html

Year Total Gas Liquids Solids Cement_Production Gas_Flaring Per_Capita

Units of million metric tons of carbon. Per capita emission estimates in metric tons of carbon.

Emiss := READPRN("Global CO2 Emissions from Fossil-Fuel Burning-1751_2006.txt")

1. Calculate Change per Year - Note there are sources other than anthropogenic

GigaTonCarbon: $ppm := 2.1 \cdot 10^9 \cdot ton$

$t := 0 .. rows(IceCO2) - 2$ $\quad IceCO2Inc_t := \left(\frac{IceCO2_{t+1,1} - IceCO2_{t,1}}{IceCO2_{t+1,0} - IceCO2_{t,0}} \right) \cdot 2.1$

$rows(CO2_{ML}) = 679$ $\quad d := 0 .. 50$ $\quad td_d := 9 + d \cdot 12$ $\quad dd := 0 .. 49$ $\quad td_{50} = 609$

$IncCO2ML_{dd} := \left(TrendCO2_{td_{dd+1}} - TrendCO2_{td_{dd}} \right) \cdot 2$ $\quad DateD_{dd} := Date_{td_{dd+1}}$

$EmissWt := Emiss^{\langle 1 \rangle} \cdot \frac{1}{1000}$ $\quad EmissLevel := 0.55 \cdot EmissWt$

$Emiss_{209,0} = 1960$ $\quad Emiss_{255,0} = 2006$ $\quad \frac{EmissWt_{255} - EmissWt_{209}}{2006 - 1960} = 0.12289$

CDIAC - Carbon Dioxide Information Analysis Center - Global Anthropogenic CO2 Emissions

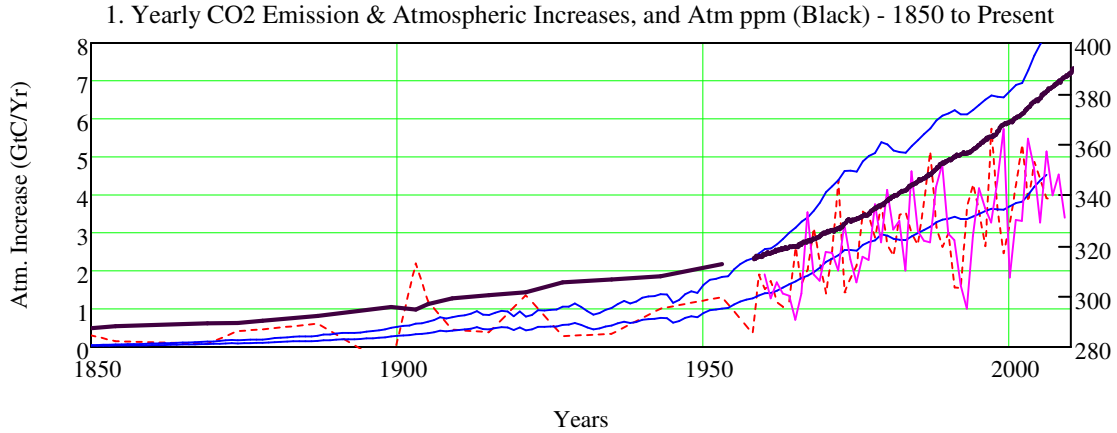

2. Global Atmospheric CO_2 Projections: IPCC Special Report Emission Scenarios (SRES)

http://www.ipcc-data.org/ancilliary/tar-isam.txt https://www.ipcc.ch/pdf/special-reports/spm/sres-en.pdf

Year A1B A1T A1FI A2 B1 B2 A1p A2p B1p B2p IS92 IS92a/SAR

ProjCO2 := READPRN("CO2 AR4 Emission Proj-Data.txt")

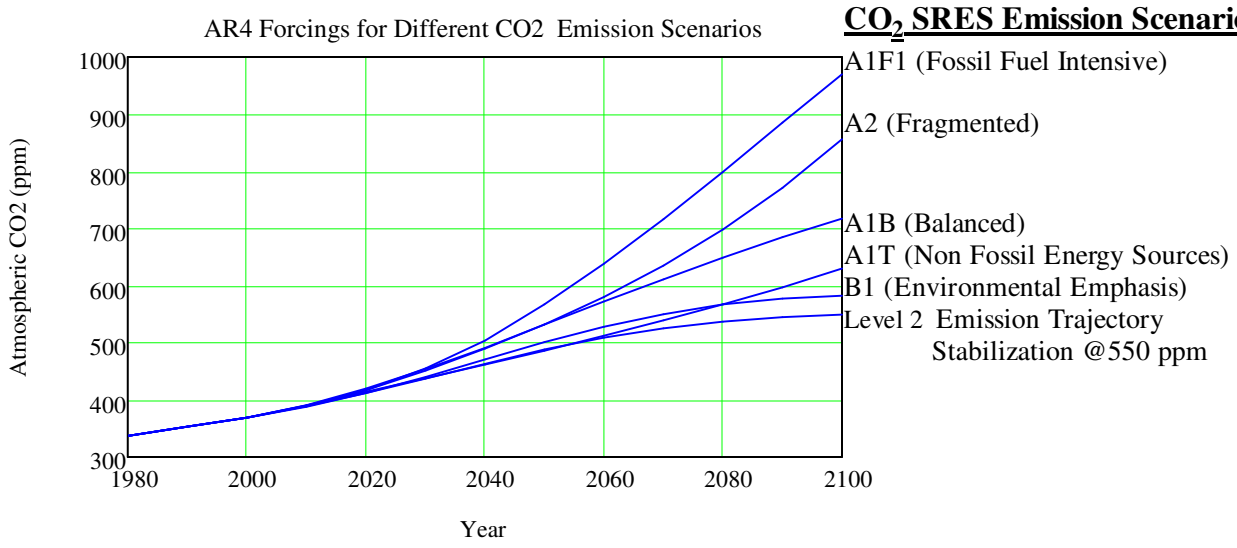

3. World Energy Production Projection

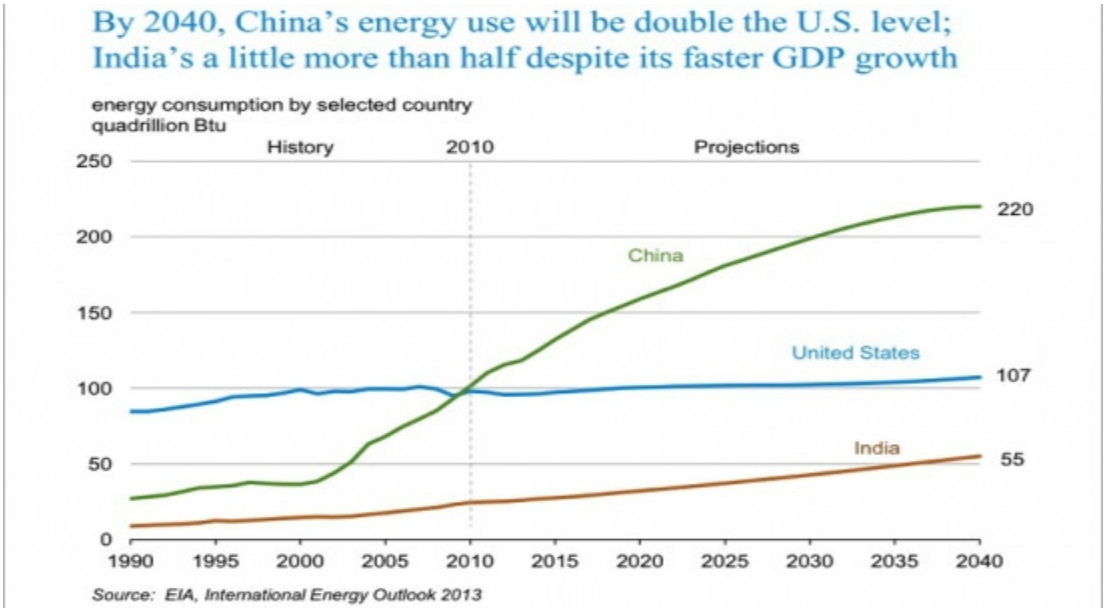

SECTION III-C. Fossil Fuel Energy Sources - CO_2 Emission Sources

1. Main Areas of Human Energy Consumption in the US

http://www.epa.gov/climatechange/ghgemissions/gases/co2.html

Electricity 38%, Transportation 32%, Industry 14%, Residential 9% and NonFossil Fuel 6%
Electricity is not a primary energy source. It is one of the most common energy carriers. generate 3 to 4 times more torque per unit energy input than all but the largest and most efficient house-sized diesel ship engines (50 percent efficient).

2. Human Contribution Relative to Other Sources of CO_2

The **burning of fossil fuels** sends **7 gigatons** (**3.27 %**) of carbon dioxide into the atmosphere each year, while the biosphere and oceans account for 440 (55.28 %) and 330 (41.46 %) gigatons, respectively—total human emissions have jumped sharply since the Industrial Revolution. Carbon is emitted naturally into the atmosphere but that the atmosphere also sends carbon back to the land and oceans and that these carbon flows have **canceled each other out** for millennia. Burning fossil fuels, in contrast, creates a new flow of carbon that, though small, is not canceled.

3. Coal Usage and Factors

Source: http://www.nationalreview.com/article/392167/social-justice-coal-robert-bryce
Coal is perfectly suited for electricity production, it's abundant, its reserves are geographically dispersed, prices are not affected by any canceled entities, and — above all — it's cheap. Coal-fired generators provide about 40 percent of all global electricity. Coal is the most carbon intensive fossil fuel.

Coal is the world's **fastest-growing form of energ**y and it has been since 1973. In 2013 alone, coal use grew by about 2 million barrels of oil equivalent per day (boe/d). That was about three times the growth seen in natural gas (which grew by about 700,000 boe/d), four times the rate of growth in wind (up by about 500,000 boe/d), and 13 times the growth in solar (which was up by about 150,000 boe/d).

China has led the rush toward coal and now accounts for fully half of global coal consumption.

Increased use of hydrocarbons results in **better living standards**. Indeed, per capita carbon dioxide emissions (like per capita electricity usage) are a reliable indicator of higher incomes.

4. Oil Production - US Drilling Rigs - December 2014

Why is the world market suddenly awash in oil? The answer: Over the past few years — thanks to rigs, rednecks, and rights — the U.S. has added the equivalent of one Kuwait and one Iran to its domestic oil and gas production.

Since 2004, **U.S. oil production is up 56 percent**, or about 3.1 million barrels a day, about the same volume as Kuwait produced last year. The dimensions of the boom in natural gas can be seen by looking solely at the Marcellus Shale in Pennsylvania, where output has jumped eight-fold since 2010 and is now about 16 billion cubic feet per day, a volume roughly equal to Iran's current natural-gas production.

U.S. oil and gas numbers are soaring because of an abundance of rigs. **More than half of all the drilling rigs on the planet are operating in the United States.** We have about 1,900 active rigs. The rest of the world combined has about 1,300.

IV. Solar Variation: Wolf Number, Sunspots, C14 SS Extrema, Irradiance, Wind

See Section XIIA for Solar Radiation Spectrum and XIIIB for Reflectance.

http://en.wikipedia.org/wiki/Solar_variation

The Sun and Climate **http://pubs.usgs.gov/fs/fs-0095-00/fs-0095-00.pdf**

Many geologic records of climatic and environmental change based on various proxy variables exhibit **distinct cyclicities that have been attributed to extraterrestrial forcing**. ... Another terrestrial observation was that the Maunder Minimum coincided with the coldest part of the Little Ice Age.

http://commons.wikimedia.org/wiki/File:Carbon-14_with_activity_labels.png

http://www.radiocarbon.org/IntCal04%20files/intcal04.14c

Read Carbon 14 Atmospheric Concentration Data

CAL BP, 14C age, Error, Delta 14C, Sigma,
YR BP ,YR BP, per mil , per mil

C14 := READPRN("Atmospheric C14 Concentration.TXT") Yr := $C14^{\langle 0 \rangle}$ + 40

SSSmooth := ksmooth(reverse(Yr), reverse($C14^{\langle 3 \rangle}$), 2000)

Detrend := reverse($C14^{\langle 3 \rangle}$) − SSSmooth

SSCycle := ksmooth(reverse(Yr), Detrend, 1000) Yr_{SS} := 2010 − Yr

Wolf number

The Wolf number (also known as the International sunspot number, relative sunspot number, or Zürich number) is a quantity which measures the number of sunspots and groups of sunspots present on the surface of the sun.

http://en.wikipedia.org/wiki/Wolf_number

The Solar Physics Group at NASA's Marshall Space Flight Center

Royal Greenwich Observatory - USAF/NOAA Sunspot Data

http://solarscience.msfc.nasa.gov/greenwch/spot_num.txt

Sunspot Monthly Averages -2013.txt: Spliced above with RecentIndices.txt data from

http://www.swpc.noaa.gov/ftpdir/weekly/RecentIndices.txt

Read Sunspot Data

YEAR MON SSN DEV

SSpots := READPRN("sunspot_num2015.txt") NumSS := $SSpots^{\langle 2 \rangle}$

YrDec := $-\left(SSpots^{\langle 0 \rangle} + \frac{SSpots^{\langle 1 \rangle} - 1}{12} - 2014\right)$ SSnotYrlv := READPRN("SN_v_tot_V2.0-1690.txt")

SSSmth := ksmooth(−YrDec, NumSS, 11) YrDec := $SSpots^{\langle 0 \rangle} + \frac{SSpots^{\langle 1 \rangle} - 1}{12}$

Solar Influences Data Analysis Center - SIDC

http://www.sidc.be/sunspot-data/ **Updated 10-23-2014**

YrMon, Year_Decimal, Monthly, Monthly Smoothed Sunspot Number, 1749 to 2014

SSN := READPRN("monthssn201409.dat") SSNYr := READPRN("yearssn2013.dat")

SSNYrSmooth := ksmooth($SSNYr^{\langle 0 \rangle}$, $SSNYr^{\langle 1 \rangle}$, 11)

NGDC - Group Sunspot Numbers (Doug Hoyt re-evaluation) 1610-1995

http://www.ngdc.noaa.gov/stp/SOLAR/ftpsunspotnumber.html#hoyt - 4bb. monthrg.dat

SSN_Hoyt := READPRN("Grp SSN-monthrg-1610-1995.dat" SSNS := ksmooth($SSNYr^{\langle 0 \rangle}$, $SSNYr^{\langle 1 \rangle}$, 10)

NGDC-Table of smoothed monthly sunspot numbers 1700-present

Year, SNN-Jan to SNN-Dec

SSNSm_Hoyt := READPRN("SmoothMonthMeanHoyt-1749-2009.txt") R := rows(SSNSm_Hoyt)

r := 0 .. R − 1 $SSH_r := \sum_{m=1}^{12} \left(SSNSm\_Hoyt_{r,m} \cdot \frac{1}{12}\right)$ $Year_H$:= $SSNSm\_Hoyt^{\langle 0 \rangle}$

Smooth Hadcrut over 11 year cycle Sun Spots: TKSmooth := ksmooth($Time_{crut}$, TCrutYr, 11)

1. TCrut Temp, Solar Proxy: Changes C14 Concentration, Number of Yearly Sunspots

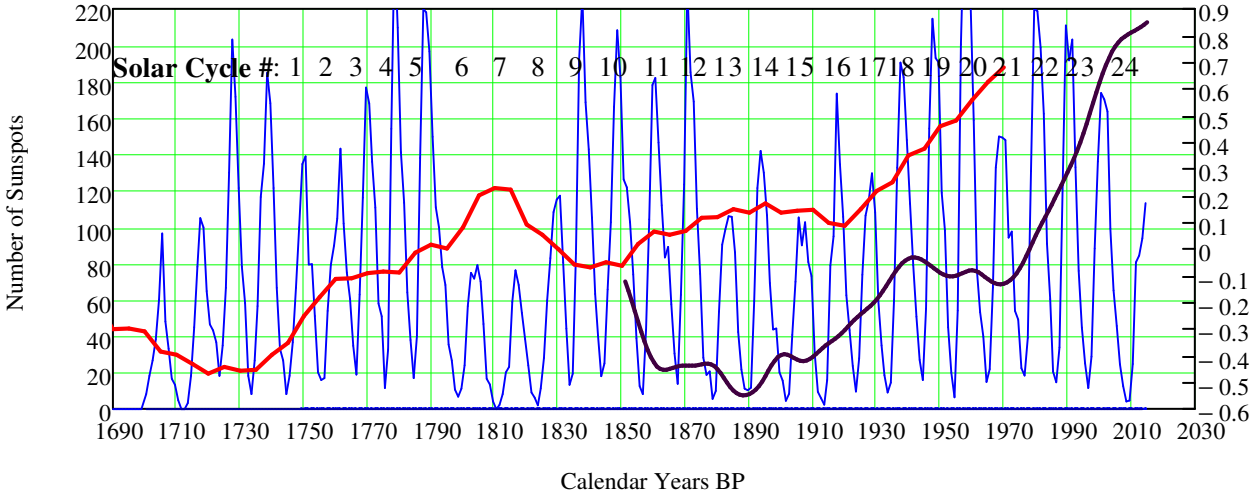

SubsetSSN := submatrix(SSNYr, 210, 313, 0, 1) SSSSNDec := ksmooth(SubsetSSN⟨0⟩, SubsetSSN⟨1⟩, 24)

2. Solar Sun Spot Epochs (910 to 2010) from C14 Concentration - Maunder Minimum

Maunder Minimum: 70 year period from 1645 to 1710 when all solar activity stopped

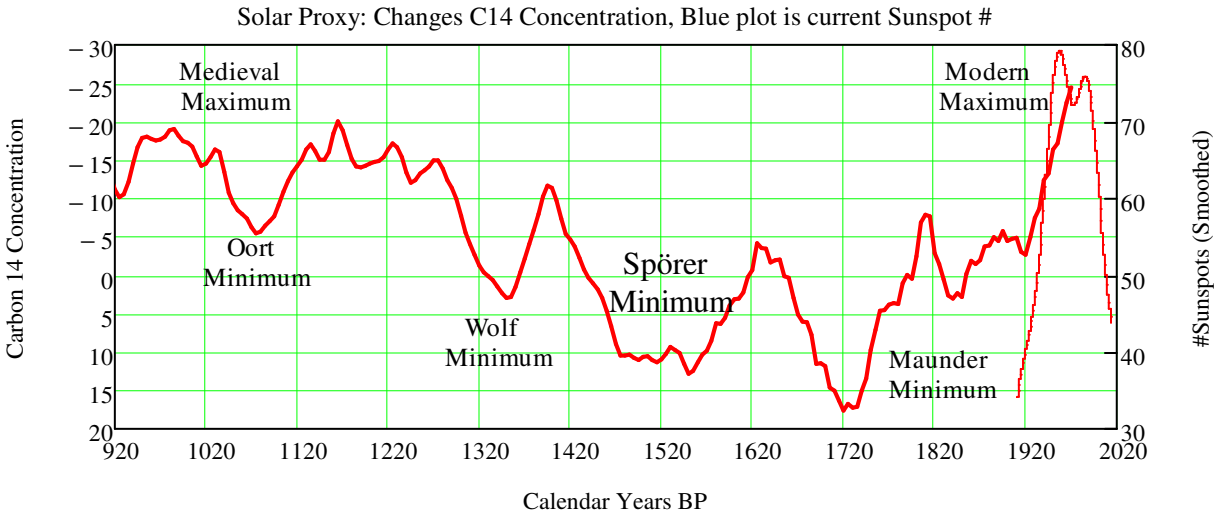

3. Extended C14 Data (Red) Smoothed Data (Dotted Blue)

Detrended Data (Solid Black) Hallstadzeit Cycles (Heavy Magenta Curve)

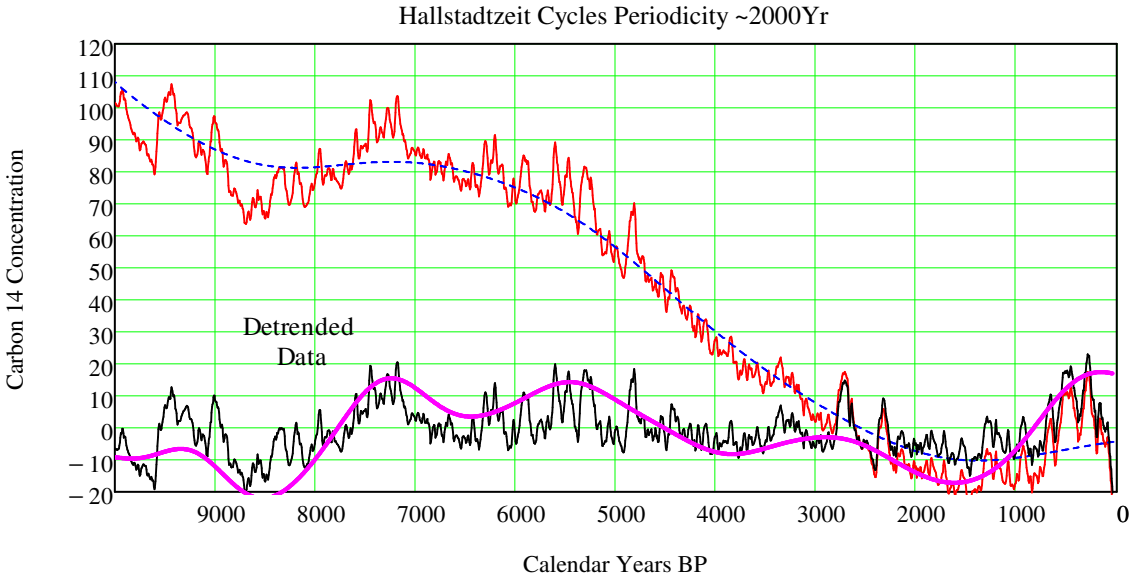

4. PMOD Total Solar Irradiance, TSI, Composite

"The Suns Total Irradiance: Cycles, Trends and Related Climate Change Uncertainties since 1978"
PMOD/WRC, Davos, Switzerland, "Unpublished data from the VIRGO Experiment on the cooperative ESA/NASA Mission SoHO"
ftp://ftp.pmodwrc.ch/pub/data/irradiance/composite
YYMMDD, epoch (1 corresponds to 1-Jan-1980), average irradiance in W/m2

$TSI_{PMOD} := READPRN("TSI.PMODF\_15.TXT")$ $TSI_{PMOD_{410,0}} = 800101$

TAM, Convert Daily to Monthly Average **TSI 2014 is Yearly**

$TSIMA06 := READPRN("TSIMonthAvg-2006Data.txt")$ $TSI_{smm} := READPRN("TSIsm8.txt")$

$TSIMon := DMAvg(TSI_{PMOD})$

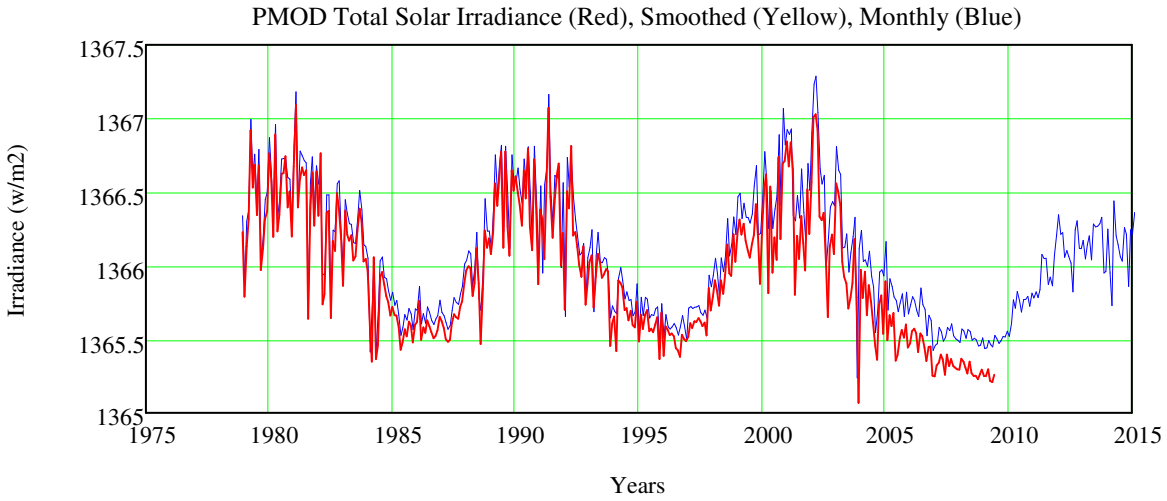

5. Reconstruction of solar irradiance since 1610, Lean 1995 (1600-1995) - Correlates to Temp

Solar Irradiance Correlates with U.S. Temp Anomaly

$HadCrutz := READPRN("hadcrut3vgl.txt")$ $rows(HadCrutz) = 32$ $cols(HadCrutz) = 14$ $nz := 0 .. 159$

$DateTSIL := READPRN("TSIpmodDate.txt")$

$TSDF_{lean} := READPRN("lean1995data.txt")$ $Yr_{lean} := TSDF_{lean}^{\langle 0 \rangle}$ $TSD_{lean} := Fill(TSDF_{lean}^{\langle 1 \rangle})$

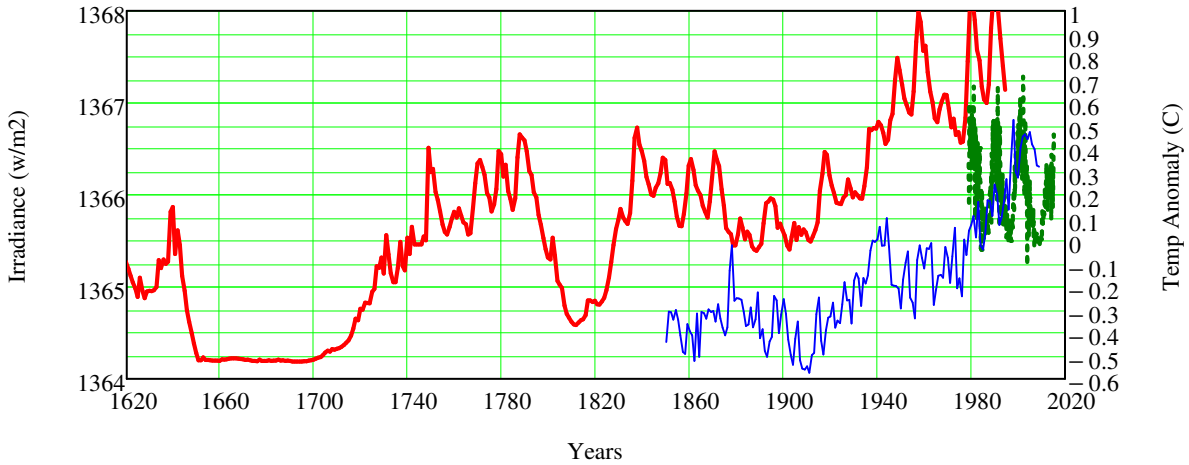

6. NASA OMNI2: Solar Wind Pressure and Decadal Trends

Solar Wind Pressure and Trends

http://omniweb.gsfc.nasa.gov/cgi/nx1.cgi
omni2_27day data from 19630130 to 20091230
Scalar B, nT, Flow pressure
YEAR DOY HR 1 2

SWPF := READPRN("OMNI_Solar_Wind_1963_27Day.dat") SWP := Fillin(SWPF)

Note the downward trend in Solar Wind Pressure since 1993, a flattening, and then renewed fall in 2005 at an equal rate, dropping to 1970 levels. This hints that we will be seeing a period of reduced solar activity - See the next SECTION on Solar Prediction.

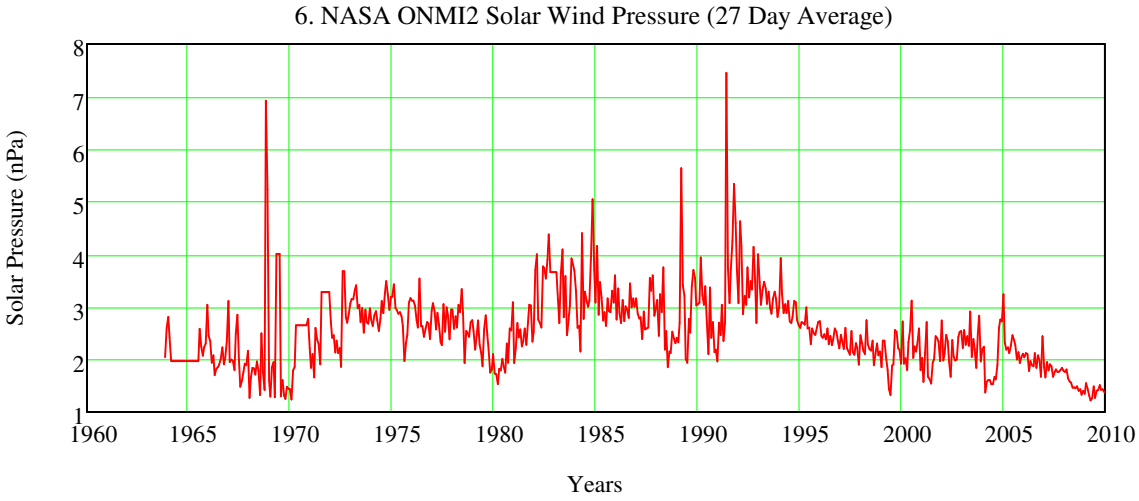

7. NASA: Solar Cycle Sunspot Prediction ==> Global Cooling - Added Cycle 24 Data

http://solarscience.msfc.nasa.gov/predict.shtml Data: HathawayMagSunspot_predict.txt

A historic low period of the Sun's activity is coming.

NASA: Solar Cycle 25 peaking around 2022 could be one of the weakest in centuries.

http://science.nasa.gov/headlines/y2006/10may_longrange.htm

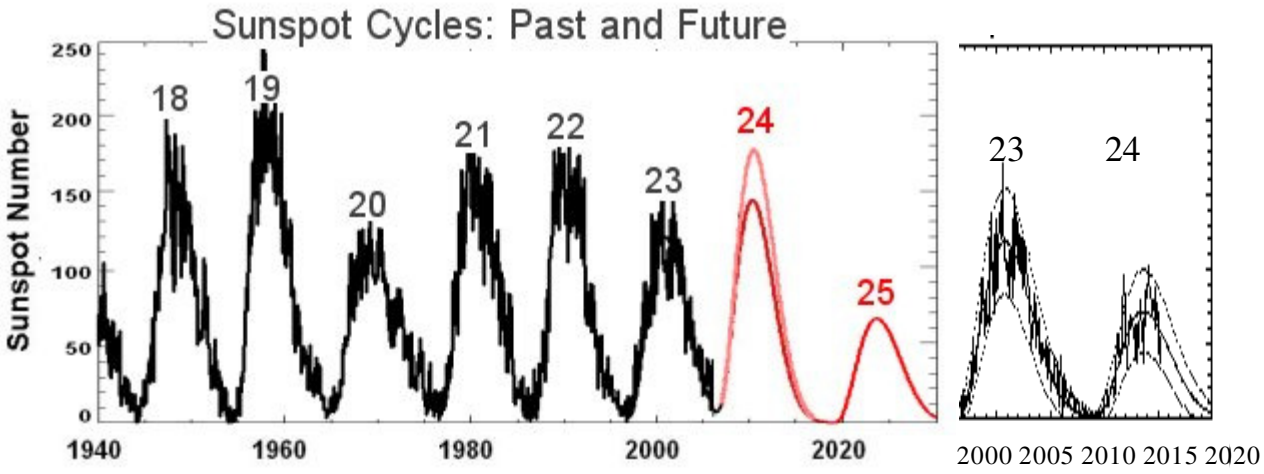

What influence does the sun have on global climate? Solar Energy.

The Sun provides the energy that drives the climate system. **Long-term variations in the intensity of solar energy reaching the Earth are believed to cause climate change on geological time-scales.** New studies indicate that **changes in the Sun''92s magnetic field** may be responsible for shorter-term changes in climate, including much of the climate of the 20th century. Also, at least one indirect effect of solar variability, the effect that changes in the **amount of UV radiation** emitted by the Sun have on the warming effect of the ozone layer, has been established. A second indirect effect, the effect that changes in solar radiation have on **cosmic-ray induced cloudiness**, has been hypothesized, but not proven. This suggested effect is being studied both by observations and in laboratory simulations.

The strength of the Sun''92s magnetic field varies through the 11-year solar cycle. When the **Sun''92s magnetic field is** strong, it reduces the number of **cosmic rays** hitting the Earth. **Laboratory experiments have shown that cosmic rays are one of the factors causing the formation of water droplets and clouds** in the atmosphere. In 1997, two Danish researchers, Svensmark and Friis-Christiansen, showed that from **1983 to 1994, there was a high degree of correlation between total cloud cover and the number of cosmic rays striking the Earth**, which in turn is correlated with the intensity of the Sun''92s magnetic field. **The changes in cloud cover, 3-4 percent, were large enough to explain much of climate change.** Additional observational studies aimed at determining whether there is a correlation between solar intensity and cloudiness are underway, and CERN, the European Organization for Nuclear Research, will be conducting laboratory experiments to determine whether simulated cosmic rays can, in fact, create the conditions for cloud formation.

Svensmark, H. and E. Friis-Christiansen, 1997: Variation of cosmic ray flux and global cloud cover –'96 A missing link in solar-climate relationships. *Journal of Atmospheric, Solar and Terrestrial Physics,* 59: 1225-32.

Svensmark, H. and N. Calder, 2007, *op cit.*

Ibid., Pg. 562.

8. Wilcox Solar Observatory Polar Observations: Correlation Magnetic Field & Sunspots

Solar Mag: http://wso.stanford.edu/Polar.html#latest SunSpot# Data: http://www.sidc.be/silso/datafiles

Year, Month, Day, N, S, Avg, Filtered N, S, Avg

MagF := READPRN("SunNSPolarMagField-XClean.txt") Date := $\left(\text{MagF}^{\langle 0\rangle} + \frac{\text{MagF}^{\langle 1\rangle} - 1}{11} + \frac{\text{MagF}^{\langle 2\rangle}}{365}\right)^{\rightarrow}$

A 20 nhz low pass filtered values eliminate **yearly geometric projection effects on Solar Mag Field Data**

Solar Magnetic Polar (N-Red & S-Blue) Field Strength and Yrly Mean Total Sunspots (Green dotted)

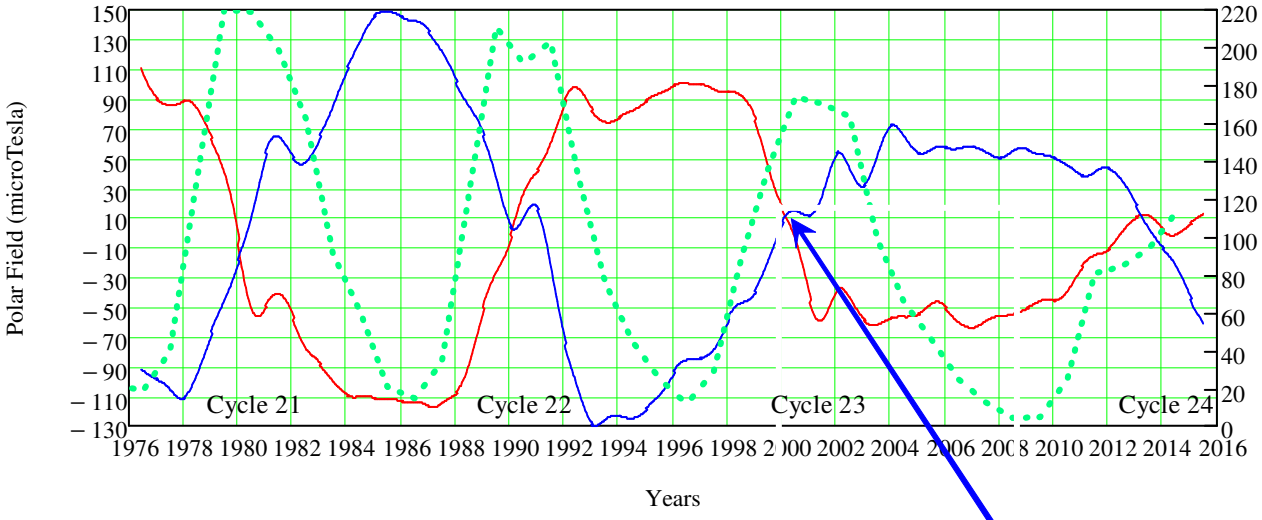

The development of the solar polar Magnetic field strength throughout a solar sunspot cycle can be used to **predict** the magnitude of the next cycle and the peak of the current cycle. Polar field **reversal**s, where the North-Red and South-Blue curves **intersect**, typically occur within a year of **sunspot maximum**.

http://science.nasa.gov/science-news/science-at-nasa/2006/10may_longrange/

2006 Hathaway Model - Single Dynamo

The **Great Conveyor Belt** is a massive circulating current of hot plasma within the Sun. It has **two branches**, north and south, each taking about 40 years to perform one complete circuit. Researchers believe the turning of the belt controls the sunspot cycle, and that's why the slowdown is important.

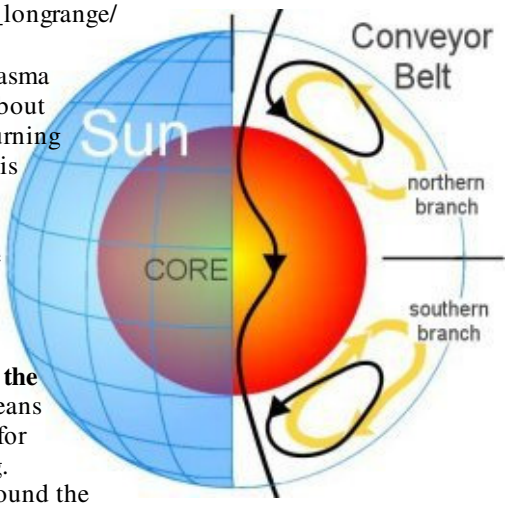

Normally, the conveyor belt moves about **1 meter per second**—walking pace," says Hathaway. "That's how it has been since the late 19th century." In recent years, however, the belt has decelerated to 0.75 m/s in the north and 0.35 m/s in the south. "We've never seen speeds so low.

According to theory and observation, the **speed of the belt foretells the intensity of sunspot activity** ~ 20 years in the future. A slow belt means lower solar activity; a fast belt means stronger activity. The reasons for this are explained in the Science@NASA story Solar Storm Warning.

"The **slowdown** we see now means that **Solar Cycle 25**, peaking around the year **2022**, could be one of the **weakest in centuries**," says Hathaway.

V. Zharkova Model - 2012, 2015 - Principal Component Analysis: Predicts Mini Ice Age during 2030s

Principal Component Analysis of Background and Sunspot Mag Field Variations During Solar 21-23 (2012)

A new model of the Sun's solar cycle is producing **unprecedentedly accurate** predictions of irregularities within the Sun's 11-year heartbeat. The model draws on dynamo effects in two layers of the Sun, one close to the surface and one deep within its convection zone. The model predicts that the **magnetic wave pairs** will become **increasingly offset** during Cycle 25, which peaks in 2022. Thus, the solar activity will **fall by 60 per cent during the 2030s** to conditions last seen during the '**mini ice age**' that began in **1645**.

Zharkova and her colleagues have found that **adding a second dynamo, close to the surface**, completes the picture with surprising accuracy. Found **magnetic wave components appearing in pairs**, originating in **two different layers** in the Sun's interior. They **both** have a frequency of **approximately 11 years**, although this frequency is **slightly different**, and they are **offset in time**. Over the cycle, the waves fluctuate between the northern and southern hemispheres of the Sun. Combining both waves together and comparing to real data for the current solar cycle, we found that our predictions showed an accuracy of 97%. The prediction results indicate that the solar activity is defined mainly by the solar background magnetic fields (SBMF) while the sunspots and their magnetic fields seem to be derivatives of the SBMF variations.

SECTION V. Solar Radiation Spectrum

1. Top of Atmosphere and 2. Sea Level

Note: Relative Importance of Water Vapor versus CO_2 absorption. Greenhouse gases—including **most diatomic** gases with two different atoms (such as carbon monoxide, CO) and all gases with three or more atoms—are able to absorb and emit infrared radiation. Though more than 99% of the dry atmosphere is IR transparent (because the main constituents—**N2, O2, and Ar—are not able to directly absorb** or emit infrared radiation), intermolecular collisions cause the energy absorbed and emitted by the greenhouse gases to be shared with the other, non-IR-active, gases.

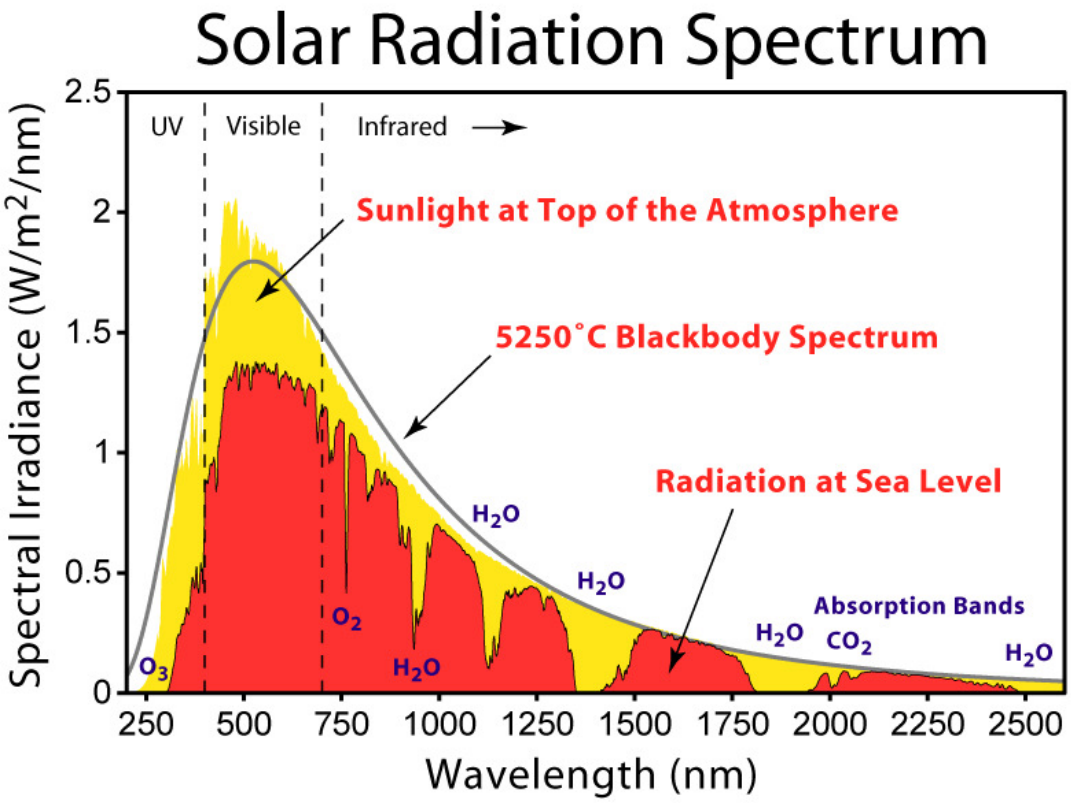

http://climatemodels.uchicago.edu/modtran/modtran.doc.html

2. Comparison of MODTRAN Model to Nimbus 3 IRIS instrument

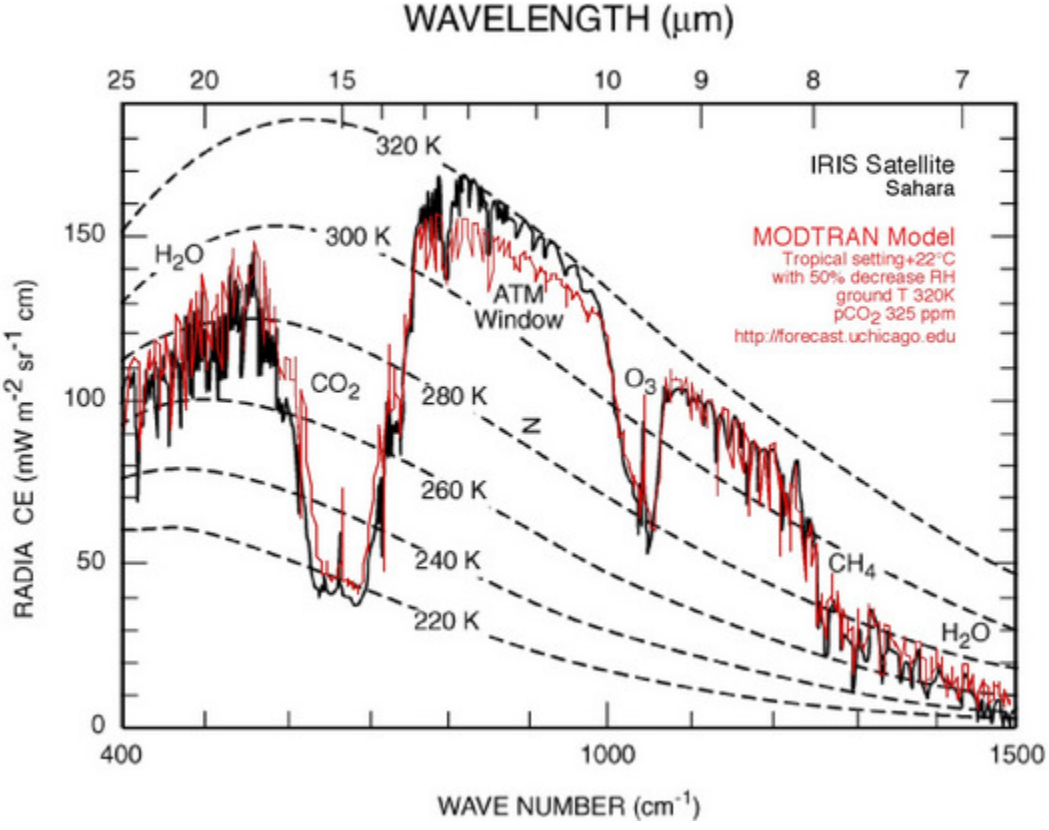

3. High Measurements of the Radiative Surface Forcing of Climate

W.F.J. Evans, North West Research Associates, Bellevue, WA; and E. Puckrin
https://ams.confex.com/ams/Annual2006/techprogram/paper_100737.htm

The earth's climate system is warmed by **35 C due** to the emission of **downward infrared radiation by greenhouse gases** in the atmosphere (surface radiative forcing) or by the absorption of upward infrared radiation (radiative trapping). **Increases in this emission/absorption are the driving force behind global warming.** Climate models predict that the release of greenhouse gases into the atmosphere has altered the radiative energy balance at the earth's surface by **several percent** by increasing the greenhouse radiation from the atmosphere. With **measurements at high spectral resolution**, this increase can be quantitatively attributed to each of several **anthropogenic gases.** Radiance spectra of the greenhouse radiation from the atmosphere have been measured at ground level from several Canadian sites using FTIR spectroscopy at high resolution. The forcing radiative fluxes from CFC11, CFC12, CCl4, HNO3, O3, N2O, CH4, CO and CO2 have been quantitatively determined over a range of seasons. The contributions from stratospheric ozone and tropospheric ozone are separated by our measurement techniques. A comparison between our measurements of surface forcing emission and measurements of radiative trapping absorption from the IMG satellite instrument shows reasonable agreement. The experimental fluxes are simulated well by the FASCOD3 radiation code. This code has been used to **calculate the model** predicted **increase in surface radiative forcing** since 1850 to be **2.55 W/m^2**. In comparison, an ensemble summary of **our measurements indicates** that an energy flux imbalance of **3.5 W/m^2** has been created by anthropogenic emissions of greenhouse gases since 1850. This experimental data should effectively end the argument by skeptics that no experimental evidence exists for the connection between greenhouse gas increases in the atmosphere and global warming.

A typical winter spectrum of the downward radiance in the **5-16 μm** wavelength range is shown in the Figure below, with the emission from several greenhouse gases identified.

Spectrum of the greenhouse radiation measured at the surface. **Greenhouse effect from water vapor is filtered out**, showing the contributions of other greenhouse gases (Evans 2006).

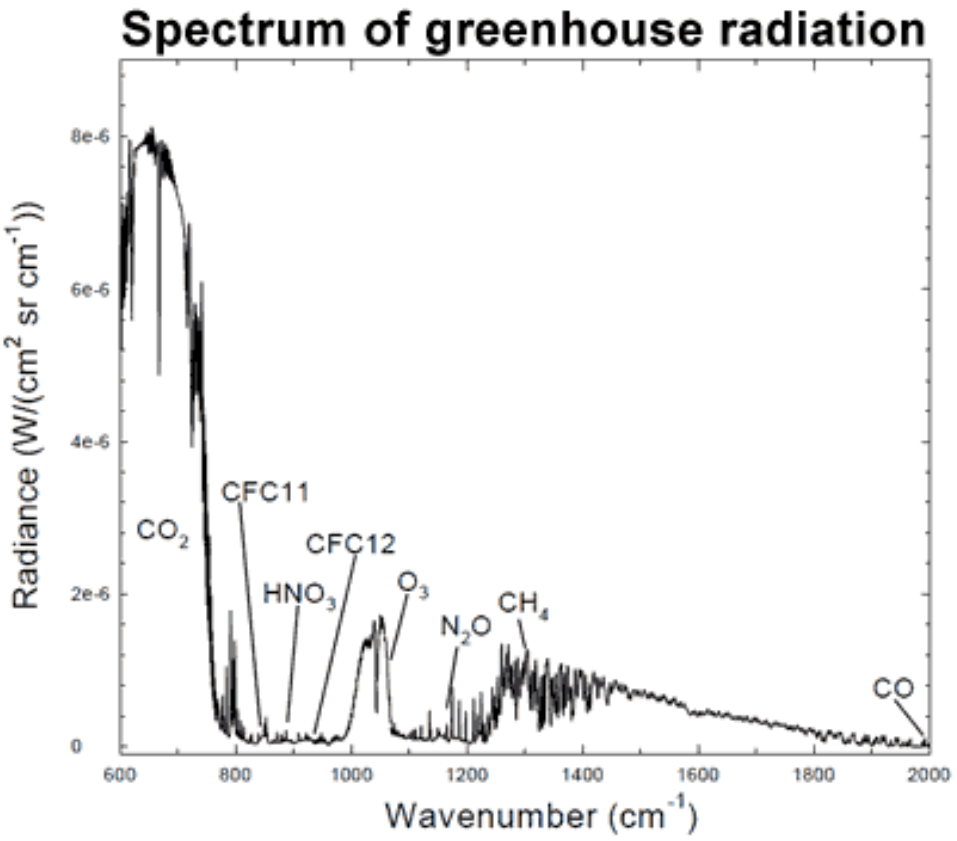

SECTION VI. Project Earthshine - Measuring the Earth's Albedo

http://www.bbso.njit.edu/Research/EarthShine/

Earth's global albedo, or reflectance, is a critical component of the global climate as this parameter, together with the solar constant, determines the amount of energy coming to Earth. **Probably because of the lack of reliable data, traditionally the Earth's albedo has been considered to be roughly constant, or studied theoretically as a feedback mechanism in response to a change in climate.** Recently, however, several studies have shown large decadal variability in the Earth's reflectance. Variations in terrestrial reflectance derive primarily from changes in cloud amount, thickness and location, all of which seem to have changed over decadal and longer scales.

A global and absolutely calibrated albedo can be determined by measuring the amount of sunlight reflected from the Earth and, in turn, back to the Earth from the dark portion of the face of the Moon (the `earthshine' or `ashen light'). For more than a decade we have been measuring the Earth's large-scale reflectance from Big Bear Solar Observatory.

"Changes in the Earth's reflectance over the past two decades" Figure 3 - Below

E. Palle, P.R. Goode, P. Montanes-Rodriguez and S.E. Koonin, Science, 304, 1299-1301, 2004a
http://bbso.njit.edu/Research/EarthShine/literature/Palle_etal_2004_Science.pdf

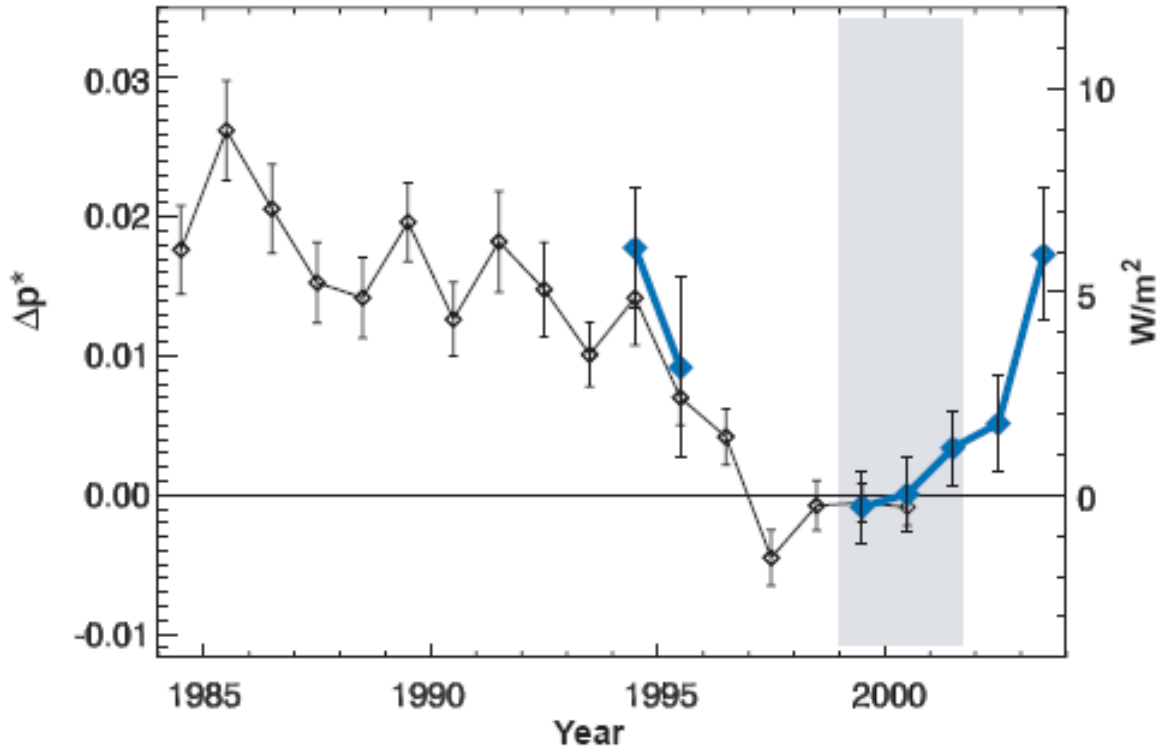

1. Figure 3 - Reconstructed annual reflectance anomalies 1984 to 2000

Reconstructed annual reflectance anomalies, Δp* (black), with respect to the mean anomaly for the regression calibration period 1999–2001 (vertical gray band). The **large error bars** result from the **seasonal variability** of Earth's albedo, which can be **15 to 20%**. Also plotted (blue) are the Earth Shine, ES, -observed annual anomalies for 1999–2003 and 1994–1995. The right hand vertical scale shows the deficit in global lSW forcing relative to 1999–2001.

The decrease in Earth's reflectance from 1984 to 2000 suggested by ISCCP data in the Graph corresponds to a change in Δp* of some –0.02, which translates into a decrease of the Bond albedo by 0.02 (Δp*/p* = ΔA/A) and an additional SW absorption, R, of **6.8 W/m²** (R = ΔA x C/4, where C = 1368 W/m² is the solar constant). This is **climatologically very significant**. For example, the latest IPCC report argues for a **2.4 W/m2 increase in CO_2 longwave forcing since 1850**. Our observational ES data extend from 1999 to 2003 and indicate a clear reversal of the ISCCP-derived reflectance trend starting in 1999 up through 2003. The increasing trend in reflectance corresponds to approximately 5 W/m², bringing the mean reflectance anomaly back to its 1980s values. Only the ES data are currently available to signal this reversal; it will be interesting to see how the proxy behaves when ISCCP data are available beyond mid-2001.

These results are difficult to attribute to monotonically increasing atmospheric greenhouse gases.

SECTION VII. 70 Year Warming Cycles

1. Analysis: Statistics of Climate Change - Temp Rise is Non Monotonic - 70 Year Cycles
Ref: "ABRUPT GLOBAL TEMPERATURE CHANGE AND THE INSTRUMENTAL RECORD," Menne
Use GISS Global Temp Data: "GISS NASA Global Temp Mean Fig2A.TXT" from Above
Break into Four 35 Year Periods: 1880 to 1910, 1911 to 1945, 1946 to 1980 and 1981 to 2010
Uses Analysis from:
http://www.leapcad.com/Climate_Analysis/Cycles_and_Trends_Average_Temp.xmcd

Note: Temperature Plateaus and then Climbs in 70 Year Cycles

$T_{abrupt} := READPRN("GAbrupt.txt")$

1. Analysis: Abrupt NOAA Global Annual Mean Temperature in 70 Year Cycles

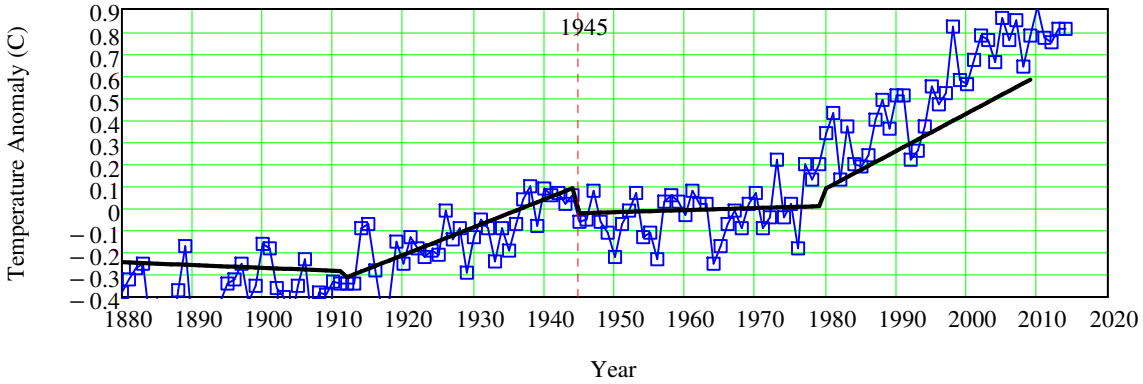

Correlation Coefficient and t Test:

$corr\left(GTemp0^{\langle 1 \rangle} \cdot 0.01, T_{abrupt}\right) = 0.94048 \qquad Stdev\left(T_{abrupt}\right) = 0.23426$

t Test: $t := 0.98622 \cdot 0.23434^{-1} = 4.2085$ These 70 year cycles are statistically significant

Section VIII. Milankovitch Cycles

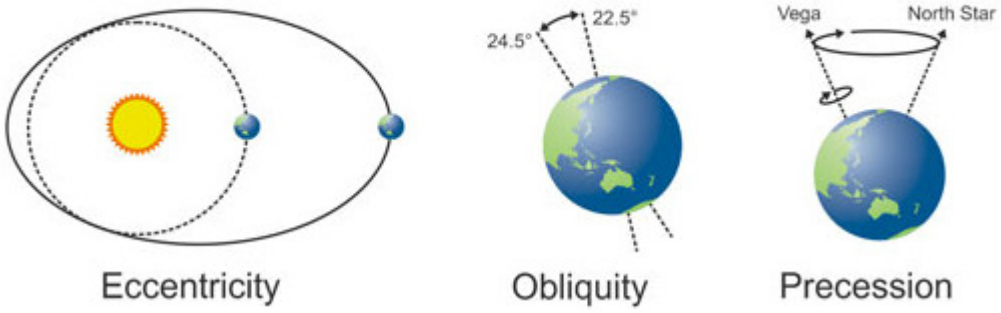

The three main orbital variations. **Eccentricity**: changes in the shape of the Earth's orbit.
Obliquity: changes in the tilt of the Earth's rotational axis. **Max 9% in Δ distance ~ 20% in Δ insolation.**
Precession: wobbles in the Earth's rotational axis.
http://www.skepticalscience.com/Why-does-CO2-lag-temperature.html

Interglacials come along approximately every **100,000 years.** This is called the **Milankovitch cycle**, brought on by changes in the Earth's orbit. There are three main changes to the earth's orbit. The shape of the Earth's orbit around the sun (**eccentricity**) varies between an ellipse to a more circular shape. The earth's axis is tilted relative to the sun at around 23°. This tilt oscillates between 22.5° and 24.5° (**obliquity**). As the earth spins around it's axis, the axis wobbles from pointing towards the North Star to pointing at the star Vega (precession).

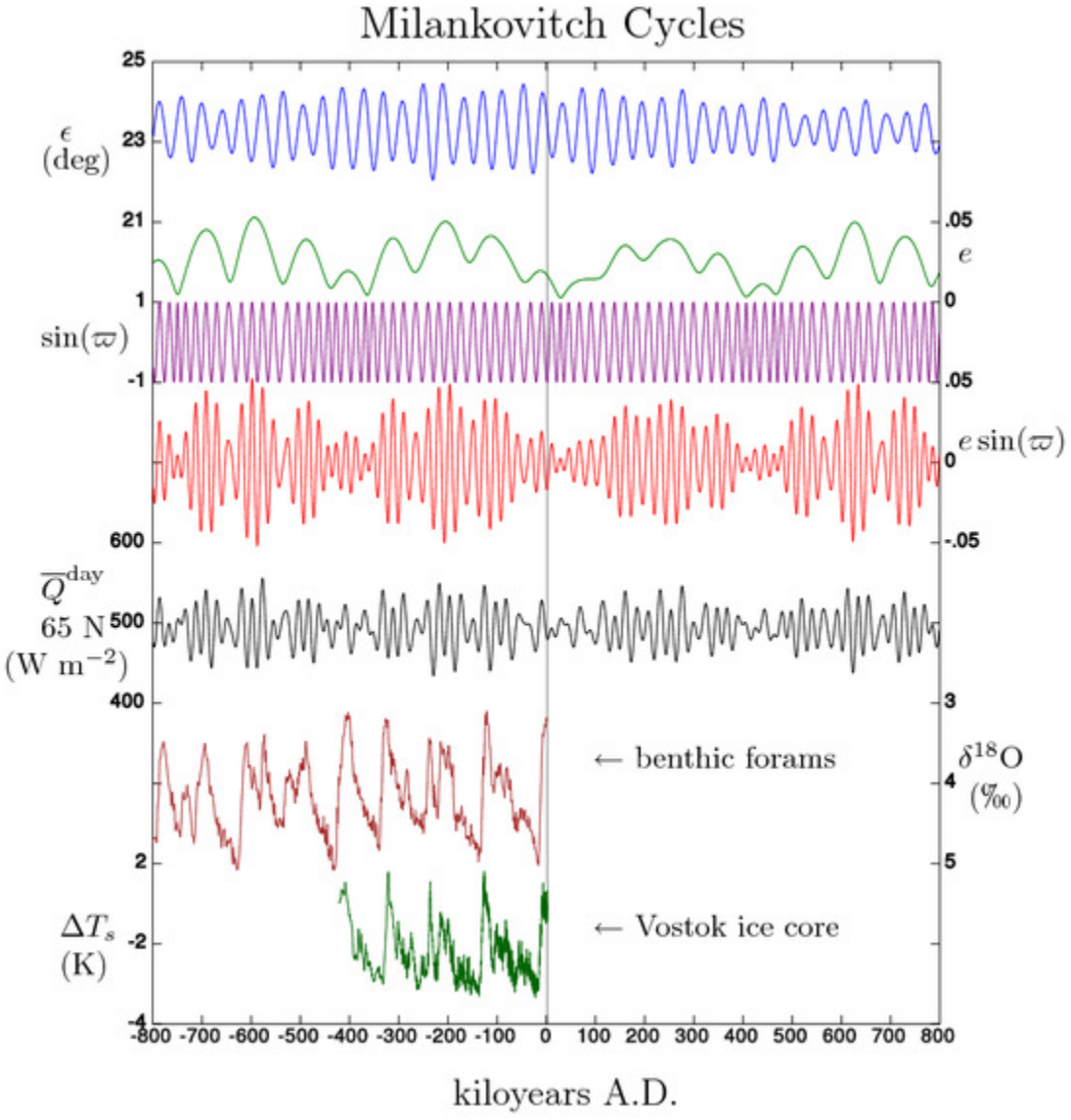

The astronomical theory of Paleoclimate after Milankovitch (1930, 1941)
http://en.wikipedia.org/wiki/Milankovitch_cycles
relates climatic change to variations of the amount of solar energy received by the Earth as a consequence of quasi-periodic changes in celestial geometry (see Imbrie & Imbrie, 1979, and Berger, 1988, for reviews). Of particular importance are variations in the eccentricity of the Earth's orbit (with dominant periods of roughly 400 kyr and 100 kyr), in the obliquity of the Earth's rotational axis relative to the orbital plane (with characteristic periods of 54 kyr and 41 kyr) and in the precession of the equinox or more exactly the eccentricity modulated precession expressed by the precessional index of Berger (1976, 1978b) (with periods of 23 kyr nd 19 kyr). The obliquity cycle is more effective in high latitudes, whereas the low latitudes are dominated by the precessional cycle.
See _Global Warming - Milankovitch.doc for list of articles
The next tipping point comes in ca. 50,000 years from now, when the Milankovich forcing almost certainly would be sufficient to start glaciation.

Solar System Orbital Simulation Data
The presence of chaos, moreover, severely limits the accuracy of orbital integrations on the time scale of **millions of years**. Chaos causes initial errors to grow exponentially in time, and so the simulated orbits diverge from the correct ones.
http://astrobiology.ucla.edu/OTHER/SSO/

1. Astronomical Solar Insolation Forcing
Early Plesitocene Glacial Cycles - Huybers
Link between glacial extent and solar forcing (orbital configuration).
ftp://ftp.astr.ucl.ac.be/pub/loutre/QSR/
BergerFILE2_90.DAT
INSOLATION DEC
Year 90NDec 60NDec 30NDec 0 Dec 30SDec 60SDec 90SDec

$$InsDec := READPRN("BergerFILE2\_90.DAT") \quad InsJun := READPRN("BergerFILE3\_90.DAT")$$

$$MeanIns := mean\left(InsJun^{\langle 4 \rangle}\right) \qquad MeanIns = 398.33779$$

$$InsSmooth := 40 \cdot \left(ksmooth\left(-InsJun^{\langle 0 \rangle}, InsJun^{\langle 4 \rangle}, 100\right) - MeanIns\right) + MeanIns$$

1. Berger: 30N June Isolation, T Vostok

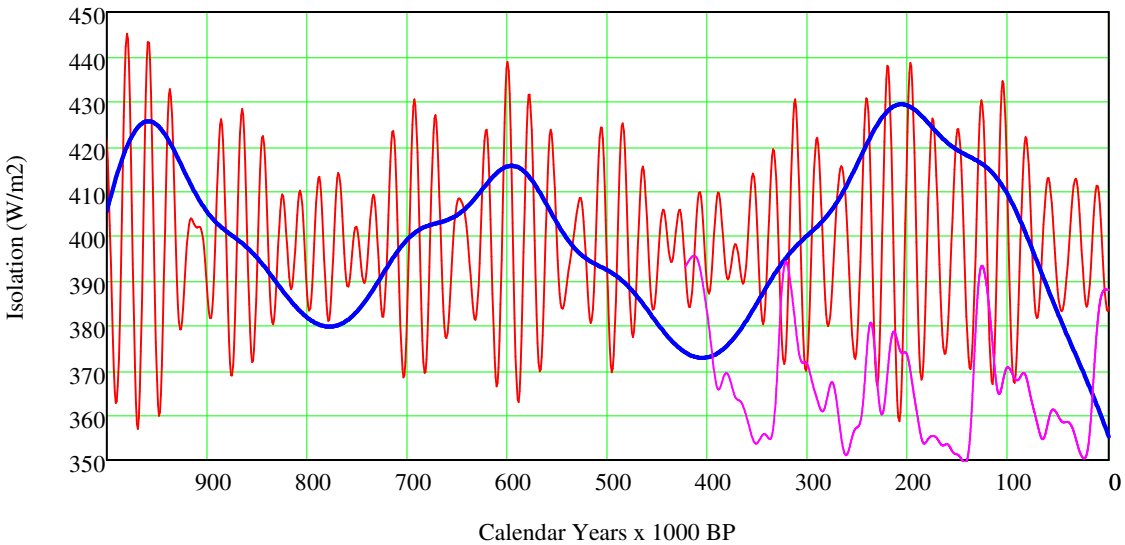

2. Milankovitch radiation for different latitudes and time periods

www.climatedata.info Average of 60 and 70 N
BP, Months 7 to 7, Annual 65N, Annual global, Global cos-weighted

$Mlnkvthh\_Ins := READPRN("Milankovitch - Isolation - ClimateCom.txt")$

$MeanMkvh := mean(Mlnkvthh\_Ins^{\langle 1 \rangle})$ $MeanMkvh = 444.08333$

$MkvhSmooth := ksmooth\left(\frac{Mlnkvthh\_Ins^{\langle 0 \rangle}}{1000}, Mlnkvthh\_Ins^{\langle 1 \rangle}, 100\right)$

$MkvhSmth := 40 \cdot (MkvhSmooth - MeanMkvh) + MeanMkvh$

2. Milankovitch Iso Annual 65N, T Vostok

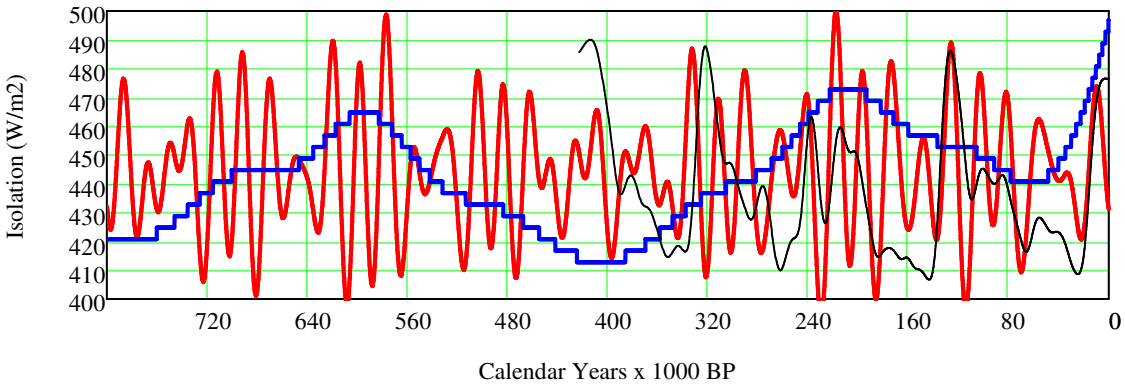

NASA Earth Observing Systems (EOS) Solar Radiation and Climate Experiment (SORCE)

An imperative for climate change planning: tracking Earth's global energy

http://lasp.colorado.edu/sorce/tsi_data/daily/sorce_tsi_L3_c24h_m29_v10_20030225_20091223.txt
nominal_date_yyyymmdd R8 f12.3 (Column 1: Nominal Data Time, YYYYMMDD) ; ; tsi_1au R8 f10.4 (Column 5: Total Solar Irradiance (TSI) at 1-AU, W/m^2)

$TSI := READPRN("Total Solar Irradiance.txt")$ $rows(TSI) = 2494$ $n := 0 .. 2493$

$TSIP := TSI^{\langle 4 \rangle}$ $TSIP_n := if(TSIP_n = 0, TSIP_{n-1}, TSI)$ $mean(TSIP) = 1361.04$ $Avg_n := 1361$

$$YrDecS_n := str2num(substr(num2str(TSI_{n,0}), 0, 4)) + \frac{str2num(substr(num2str(TSI_{n,0}), 4, 8))}{1231}$$

$TSIPs := medsmooth(TSIP, 31)$

The sun has progressed from an active part of the sunspot cycle in 2003 to a very quiet phase in 2008 through 2010. The net change is a decrease in TSI of 0.5 W/m² -for an ASR of 0.1 W/m2
For more studies and conclusions on recent solar effects see
http://www.skepticalscience.com/solar-activity-sunspots-global-warming.htm

3. SORCE Total Solar Irradiance-31 Day Median Fit

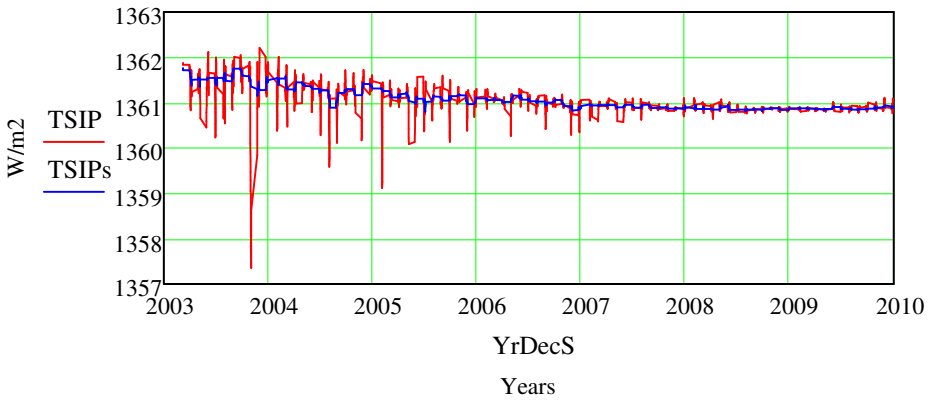

SECTION IX. Climate Cycle Analysis - Wavelets

These are Very Detailed Analyses - Go to: http://www.leapcad.com/Climate_Analysis.html

Refer to the Separate Worksheets

Climate Cycle Analysis: Solar Insolation

1. Multiresolution Wavelet Analysis
2. Adaptive Hilbert-Huang Transformation Analysis
3. Astronomical Earth Orbit Analysis

SECTION X. ENSO-2014 AND PDO (ENSO - The Southern Oscillation)

http://www.leapcad.com/Climate_Analysis/Empirical_Model_ENSO_Solar_VolcAero_Anthro.pdf

Multi Variate ENSO Index: http://www.esrl.noaa.gov/psd/people/klaus.wolter/MEI/mei.html

MV E I Data Format: Year, ENSO (Jan, Feb,...Dec)

El Niño/Southern Oscillation (ENSO) is the most important coupled ocean-atmosphere phenomenon to cause global climate variability on interannual time scales. Here we attempt to monitor ENSO by basing the **Multivariate ENSO Index (MEI)** on the six main observed variables over the tropical Pacific. These six variables are: sea-level pressure (P), zonal (U) and meridional (V) components of the surface wind, sea surface temperature (S), surface air temperature (A), and total cloudiness fraction of the sky (C).

MEIData := READPRN("MultiVariate ENSO Index.TXT")

1. ENSO Index - 1950 to 2014

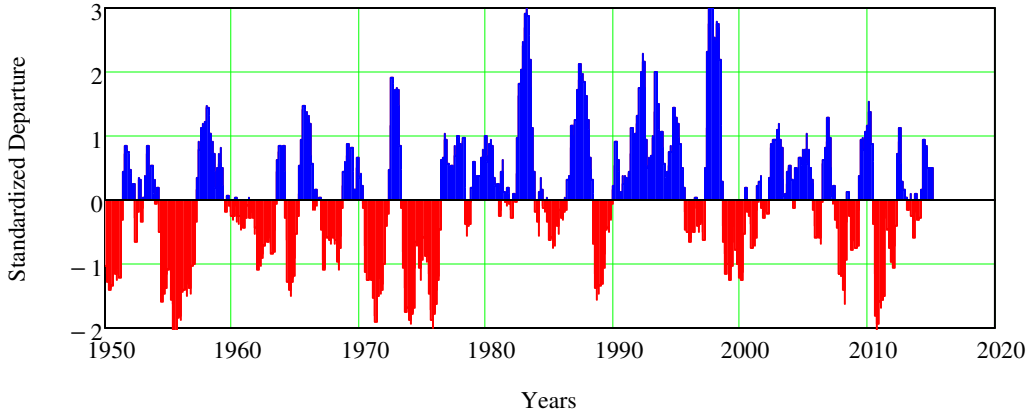

Pacific Decadal Oscillation (PDOI) Index from 1900 to 2014

Note: ENSO and PDO are not statistically independent. They have a 47% correlation.

http://jisao.washington.edu/data/pdo/ Year, Jan to Dec

PDO := READPRN("PDO_Index2014.txt") R := rows(PDO) rr := 0 .. (R − 1)·12 + 11

PDOx := submatrix(PDO, 0, R − 1, 1, 12)

$$PDOYr_{rr} := \left(PDO^{\langle 0 \rangle}\right)_{floor\left(\frac{rr}{12}\right)} + \frac{mod(rr,12)}{12}$$

$$PDOI_{rr} := PDOx_{floor\left(\frac{rr}{12}\right),mod(rr,12)} \quad PDOPlus := (\Phi(PDOI)\cdot PDOI) \quad PDOSm := ksmooth(PDOYr, PDOI, 20)$$

2. PDO Index - 1900 to 2010

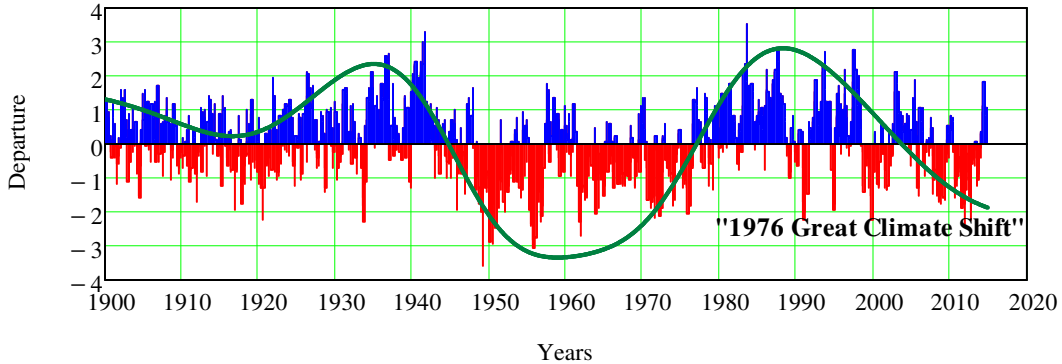

SECTION XI. Energy Balance Modeling and Wavelet Analysis

1. Stefan-Boltzmann Law of Radiation - Temp of Earth

Transmittance Stefan-Boltzmann constant

$R_{orbit} := 1.5 \cdot 10^{11} m$ $R_{sun} := 7 \cdot 10^{8} m$ $T_{sun} := 5800 K$ $\alpha := 1$ $\sigma := 5.6704 \cdot 10^{-8} \frac{watt}{m^2 \cdot K^4}$

Absorption

$$Power_{sun} := \alpha \cdot \pi \cdot R_{earth}^{2} \cdot \sigma \cdot T_{sun}^{4} \left(\frac{R_{sun}}{R_{orbit}} \right)^{2} \qquad Power_{sun} = 1.78581 \times 10^{17} W$$

$$A_{earth} := \frac{1}{2} 4 \cdot \pi \cdot R_{earth}^{2} \qquad \frac{Power_{sun}}{0.5 \cdot A_{earth}} = 1397.45951 \cdot \frac{W}{m^2}$$

The flux of the solar radiation energy received by the Earth ~ 1370 W/m^2

Emission

albedo of earth: $\alpha_{earth} := 0.7$

$$Temp_{earth} := \left[\frac{\alpha_{earth}}{4} \cdot \left(\frac{R_{sun}}{R_{orbit}} \right)^{2} \right]^{\frac{1}{4}} T_{sun} \qquad Temp_{earth} = 256.26594 K$$

Temp in Celcius

$257 - 273 = -16$

The earth is warmer than -16C. This actual warmer temperature (~20C) results from the Greenhouse Effect. Further evidence is provided by the moon, which has not atmosphere. Same sunlight, but temps range from -173C to 100C

2. Simple 1D Latitudinal Energy Balance Model - From Climate Modelling Primer, McGuffe

Details: http://leapcad.com/Climate_Analysis/1D_Zonal_Globall_Temperature-Energy_Balance_Model.xmcd

Energy flows into Earth through radiation from the Sun and out of Earth by reflection and radiation. There are latitudinal variations. The flow of energy into Earth and the flow of energy out of Earth must be equal if Earth is to maintain a stable temperature. H_0 is the extraterrestrial solar flux (w/m^2). In the zonal model, we need to be able to calculate the total energy received from the sun per unit time. This is given by $\pi R^2 H_0$. The average extraterrestrial solar flux over the entire surface can by calculated by $H_0/4$.

Mathcad Simulation Results: 1-D Effusive EBM Analytic Model (Magenta Plots)

To is the planetary, globally averaged temperature, T2 is 2/3 of the Temp difference from the poles to equator, Tpe. The ice sheet edge (T = -10C) is above 73.74°, with ice albedo, α_{ice}.

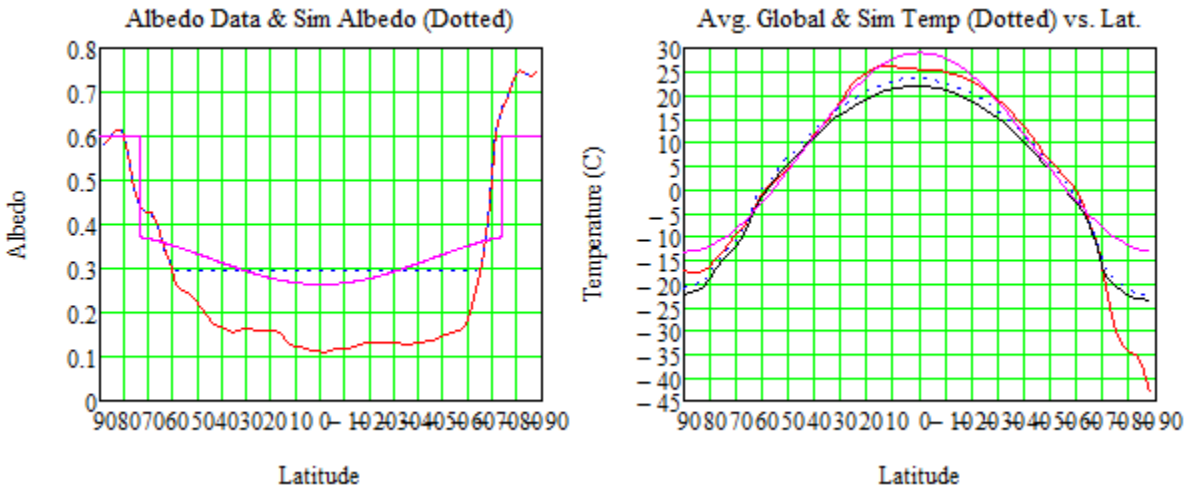

3. Wavelet Adaptive Hilbert-Huang Transformation Analysis - Empirical Mode Decomposition of Temperature

http://www.leapcad.com/Climate_Analysis/EMD_HHT.xmcd

Load Wavelet Transformation Functions:

Reference:C:\Users\Tom\Documents\%%_AEPOF wwwLCcom\www\Climate_Analysis\EMD Extrema.xmcd(R)

Reference:C:\Users\Tom\Documents\%%_AEPOF wwwLCcom\www\Climate_Analysis\EMD HHT Function.xmcd(R)

TempMill7 := READPRN("Temp 7 Reconstructions-briffa.txt") t := 1.. 988 Note: Array Origin = 1

gsta := READPRN("gsta.dat") Yr := gsta$^{\langle 1 \rangle}$ T := gsta$^{\langle 2 \rangle}$

$Y987_t := TempMill7_{t,1} - 1000$ $T987_t := TempMill7_{t,7} + 0.2$ RT := rows(T)

rows(extrema(T)) = 89 HHT := eemd(T, 0, 1) cols(HHT) = 8

r := 1.. RT $X_r := r$ Residual := HHT$^{\langle 6 \rangle}$ + HHT$^{\langle 7 \rangle}$ + HHT$^{\langle 8 \rangle}$

Ext := extrema(T) RExt := rows(Ext) spmax := submatrix(Ext, 1, $Ext_{RExt,2}$, 1, 2)

spmin := submatrix(Ext, $Ext_{RExt,2}$ + 1, RExt − 2, 1, 2) up_{sp} := cspline(spmax$^{\langle 1 \rangle}$, spmax$^{\langle 2 \rangle}$)

upper := interp(up_{sp}, spmax$^{\langle 1 \rangle}$, spmax$^{\langle 2 \rangle}$, X)

low_{sp} := cspline(spmin$^{\langle 1 \rangle}$, spmin$^{\langle 2 \rangle}$) lower := interp(low_{sp}, spmin$^{\langle 1 \rangle}$, spmin$^{\langle 2 \rangle}$, X)

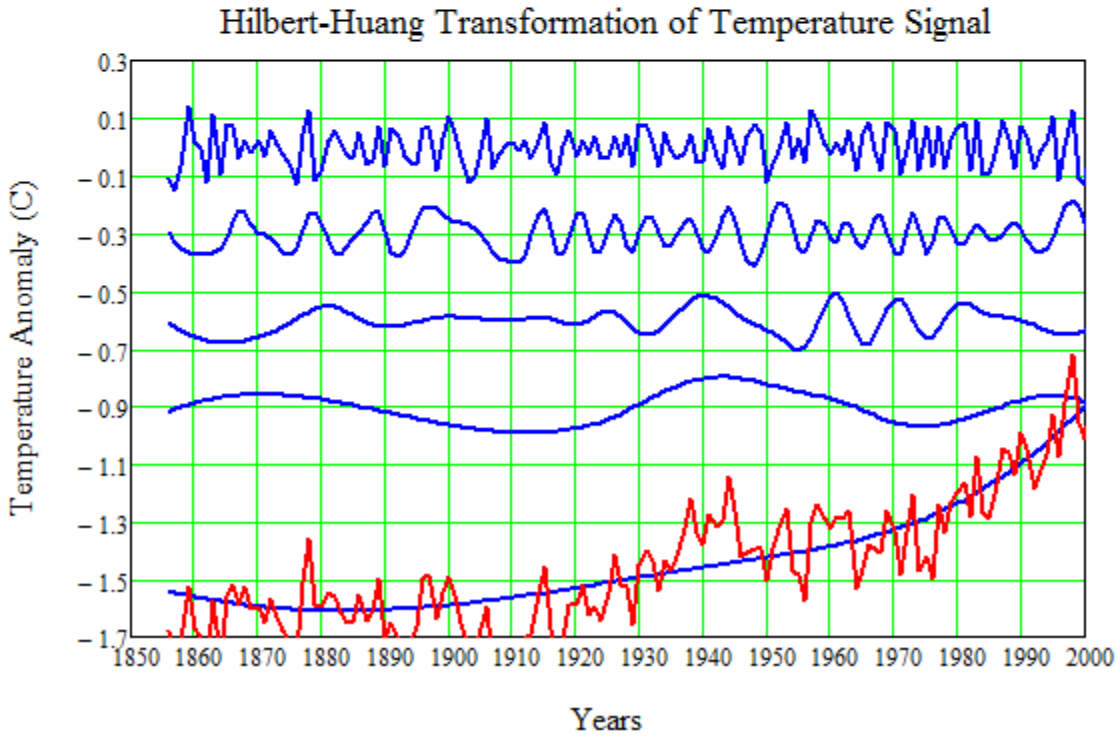

SECTION XII. More Complex Models

Go to Link: http://www.leapcad.com/Climate_Analysis.html

Climate Model Papers: General Circulation

- GISS ModelE (See http://www.giss.nasa.gov/tools/modelE/)
- Efficient Three-D Global Model - GISS Model II
- Educational GISS Model II

Testing the Anthropogenic Greenhouse Gas Global Warming Model
Looking for Unique Fingerprints of AGW

SECTION XIII. Model: Global Temp Reproduced by CO2 and Natural Forcings

Test #0. Use ENSO, Irradiance, Volcanic Aerosols, and Anthropogenic Effects to Create an Empirical Temp Model

See http://www.leapcad.com/Climate_Analysis/Empirical_Model_ENSO_Solar_VolcAero_Anthro.pdf
Reference "Some statistical aspects of anthropogenic and natural forced global temperature change", Schonwiese and Bayer, 1995.
Empirical Multivariate Regression Model by Combining ENSO (E), Irradiance (S), Volcanic Aerosols (V), CO_2 Anthropogenic Forcing Effects (A) to generate Multi-Variate regression coefficients of Global Temperature Anomaly data. The resulting model has an R^2 of 0.84, i.e. it **captures 84% of the variation of Global Temperature**. This model is then used to make decadal temperature projections based on predictions for these four climate variables.
Monthly mean surface temperature anomalies ΔT_{MS} are reconstructed as a **Linear Regression Equation**:

$$\Delta T_{MS}(t) = co + c_E \cdot E(t - \Delta t_E) + c_V \cdot V(t - \Delta t_V) + c_S \cdot S(t - t_S) + c_A \cdot A(t - t_A)$$

Where E, V, S and A are a AR(1) time series with **optimized lags** of $\Delta t_E = 7, \Delta t_V = 8$, and $\Delta t_S = 2$ months and $\Delta t_A = 17$ years. The lags are chosen to maximize the proportion of global variability that the statistical model captures and are spatially invariant. The fitted coefficients are obtained by multiple linear regression against the instrumental surface temperature record (HadCRUT4). The Temp data was median smooth within a 7 month period.

Multiforced regression models based on observational temperature data are able to **reproduce both a major part of natural fluctuations (decadal time scale) & a trend which may be due to GHG forcing**. Moreover, **future extrapolatior** of the GHG forced temperature trend show a magnitude which is **similar to Global Climate Model** projections.

Compare Anthropogenic (CO2) Forcing Component - to Temp Data

b4*z4 (Green Line) is the Optimized Match of Effects of CO_2 Forcing to Global Temperature Data

IPCC CO_2 Log Forcing Function used in Regression Model. Co = 340 ppm.

$$Co := 340 \qquad \Delta F_{IPCC}(C) := 6.3 \ln\left(\frac{C}{Co}\right)$$

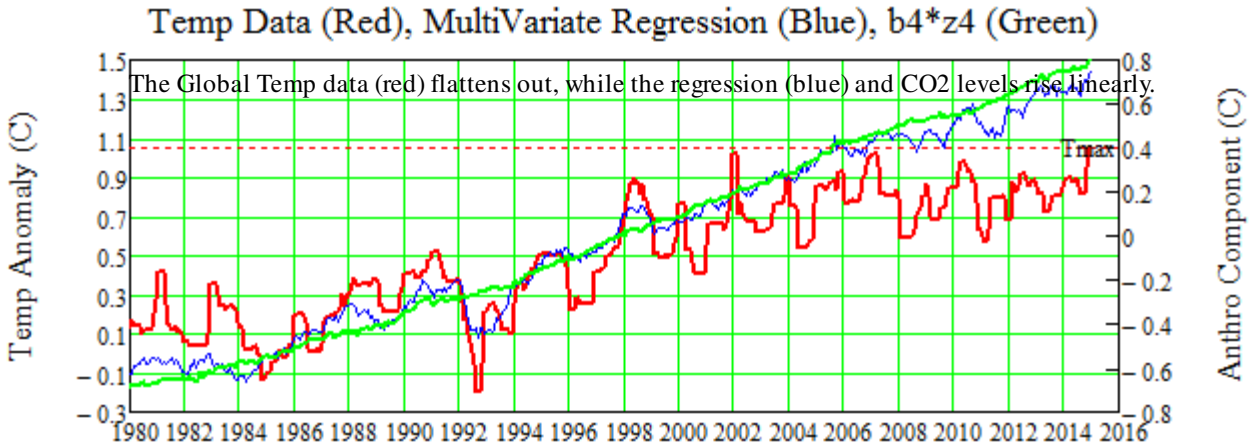

$corr(Y, \Delta T) = 0.9038$ $\qquad RSquare := corr(Y, \Delta T)^2 = 0.81685$ $\qquad corr(Y, \Delta Ts)^2 = 0.72544$

Correlation to Global Temp between:
Y (ΔTemp) and x1 (ENSO) = - 3.5%
Y (ΔTemp) and x2 (Volcanic Aero) = - 49%
Y (ΔTemp) and x3 (Solar) = - 8.5%
Y (ΔTemp) and x4 (Anthropogenic) = 87%

CO_2 has ten times the correlation than Solar

$$CORR = \begin{pmatrix} 1 & 0.35061 & -0.11702 & -0.23532 & -0.05022 \\ 0.35061 & 1 & 0.01393 & -0.3596 & -0.48887 \\ -0.11702 & 0.01393 & 1 & 0.12867 & 0.08534 \\ -0.23532 & -0.3596 & 0.12867 & 1 & 0.87369 \\ -0.05022 & -0.48887 & 0.08534 & 0.87369 & 1 \end{pmatrix} \begin{matrix} x1 \\ x2 \\ x3 \\ x4 \\ y \end{matrix} \begin{pmatrix} ENSO \\ Aerosols \\ Solar \\ CO2 \\ \Delta Temp \end{pmatrix}$$

SECTION XIV Testing the Anthropogenic Greenhouse Gas Model

Looking for Unique Fingerprints of AGW - Continued

Test #1. Spectral signatures of climate change in IR spectrum between 1970 and 2000

"Spectral signatures of climate change in the Earth's infrared spectrum between 1970 and 2006", Chen et al. (2007

Chen et al. showed that increased CO2 is preventing LW radiation from escaping the atmosphere and this decreasing LW radiation is accurately being predicted by climate models.

The observed TES – IRIS and simulated 2006 – 1970 difference spectra are shown in Figure 3. The background offset in the lower wavenumber window discussed previously when comparing the observed and modelled brightness temperature spectra (Figure 1 and Figure 2) is not apparent when comparing the observed and modelled difference spectra. Instead the feature cancels out and the background is seen to match well over the wing of the 15 µm CO_2 band and in the window regions. This emphasizes the importance of looking at the raw spectra as well as the difference spectra. The modelled 2006 – 1970 difference in the methane signal is shallower than the observed case, which is due to the model calculating a deeper signal for 1970 than was observed.

CONCLUSIONS

The TES data compare very well with the IRIS data, suggesting successful normalization of the different instrument characteristics. The TES and IRIS difference spectrum covers the time range of 1970 – 2006, a period of 36 years. Simulated spectra represent the state of the HadGEM1 coupled model for 1970 and 2006. Changing spectral signatures in CH_4, CO_2, and H_2O are observed, with the difference signal in the CO_2 matching well between observations and modelled spectra. The methane signal is deeper for the observed difference spectrum than the modelled difference spectrum, but this is likely due to incorrect methane concentrations or temperature profiles from 1970. In the future, we plan to extend the analysis to more spatial and temporal regions, other models, and to cloudy cases.

"This experimental data should effectively end the argument by skeptics that no experimental evidence exists for the connection between greenhouse gas increases in the atmosphere and global warming."

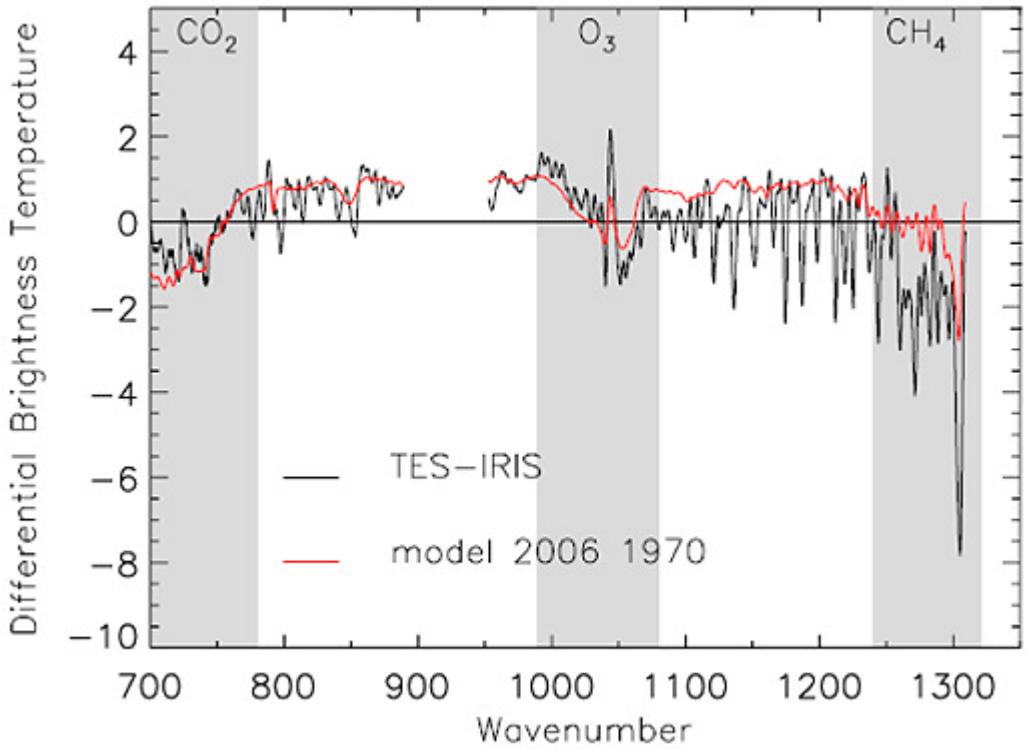

Observed difference spectrum (black line) between 2006 and 1970 (TES – IRIS) and the simulated difference spectrum (red line) for the same time interval.

Test #2. Natural Forcing alone cannot account for global warming - IPCC - 2007 WG1-AR4

Temperature changes relative to the corresponding average for 1901-1950 (°C) from decade to decade from 1906 to 2005 over the Earth's continents, as well as the entire globe, global land area and the global ocean (lower graphs). The black line indicates observed temperature change, while the coloured bands show the combined range covered by 90% of recent model simulations. Red indicates simulations that include natural and human factors, while blue indicates simulations that include only natural factors. Dashed black lines indicate decades and continental regions for which there are substantially fewer observations.

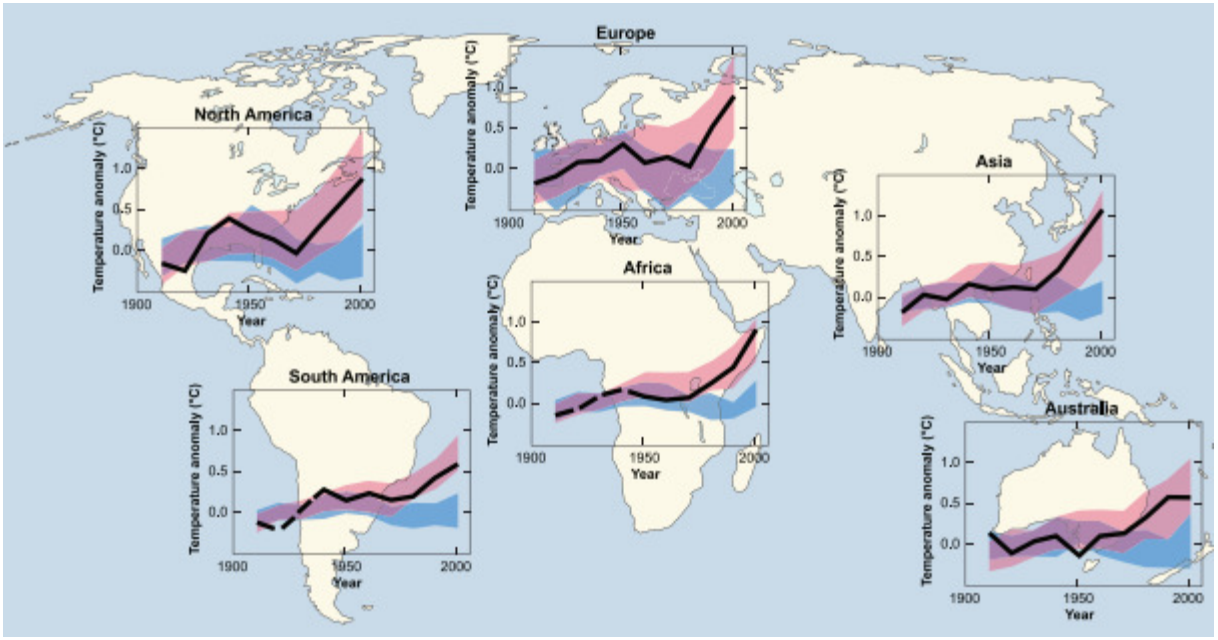

Test #3. Warming over land is greater than over oceans - IPCC - 2007 WG1-AR

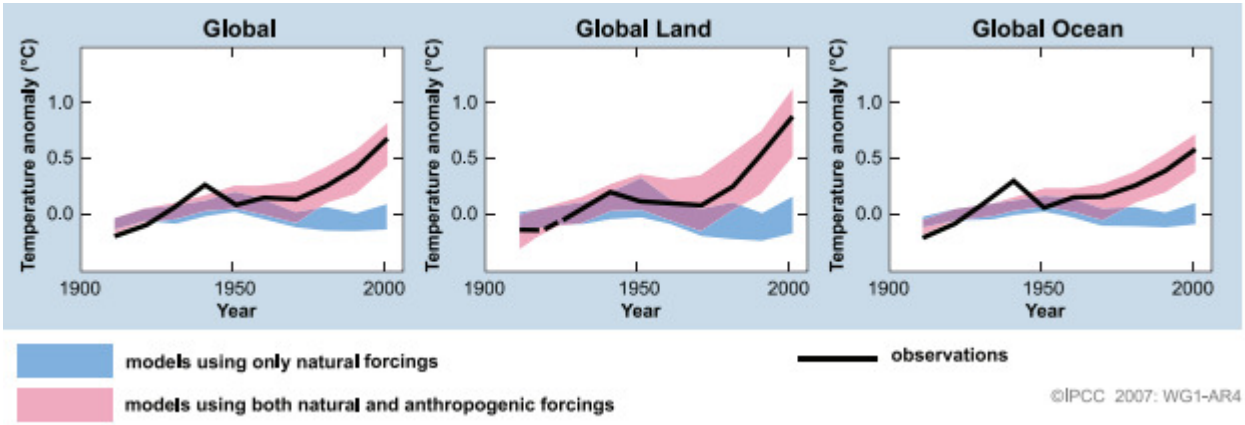

Test #4.
AGW (GH Effect) requires the lower and mid troposphere to be warmer than the surface.

Reconciling Observations of Global Temperature Change

Panel on Reconciling Temperature Observations, National Research Council, 2000

FINDINGS - 21

Based on current estimates, the lower to mid-troposphere has warmed less than the earth's surface during the past 20 years. For the time period from 1979 to 1998, it is estimated that on average, over the globe, surface temperature has increased by 0.25 to 0.4 ℃ and lower to mid-tropospheric temperature has increased by 0.0 to 0.2 ℃.

Test #5: AGW (GH Effect) requires the stratosphere to cool

Stratosphere Data: http://www.nsstc.uah.edu/data/msu/t4/uahncdc_ls_5.6.txt

Year Mo Globe Land Ocean NH Land Ocean SH Land Ocean Trpcs Land Ocean NoExt Land

$StratTemp := READPRN("LowStrat - uahncdc_ls_5.6.dat")$ $Year_{strat} := StratTemp^{\langle 0 \rangle} + \frac{StratTemp^{\langle 1 \rangle} - 1}{12}$

$SmoothGlobe := medsmooth(StratTemp^{\langle 2 \rangle}, 11)$ $SmoothTropics := medsmooth(StratTemp^{\langle 11 \rangle}, 11)$

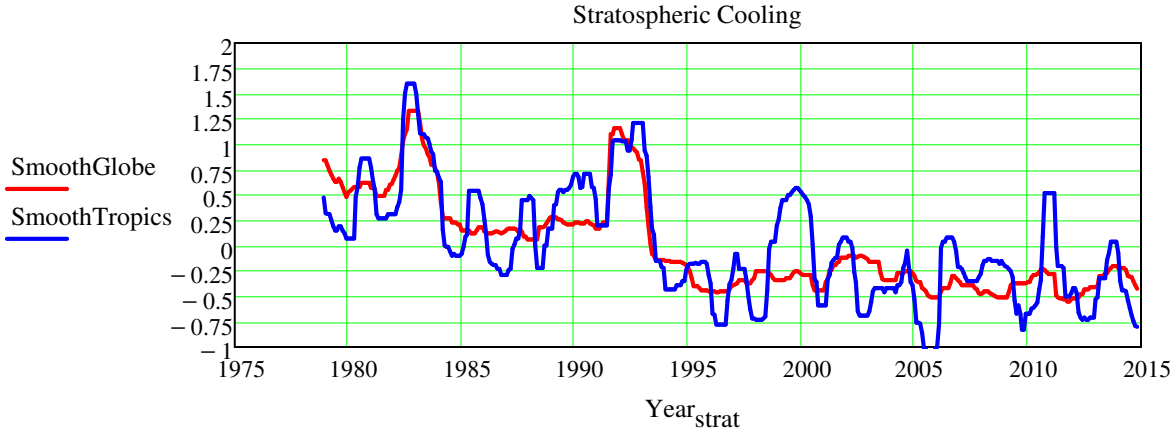

Test #6 Asymmetric diurnal temp change - Nights warming faster than days

If an increased greenhouse effect was causing warming, we would **expect nights to warm faster** than days. This is because the **greenhouse effect operates day and night.**

Global observed changes in daily climate extremes of temperature and precipitation, Alexander, JOURNAL OF GEOPHYSICAL RESEARCH, VOL. 111, D05109, **2006**

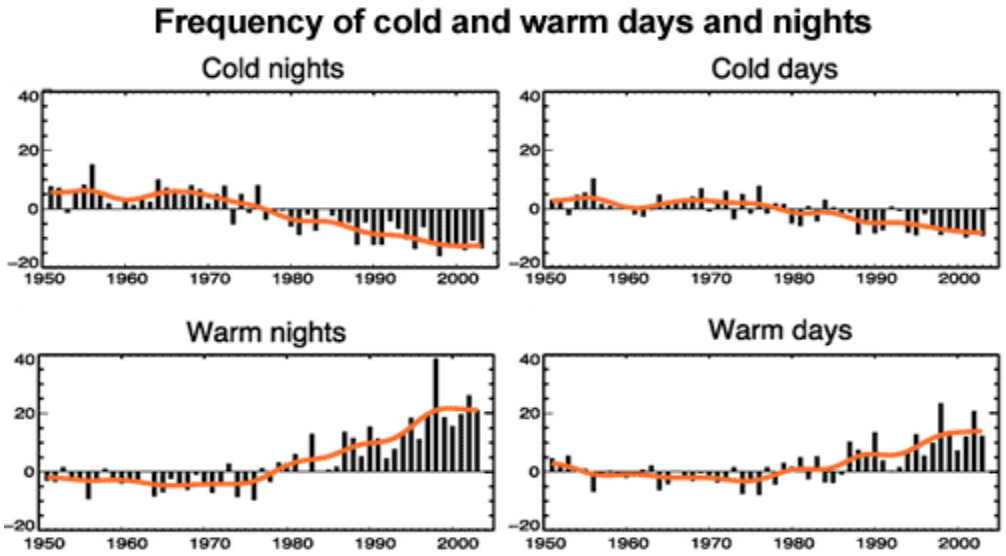

Graph Above: Observed trends (days per decade) for 1951 to 2003 in the number of extreme cold and warm days and nights per year. Cold is defined as the bottom 10%. Warm is defined as the top 10%. Orange lines show decadal trend (IPCC AR4 FAQ 3.3 adapted from Alexander 2006).

Below: Updated: Warm nights/days, TN90p/TX90P www.metoffice.gov.uk/hadobs/hadex2/Donat_etal2013.pdf

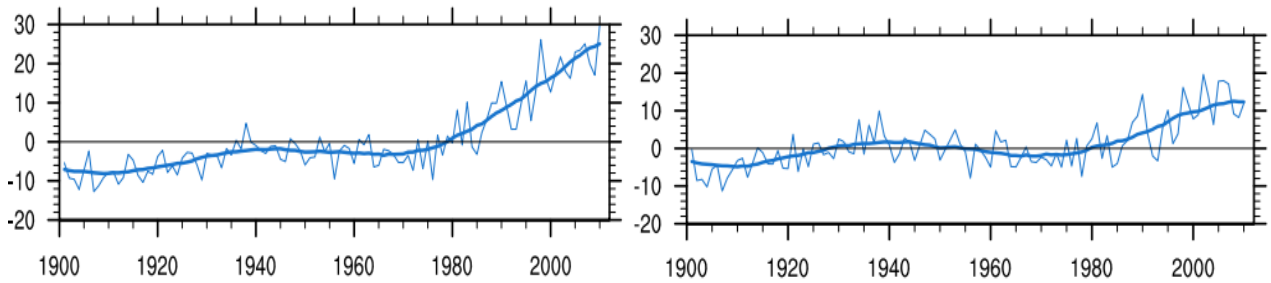

Test #7 Measure - Global Atmospheric Downward Longwave Radiation 1973-2008

JOURNAL OF GEOPHYSICAL RESEARCH, VOL. 114, D19101, doi:10.1029/2009JD011800, 2009 Wang and Liang
Evaluation of two widely accepted methods to estimate global atmospheric **downward longwave radiation (L_d)** under **both clear and cloudy** conditions, using meteorological observations from 1996 to 2007 at 36 globally distributed sites, operated by the Surface Radiation Budget Network (SURFRAD),we applied them to globally available meteorological observations to estimate **decadal variation in L_d.** The decadal variations in global L_d under both clear and cloudy conditions at about 3200 stations from 1973 to 2008 are presented. We found that daily L_d **increased at an average rate of 2.2 W m^{-2} per decade from 1973 to 2008**. The rising trend results from increases in **air temperature, atmospheric water vapor, and CO_2 concentration.** The L_d is estimated by

$$L_d := (1 - f)\cdot L_{dc} + f\cdot\sigma T_a^{\,4}$$

where f is the cloud fraction, L_{dc} clear-sky radiation, σ is the Stefan-Boltzman constant, and T_a is air temp

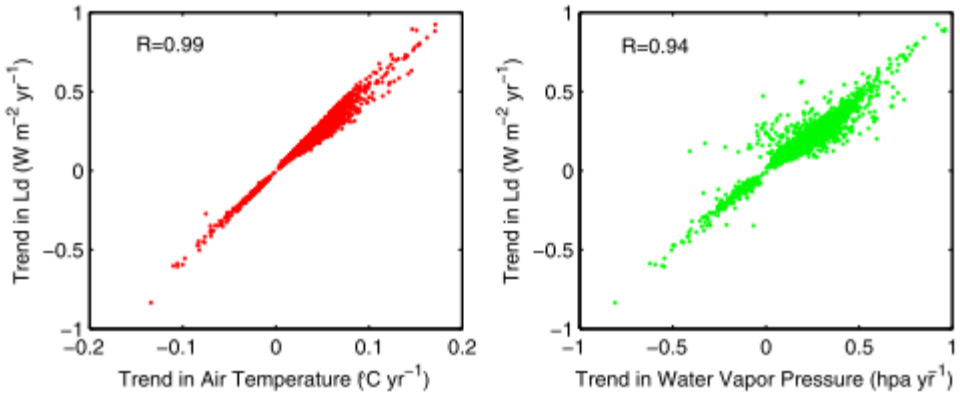

Figure 6. The scatterplots of linear trends in L_d as a function of trends in air temperature (red) and water vapor pressure (green) at the stations shown in Figure 5. One point in the figure represents one station. The correlations of the trends in air temperature, relative humidity, and water vapor pressure are also shown.

Test #8 Observational determination of surface radiative forcing by CO_2 2000 to 2010

Observational determination of surface radiative forcing by CO_2 from 2000 to 2010
D. R. Feldman, W. D. Collins, P. J. Gero, M. S. Torn, E. J. Mlawer & T Shippert, Nature 519, 339–343 (19 March 2015)

The climatic impact of CO2 and other greenhouse gases is usually quantified in terms of radiative forcing, calculated as the difference between estimates of the Earth's radiation field from pre-industrial and present-day concentrations of these gases. Radiative transfer **models** calculate that the increase in CO2 since 1750 corresponds to a global annual-mean radiative forcing at the tropopause of **1.82 ± 0.19 W m–2** (ref. 2). However, despite widespread scientific discussion and modelling of the climate impacts of well-mixed greenhouse gases, there is **little direct observational evidence** of the radiative impact of increasing atmospheric CO2. Here we present observationally based evidence of **clear-sky** CO2 surface radiative forcing that is **directly attributable** to the **increase**, between 2000 and 2010, of **22 parts per million atmospheric CO_2.**

The time series of this forcing at the **two locations**—the Southern Great Plains (SGP) and the North Slope of Alaska (NSA)—are derived from Atmospheric Emitted Radiance Interferometer spectra.The time series both show statistically significant trends of **0.2 W m–2 per decade** (with respective uncertainties of ±0.06 W m–2 per decade and ±0.07 W m–2 per decade) and have seasonal ranges of 0.1–0.2 W m–2. This is **only ten per cent of the trend in downwelling longwave radiation.** These results confirm theoretical predictions of the atmospheric greenhouse effect due to **anthropogenic** emissions, and provide **empirical evidence of how seasonal and rising CO_2 levels,** mediated by temporal variations due to photosynthesis and respiration, **are affecting the surface energy balance**.

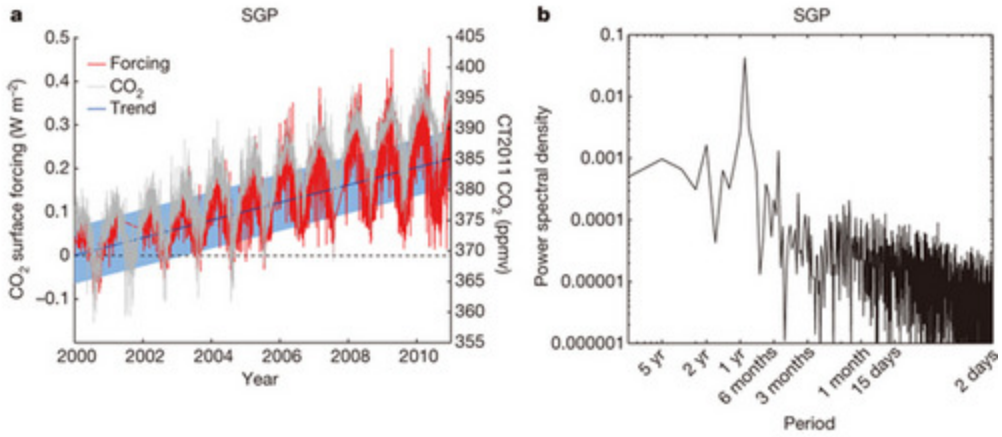

SECTION XV. Geologic and current nonlinear multiyear cycles in sea level

Effects Associated with Increased Temperatures in General

1. Non Linear Trend: Holocene Sea Level Rise - 8000 BP

Variations in sea level during the Holocene (10,000 BC, the time since the end of the last major glacial epoch).

Adjusted for glacial isostatic motion. See "Refining the eustatic sea-level curve since the Last Glacial Maximum using far- and intermediate-field sites", Fleming, Kevin (1998). Earth and Planetary Science Letters 163 (1-4): 327-342. "Modeling Holocene relative sea-level observations from the Caribbean and South America", Quaternary Science Reviews 24 (10-11): 1183-1202, Milne

$SLHol := READPRN("Holocene\_Sea\_Level.txt")$ $r := 0 .. rows(SLHol) - 1$ $cc := 0 .. 1$

$SLHolBP_{r,0} := -SLHol_{r,0}$ $SLHolBP_{r,1} := SLHol_{r,1}$

$SLHolC := READPRN("Holocene\_Sea\_Level4.txt")$ $r := 0 .. rows(SLHolC) - 1$ $cc := 0 .. 1$

$SLHolBPC_{r,0} := -SLHolC_{r,0}$ $SLHolBPC_{r,1} := SLHolC_{r,1}$ $SSSHol := csort(SLHolBPC, 0)$

$X := SSSHol^{\langle 0 \rangle}$ $Y := SSSHol^{\langle 1 \rangle}$ $w := 33$ $m := \frac{w-1}{2}$ $n := rows(Y)$ $i := 0 .. n-1$

$$mvg\_avg_i := if\left[i < m, \frac{\sum_{j=0}^{2\cdot i} Y_j}{(2\cdot i)+1}, if\left(i > n-1-m, \frac{\sum_{j=2\cdot i-n+1}^{n-1} Y_j}{2n-1-2\cdot i}, \frac{\sum_{j=i-m}^{i+m} Y_j}{w} \right) \right]$$

2. Holocene Sea Level Rise - 8000 BP

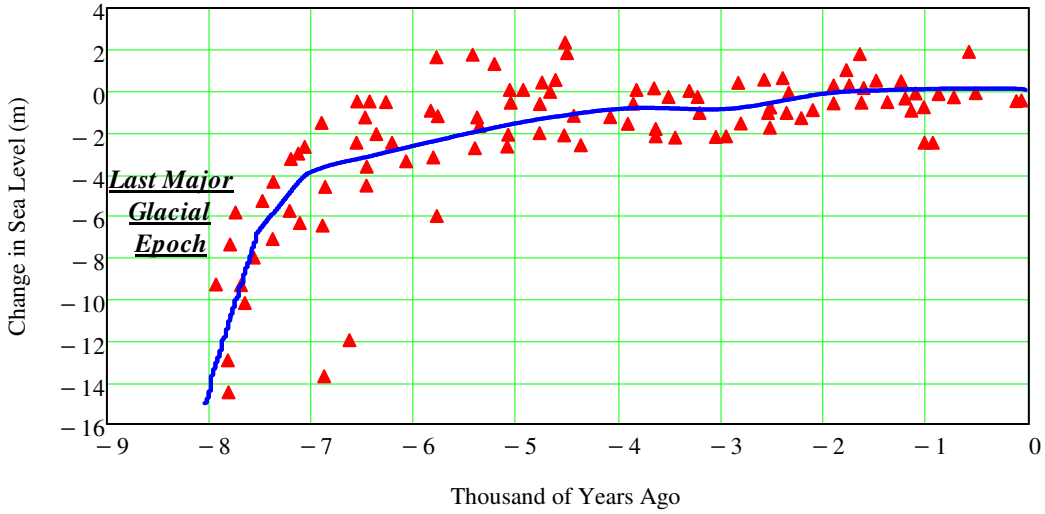

3. Shutdown of thermohaline circulation

There is some speculation that global warming could, via a shutdown or slowdown of the thermohaline circulation, trigger localized cooling in the North Atlantic and lead to cooling, or lesser warming, in that region.[76] This would affect in particular areas like Scandinavia and Britain that are warmed by the North Atlantic drift

1. Non Linear Trend: Global Sea Level vs Time - 1800 to 2014 - Anomalous increased rate since 1990

Jevrejeva, S., Grinsted, A., Moore, J. and S. Holgate. , J. Geophys. Res., 111, C09012, 2006
Global Sea Level Reconstruction Data http://www.pol.ac.uk/psmsl/author_archive/jevrejeva_etal_gsl/
%time, gsl_rate (mm), gsl_rate_error (mm), gsl (mm), gsl_error(mm)

Proudman Oceanographic Laboratory
http://www.pol.ac.uk/psmsl/author_archive/church_white/
church_white_grl_gmsl.txt
years, GMSL in millimeters, One-sigma error in millimeters.
Note: Data agrees with Global mean sea level from TOPEX/Poseidon, Jason-1, and Jason-2

U of Colorado Sea Level Research Group Sat Data
http://sealevel.colorado.edu/files/2014_rel5/sl_ns_global.txt
SatSL: Sat 2015 Global Mean Sea Level Time Series
Seasonal signal removed.
Data Format: Years, mm

SeaLevel := READPRN("Global sea level data.txt")
SL_CWF := READPRN("church_white_gmsl.txt")

SLI := submatrix(SeaLevel, 630, rows(SeaLevel) − 1, 0, 3)

Time := SeaLevel$^{\langle 0 \rangle}$ Time2 := SL_CWF$^{\langle 0 \rangle}$

SL := SeaLevel$^{\langle 3 \rangle}$ SL_CW := SL_CWF$^{\langle 1 \rangle}$

SatSL := READPRN("sl_ns_global2015.txt")

The Proudman raw and regression data gives a reference level for 2007.5 of ~ 137 mm and U of Col of 36.5 mm.
Add 100 mm to U of Col data to match up.

SatSLM := SatSL$^{\langle 1 \rangle}$ + 100

Sr := line(SLI$^{\langle 0 \rangle}$, $\overrightarrow{\text{SLI}^{\langle 3 \rangle}}$) $SL_{reg}(year) := Sr_0 + Sr_1 \cdot (year)$ $SL_{reg}(2007.5) = 136.58959$ $Sr_1 = 1.71045$

http://www.psmsl.org/products/reconstructions/gslGPChange2014.txt
%time, gsl_rate (mm), gsl_rate_error (mm), gsl (mm), gsl_error(mm)
Jevrejeva et al 2014
SLJ := READPRN("gslGPChange2014.dat")

SR := line(SatSL$^{\langle 0 \rangle}$, SatSLM) $SR_1 = 3.24825$

Sea level rise, Sr, of 1.7 mm/year began 1860, well before large scale CO_2 emissions
However, after 1990 the rate (SR) increased to 3.25 mm/year.

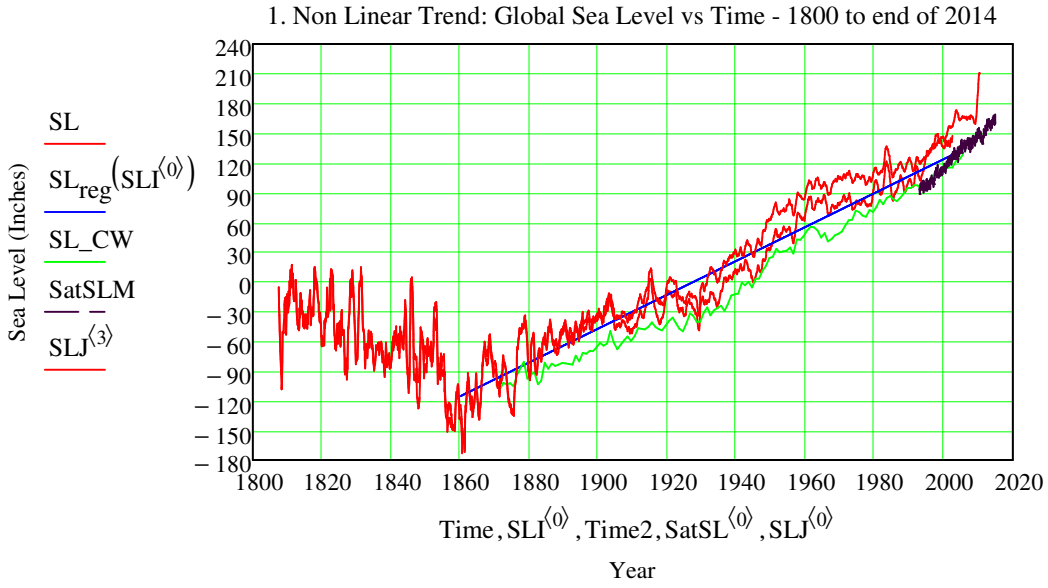

SECTION XVI "Extracting a Climate Signal from 169 Glacier Records", J. Oerlemans, 2005

Table S2. Global mean temperature reconstructed from glacier records compared to other temperature series. Glaciers Temp Reconstruction (Blue), Mann et al. Proxy (Red), Jones and Moberg Proxy (Green)

TempGlacier := READPRN("Extracting a Climate Signal from 169 Glacier Records Data.csv")

$$\frac{dL'(t)}{dt} = -\frac{1}{\tau}[cT'(t) + L'(t)] \qquad T'(t) = -\frac{1}{c}\left[L'(t) + \tau\frac{dL'(t)}{dt}\right]$$

Climate sensitivity depends in particular on the surface slope (a geometric effect) and the annual precipitation (a mass-balance effect). Glaciers in a wetter climate are more sensitive, and this is taken into account. Using a first-order theory of glacier dynamics, changes in glacier length were related to changes in temperature. Here, t is time, L' is the glacier length with respect to a reference state, and T is a temperature perturbation (annual mean) with respect to a reference state. As a result, in the sample of 169 glaciers, c varies by a factor of 10, from ~1 to ~10 km/K. Values of τ vary from about 10 years for the steepest glaciers to a few hundreds of years for the largest glaciers in the sample with a small slope (the glaciers in Svalbard). Most of the values are in the range of 40 to 100 years.

Glaciers Temp Reconstruction (Blue), Mann et al. Proxy (Red), Jones and Moberg Proxy (Green)

1. Glacier Global Temp Reconstruction & Ts - 1600 to 2000

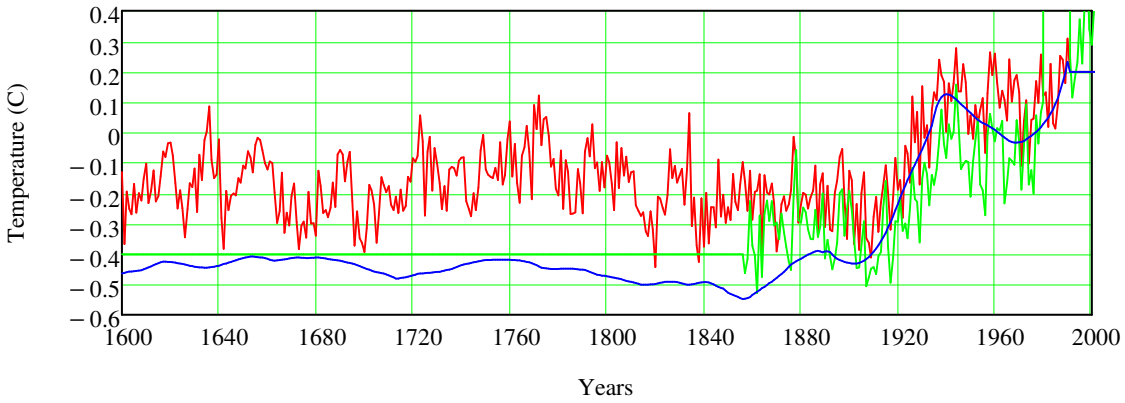

Glacier Mass Balance and Regime: Data of Measurements and Analysis OP55_glaciers.pdf
Institute of Arctic and Alpine Research, University of Colorado, Boulder, Colorado
http://instaar.colorado.edu/index.html

Appendix 3: Annual data on glacier regime - Averaged AAR calculations

Averaged annual or net mass balance calculations, pg. 79, <bn>, (mm)

ANMB := READPRN("Averaged annual or net mass balance calculations OP55.TXT")

$$\text{CumNMB} := \left(\text{ANMB}^{\langle 3\rangle} - \text{ANMB}_{4,3}\right)\cdot 10^{-3}$$

2. Glacier Cumulative Mass Balance, Thickness (m) - 1950 to 2000

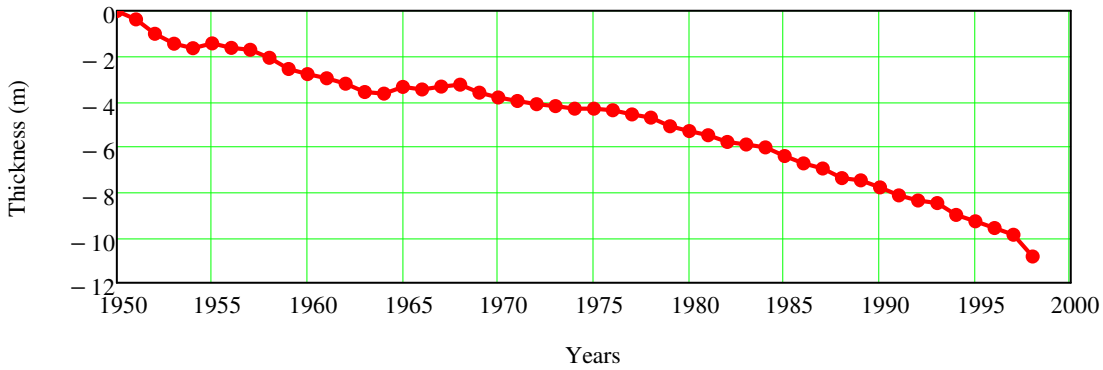

3. Vostok Ice Core Data, Ratio $^{18}O/^{16}O$ (High-->Warm) ==> Continental Glaciers over past 10^6 years

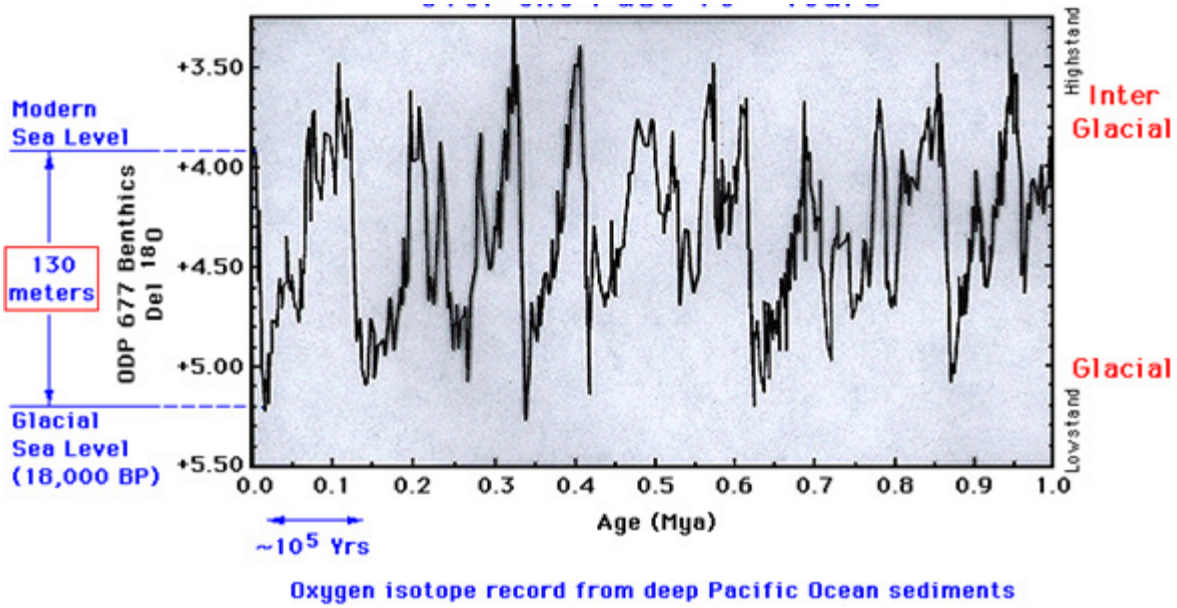

Oxygen isotope record from deep Pacific Ocean sediments

SECTION XVII. Snow Coverage in the Northern Hemisphere

Snow cover, the **whitest natural surface on the planet, reflects** roughly **90 percent of the sunlight** that reaches it. **Snow-free ground absorbs** anywhere from **four to six times more solar radiation** than snow-covered Earth. Though some snow cover occurs in the Southern Hemisphere or on Northern Hemisphere sea ice, **nearly all of the Earth's seasonal snow cover happens over land in the Northern Hemisphere.**

Changes over time

http://www.climate.gov/news-features/understanding-climate/2013-state-climate-snow-northern-hemisphere
From 1970 - Climate.gov

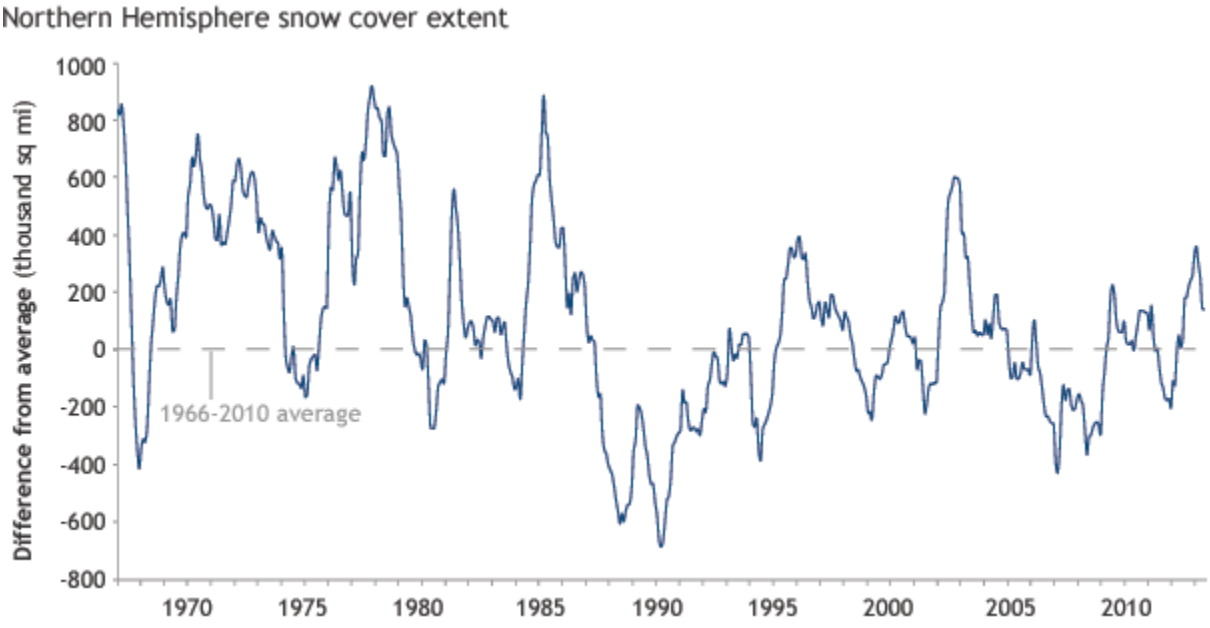

Rutgers Snow Coverage Data - From 1965

http://climate.rutgers.edu/snowcover/table_area.php?ui_set=1&ui_sort=0

Million sq. km

Row Year Month N. Hemisphere Eurasia N. America N. America (no Greenland)

$Snow := READPRN("gsl\ snow\ data.dat")$ $Yr\_snow := Snow^{\langle 1 \rangle} + \frac{Snow^{\langle 2 \rangle} - 1}{12}$

$LSnow := line\left(Yr\_snow, Snow^{\langle 3 \rangle}\right)$ $Lin\left(Yr_{snow}\right) := LSnow_0 + LSnow_1 \cdot \left(Yr_{snow}\right)$

$PerCentSnowDecrease := \frac{Lin(2014) - Lin(1965)}{Lin(1965)} \cdot 100$ $PerCentSnowDecrease = -13.69749$

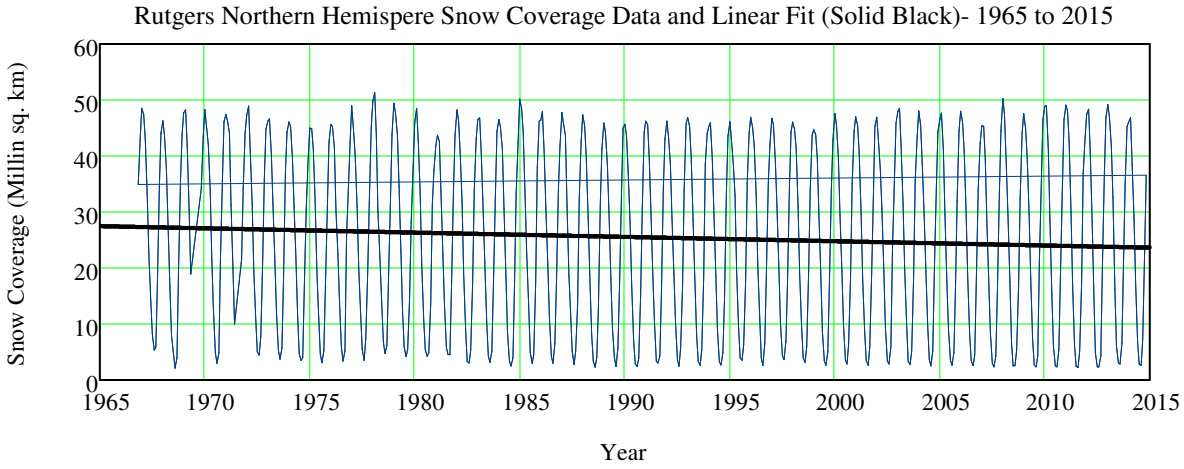

SECTION XVIII. Cryosphere -Sea Ice Extent -North & South Hemispheres

National Snow and Ice Data Center - North Year Month Day Extent (Millions sq km) Decimal Yr

ftp://sidads.colorado.edu/DATASETS/NOAA/G02135/north/ /south/daily/data/SH_seaice_extent_final.csv

$SeaIce := READPRN("Sea\_ice\_extent\_final\_North.TXT")$ $SeaIceNS := ksmooth\left(SeaIce^{\langle 4 \rangle}, SeaIce^{\langle 3 \rangle}, 30\right)$

$WRITEPRN("SeaIceAreaSSmooth.txt") := SeaIceN$ $SeaIceSmooth := READPRN("SeaIceAreaSmooth.txt")$

$SeaIceSouth := READPRN("SH\_seaice\_extent\_final.txt$ $SeaIceSS := ksmooth\left(SeaIceSouth^{\langle 4 \rangle}, SeaIceSouth^{\langle 3 \rangle}, 30\right)$

$WRITEPRN("SeaIceAreaSSmooth.txt") := SeaIceSS$ $SeaIceSSmooth := READPRN("SeaIceAreaSSmooth.txt")$

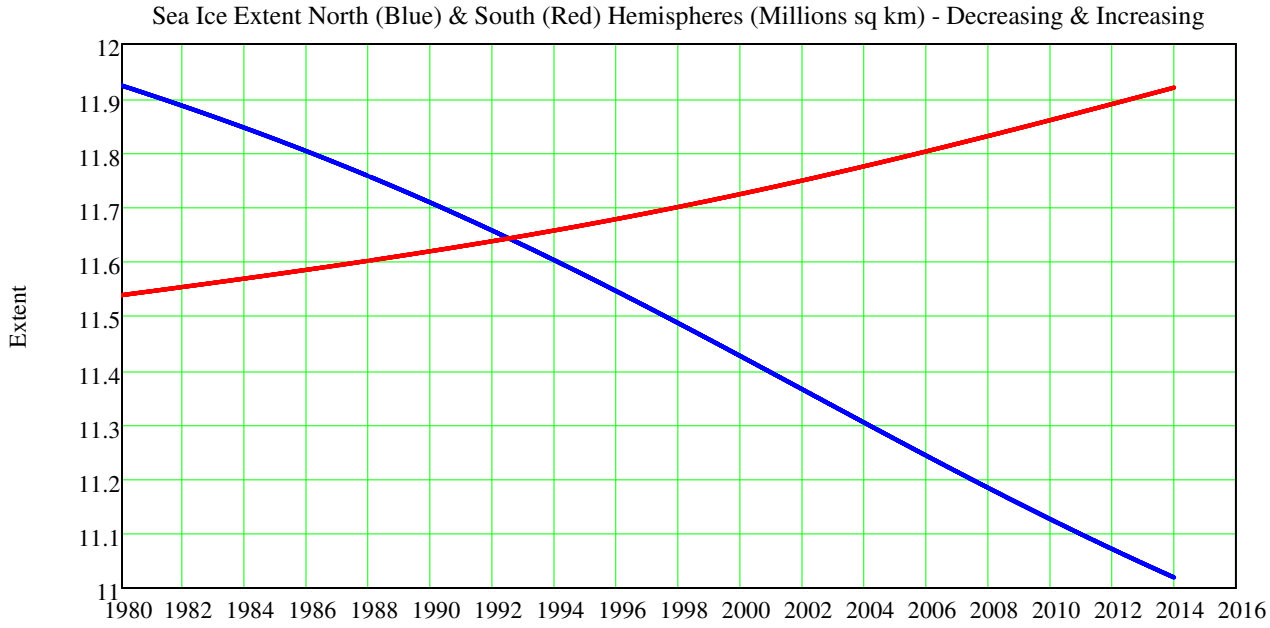

Calculate the Net Change: $\text{NetSeaIce} := \frac{\text{SeaIceSSmooth} + \text{SeaIceSmooth}}{\text{SeaIceSSmooth}_0 + \text{SeaIceSmooth}_0} \cdot 100$

2.5% Global Extent of Sea Ice Loss since 1980

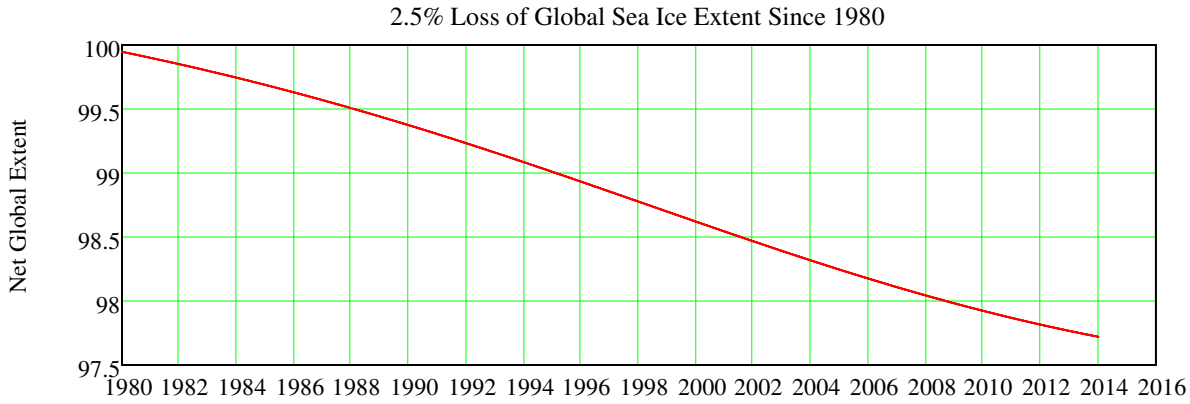

SECTION XIX. Model Predictions for Tropical Atmospheric Warming

http://www.climatechange.gov.au/en/climate-change/science.aspx
http://www.drroyspencer.com/wp-content/uploads/Spencer_EPW_Written_Testimony_7_18_2013_updated.pdf

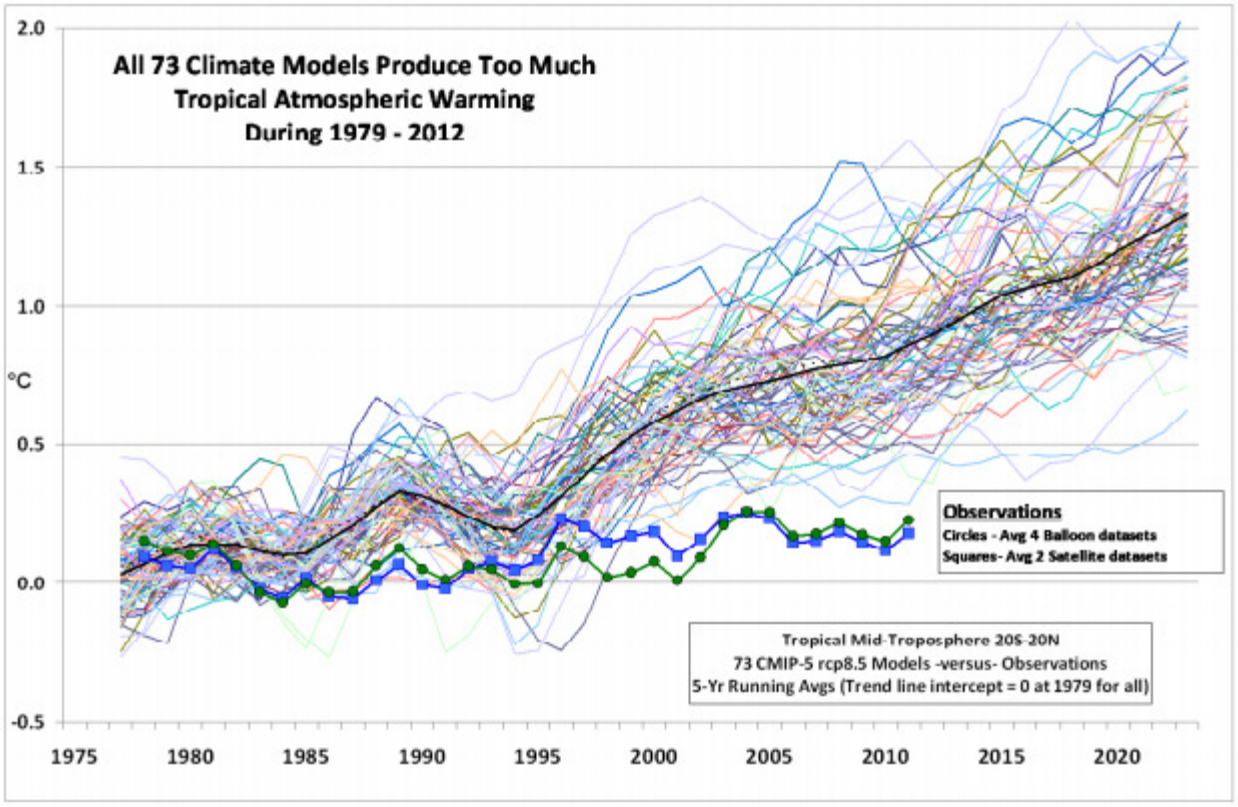

SECTION XX. Extreme Weather Getting Worse (NOAA Data)?

Decadal to Century Scale Trends in North American Snow Extent in Coupled Atmosphere-Ocean General Circulation Models - Columbia University, Geophysical Research Letters, 32:L18502, doi: 10.1029/2005GL023394.
http://www.eee.columbia.edu/research-projects/water_resources/climate-change-snow-cover/index.html

Continental-scale snow cover extent (SCE) is a potentially sensitive indicator of climate change, since it is an integrated measure of multiple hydroclimatological processes, and it is the most prominent seasonal land surface feature in the extratropical Northern Hemisphere. Conversely, feedback processes may cause SCE changes to in turn affect the direction and magnitude of other climate changes across the globe. In this study, current and future decadal trends in winter North American SCE (NA-SCE) are investigated, using 9 **general circulation models (GCMs)** of the global atmosphere-ocean system participating in the upcoming Intergovernmental Panel on Climate Change Fourth Assessment Report (IPCC-AR4).

Simulated annual time series of January NA-SCE spanning the 20th and 21st centuries are shown for all nine models in figure 1, based on a set of current and hypothesized future socioeconomic developments with associated greenhouse gas emissions, designated the 20C3M and SRESA1B scenarios, respectively. This exemplifies the considerable uncertainties that still plague GCM simulations. Nevertheless, all nine models exhibit a clear and statistically significant decreasing trend in 21st century NA-SCE, although the magnitude of the trend varies between models.

1. Simulated annual time series of January NA-Continental Scale Snow Coverage from 1850

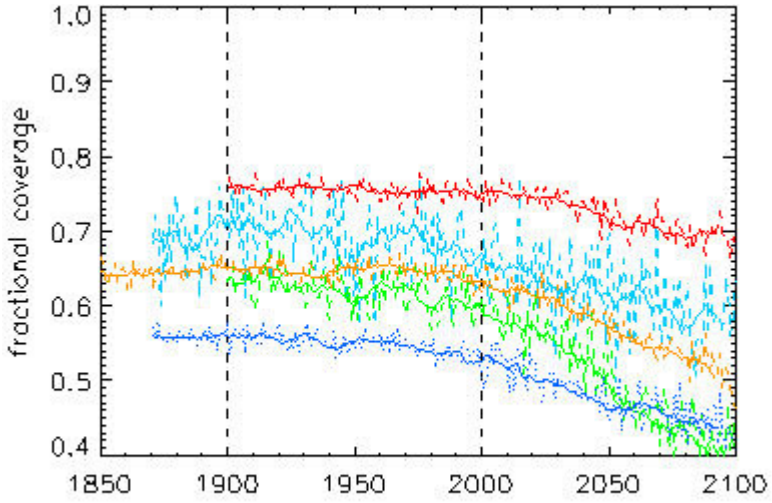

2. Rutgers Snow Lab (Plot Only Jan & Feb Data):

http://climate.rutgers.edu/snowcover/files/moncov.nhland.txt

Snow := READPRN("Rutgers-moncov.nhland2014.tx S := SJan(Snow) Sw := SWin(Snow)

$S^{\langle 1 \rangle} := S^{\langle 1 \rangle} - \text{mean}\left(S^{\langle 1 \rangle}\right)$ L := line$\left(S^{\langle 0 \rangle}, S^{\langle 1 \rangle}\right)$ Fit := $L_0 + L_1 \cdot S^{\langle 0 \rangle}$

$Sw^{\langle 1 \rangle} := Sw^{\langle 1 \rangle} - \text{mean}\left(Sw^{\langle 1 \rangle}\right)$ Lw := line$\left(S^{\langle 0 \rangle}, Sw^{\langle 1 \rangle}\right)$ Fitw := $Lw_0 + Lw_1 \cdot S^{\langle 0 \rangle}$

Is slope of trend increasing(+) or decreasing (-)? $L_1 = 0.01255$ $Lw_1 = 0.02867$

2. North Hemisphere Snow Cover Anomalies (December & January). Trend Line (Blue)

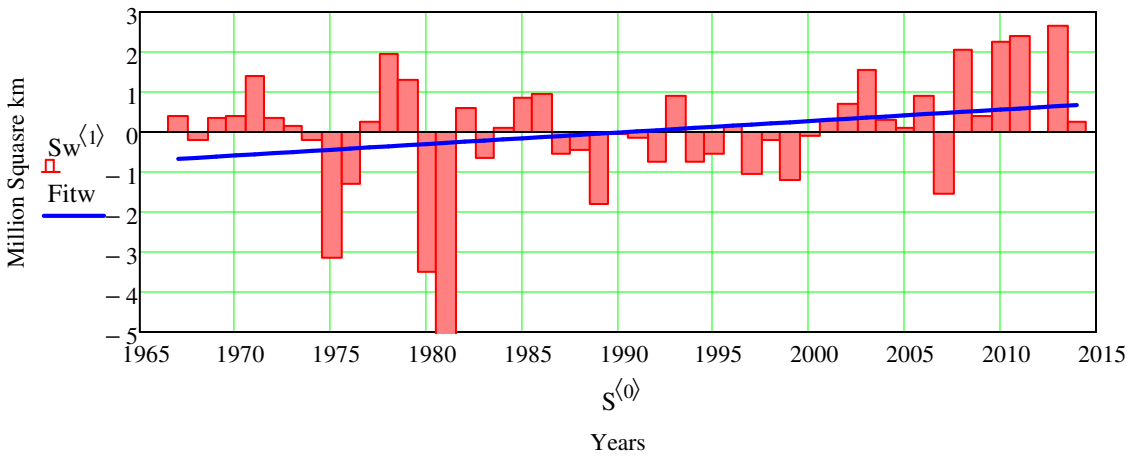

3. US Percentage Area Very Warm, Very Cold

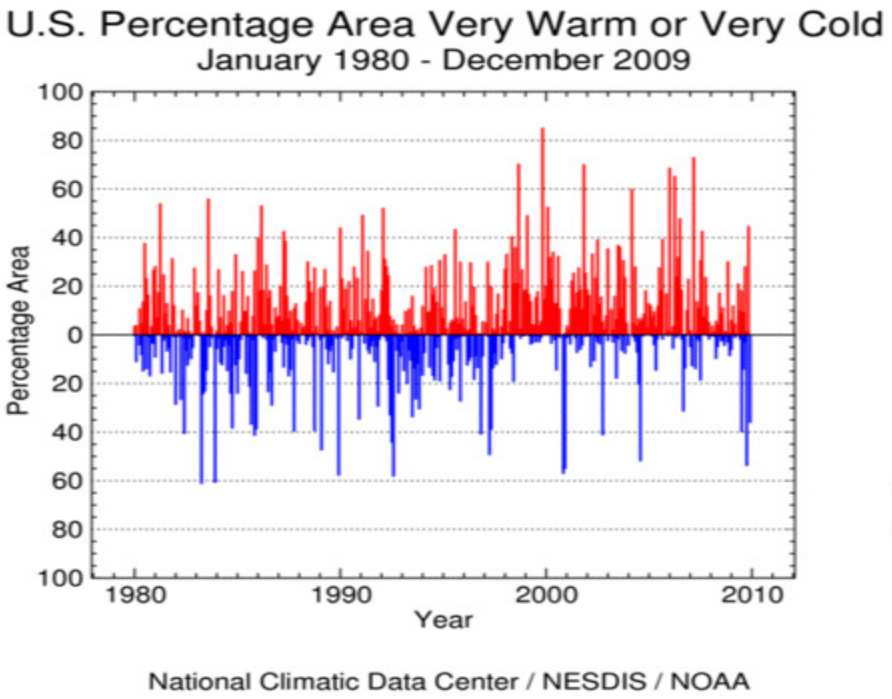

Red - Very Warm
Blue - Very Cold

4. USDA Economic Research Service: Worst Droughts 1930s

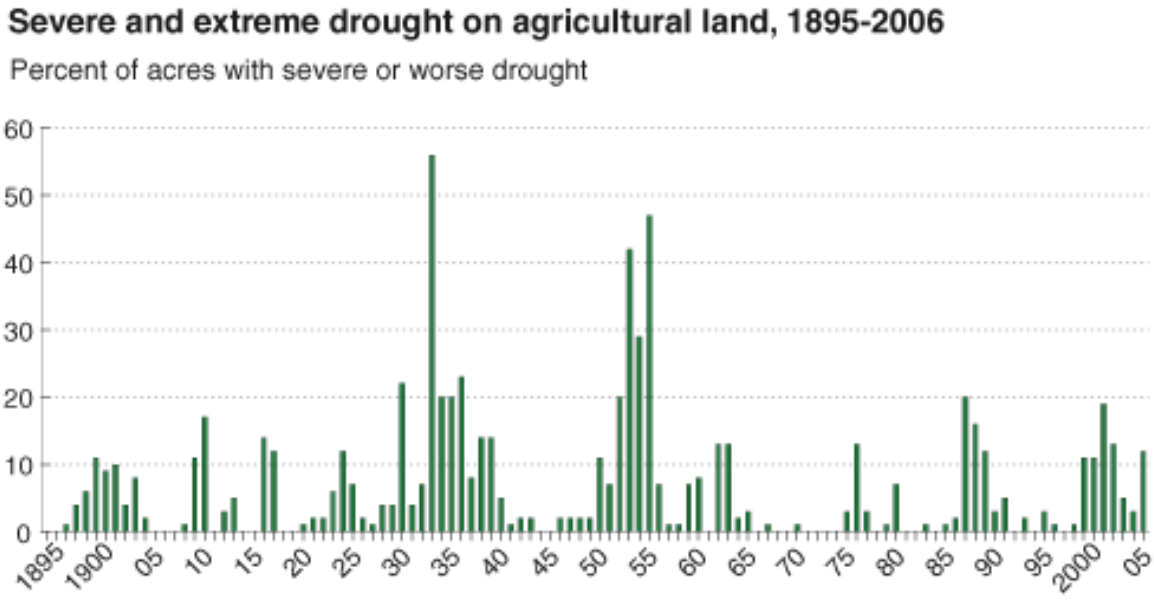

Note: Percentage of land is based on current land use for agriculture, including land in crops, pasture, range, and USDA's Conservation Reserve Program.

Source: National Oceanic and Atmospheric Administration.

Amber Waves: US Department of Agriculture, Economic Research Service, May 2007

5. NOAA: Rainfall/Wetness Data

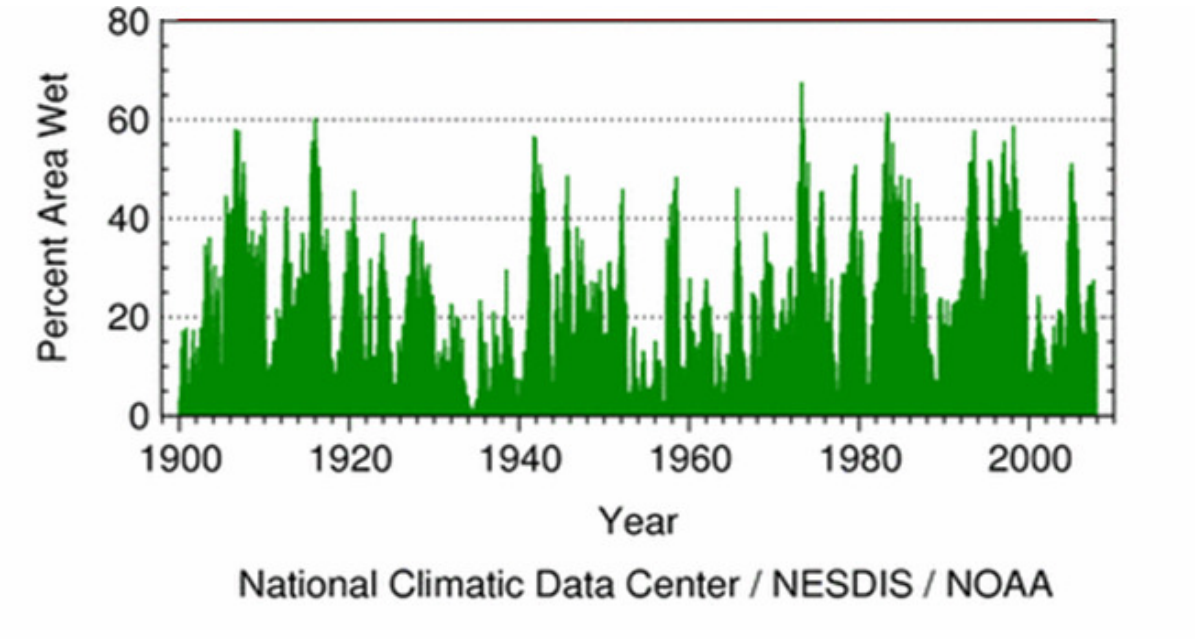

6. Lessoning Predicted Impact of Global Warming on Sea Level Rise by 2100

Trend of PCC Predictions: Sea Level Rise by 2100

- **Al Gore's** 'An Inconvenient Truth' 2006 — 240 inches
- IPCC 'Scientific Assessment' **2001** — 6 to 34 inches
- IPCC 'Summary for Policymakers' **2007** — 6 to 23 inches
- IPCC 'Scientific Assessment' **2007** — 6 to 17 inches

Over the 20th Century (**Natural Causes**), sea-levels globally have risen about 6 to 8 inches

7. Hurricane Frequency - Getting Worse? No.

For Analysis See: http://www.leapcad.com/Climate_Analysis/Hurricane_Frequency.pdf

Plot Number: Hurricanes (Blue), Hurricanes with Landfalls (Black) and Cat 3 Hurricanes (Red)

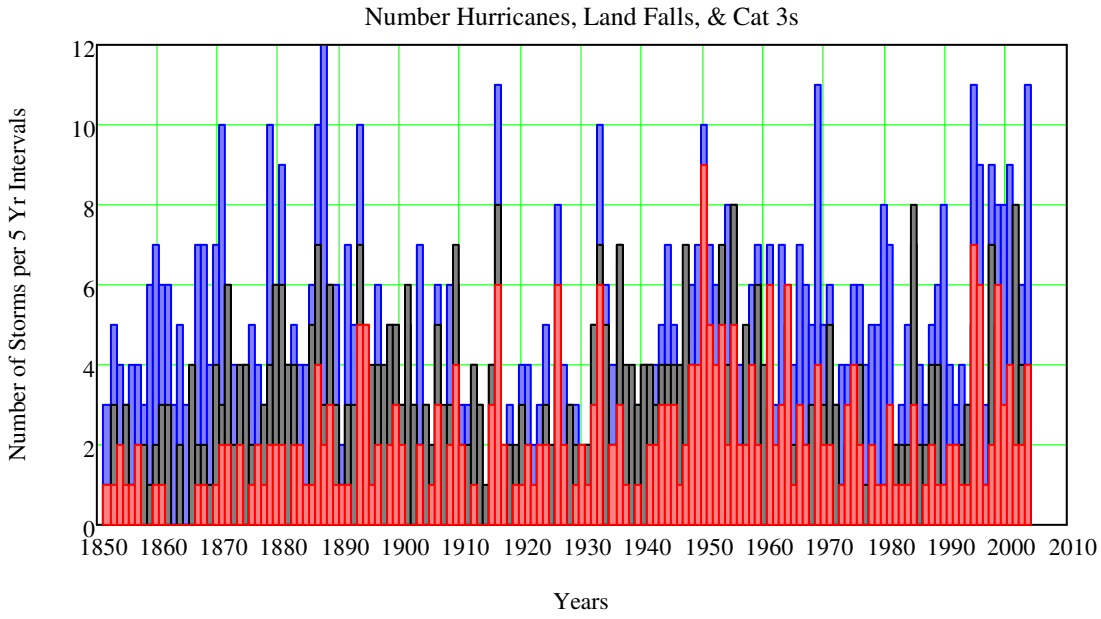

8. NWS US Tornadoes - Getting Worse

http://climate.rutgers.edu/stateclim_v1/robinson_pubs/refereed/Kunkel_et_al_2013.pdf

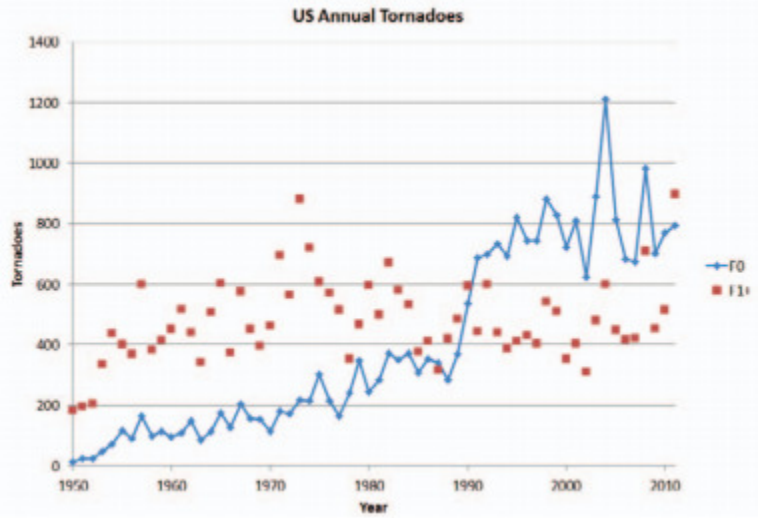

Reported tornadoes in NWS database from 1950 to 2011.

9. NOAA National Climate Extremes Index - Getting Worse

http://www.ncdc.noaa.gov/extremes/cei/graph

CEI := READPRN("NOAANationalClimateExtremesIndex.txt")

LX := line(CEI^⟨0⟩, CEI^⟨1⟩) FitX := $LX_0 + LX_1 \cdot CEI^{\langle 0 \rangle}$

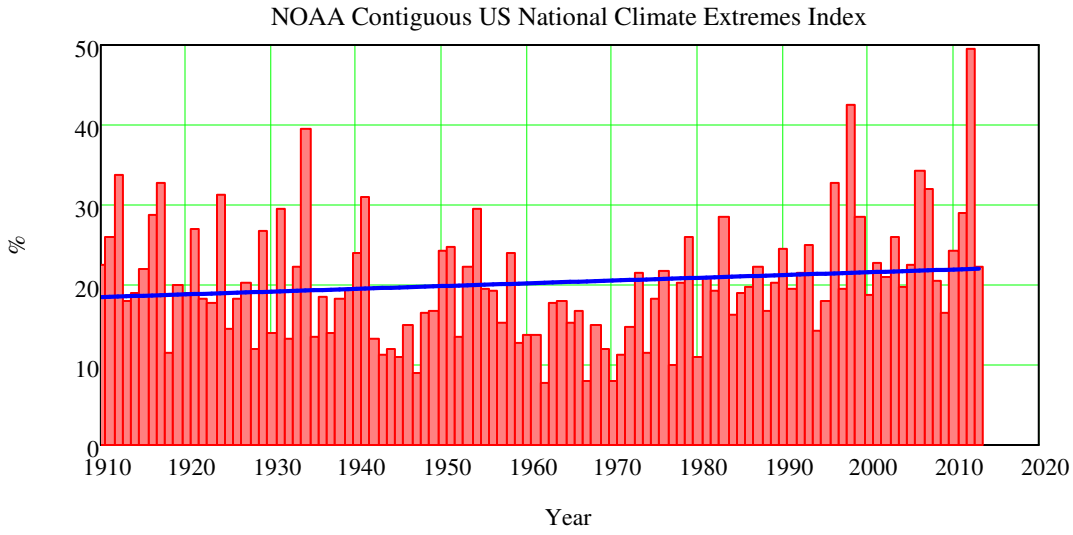

10. Destabilzed Polar Vortex (USA Winters of 2009-2013)

In the Arctic in the past, frigid air is typically trapped in a tight loop known as the polar vortex. This super-chilled air is not only **cold, it also tends to have low barometric pressure** compared to the air outside the vortex. The **surrounding high-pressure zones push in on the vortex** from all sides so the cold air is essentially "fenced in" above the Arctic, where it belongs.

As the Arctic region **warms faster** than most other places, **however**, the **Arctic sea ice melts more rapidly** and for longer periods each year, and is unable to replenish itself in the briefer, warmer winter season. This can **destabilize the polar vortex and raises the barometric pressure** within it. For several winter seasons (2009/2010, 2010/2011, and 2012/2013), the polar vortex was notably unstable.

This effect is climate, per se, but it is a tread.

SECTION XXI.
The Tradeoff Between Improvement of Human Condition vs. Climate Change

The Improvement in Human Condition Dwarfs the Rise in CO_2 Levels

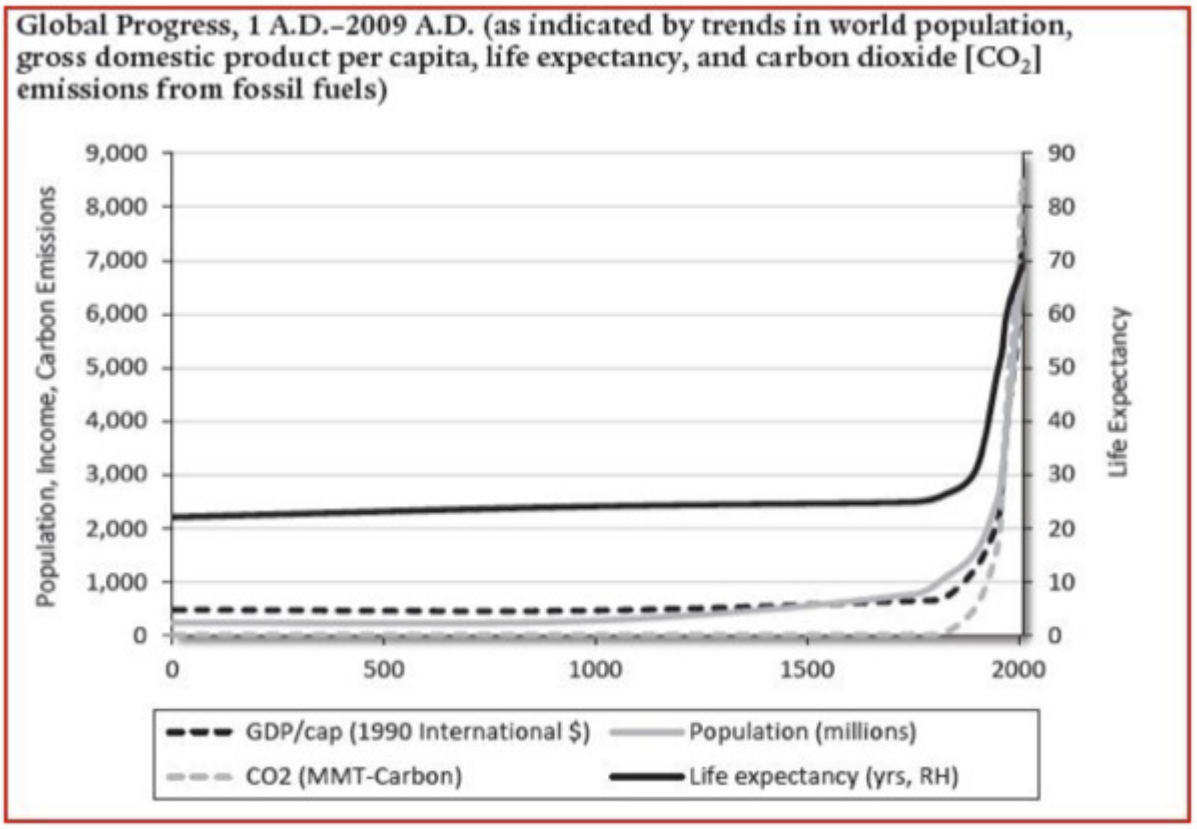

APPENDIX

AI. Types of GISS NASA Data Sources and New versus Old Differences:

GISTEMP Indices

Land-Ocean Temperature index (LOTI, i.e. the index that **includes weather station data and sea surface temperature** data to give a global anomaly index with wide spatial coverage) ("GLB.Ts**+dSST**.txt").

Met station index, which **only uses weather station data** ("GLB.Ts.txt") which doesn't't have as much coverage and has a substantially larger trend reflecting the relative predominance of faster-warming continental data in the average.

Old versus New differences are tiny, and mostly reflect slightly more data in the earlier years in the latest data and the different homogenization in GHCN v3 compared to GHCN v2 (which was used up to Dec 2011). The the biggest difference in trend (between 2006 and today), is a mere 0.05ºC/Century, and from 2008 to 2012 it is only 0.003ºC/Century.

HADCRUT - Climatic Research Unit (University of East Anglia) in conjunction with the Hadley Centre
http://www.cru.uea.ac.uk/cru/data/temperature/
CRUTEM4: Land air temperature anomalies
CRUTEM4v: Variance adjusted version of CRUTEM4
CRUTEM3: **Land air** temperature anomalies - superseded by CRUTEM4
CRUTEM3v: **Variance adjusted** version of CRUTEM3 (superseded by CRUTEM4v)
HadSST3: Sea Surface